



Tank Shell Design According to Eurocodes and Evaluation of Calculation Methods

Dimensionering av cisternvägg enligt Eurokod samt utvärdering av beräkningsmetoder

Malin Pluto

Faculty of Health, Science and Technology

Degree Project for Master of Science in Engineering, Mechanical Engineering

30 hp

Supervisor: Jens Bergström

Examiner: Pavel Krakhmalev

2018-07-25

Abstract

Tanks are storage vessels for liquids. They can have different appearances; some are short and wide, others are tall and slim, some are small, others are large. In this thesis a tank of 6 m in both diameter and height has been used to obtain numerical results of the stresses in the tank. Tanks are most often thin-walled with stepwise variable shell thickness with thicker wall sections at the bottom of the tank and thinner at the top. Since they are thin walled they are susceptible to buckling and there are conditions the shell construction must meet. The conditions that has to be met are determined by the laws and regulations that govern tank design. The National Board of Housing, Building and Planning (Boverket) is the new Swedish authority for rules of tank design and the Eurocodes are the new family of standards that should be followed. Sweco Industry AB is the outsourcer of this thesis and wants to clarify what rules that apply now when the Eurocodes are to be followed. The thesis project has produced a calculation document in Mathcad for tank shell design according to the Eurocodes with stress calculations according to membrane theory and linear elastic shell analysis. This thesis has also produced a comparison of stresses calculated using membrane theory, linear elastic shell analysis and finite element method (FEM). The comparison has been made for numerical results given for an arbitrarily designed tank wall.

The loads acting on the tank included in the description were self-weight, internal and hydrostatic pressure as well as wind and snow loads. The loads were described in accordance with the Eurocodes. Some assumptions had to be made where the standard was vague or deficient in order to make calculations by hand possible. For example, the wind load had to be described as an axisymmetrically distributed load rather than an angularly varying. The stresses in the tank wall were calculated through creating free-body diagrams and declaring equations for force and moment equilibrium. The loads and boundary conditions were set in a corresponding manner in the FEM software Ansys as in the calculation document in order to obtain comparable results. When compared, the stress results calculated with membrane theory and FEM were quite similar while the stresses calculated with linear analysis were a lot larger. The bending moments were assumed to be too large which make the results of the linear analysis dominated by the moments. The arbitrarily dimensions set for the tank did thus not fulfill the conditions when linear analysis was used but did so for membrane theory and FE-analysis.

Since the results calculated with membrane theory were very close to FEM in most cases, even without expressions for local buckling, it was assumed to be an adequate method in this application. Expressions for local buckling are although needed for the meridional normal stress. The conclusions of the results obtained are that membrane theory is a simple and adequate method in most cases. Linear analysis thus becomes redundant since it is more complicated and more easily leads to faulty results. Furthermore it cannot be used for higher consequence classes than membrane theory. FEM, with a computer software such as Ansys, is although the most usable calculation method since it can conduct more complicated calculations and is allowed to be used for all consequence classes.

Keywords: Tank, Eurocode, Membrane theory, Linear elastic shell analysis, Finite element method

Sammanfattning

Cisterner är behållare för lagring av vätska. De kan se ut på olika sätt; vissa är korta och breda, andra är höga och smala, vissa är små, andra är stora. I detta arbete har en cistern med 6 m i både diameter och höjd använts för att erhålla numeriska resultat av spänningarna i cisternen. Oftast är cisterner tunnväggiga med stegvis variabel manteltjocklek där väggen är tjockare nertill än upptill. Eftersom att de är tunnväggiga är de också benägna att buckla, vilket det finns villkor som skalkonstruktioner ska uppfylla för att undvika. Vilka villkor som ska uppfyllas bestäms av de lagar, regler och förordningar som finns för cisterner. Boverket är den nya myndigheten som skriver de förordningar som cisternsdesign ska följa. Eurokoderna är den nya samling av standarder som ska följas. Sweco Industry AB är uppdragsgivare till uppsatsen och vill reda ut vad som gäller i och med att Eurokoderna nu ska följas. Uppsatsen har tagit fram ett beräkningsdokument i Mathcad för cisternväggsdesign enligt Eurokoderna med spänningsberäkning enligt membranteori och linjärelastisk skalanalys. Uppsatsen har även framfört en jämförelse mellan spänningarna beräknade av membranteori, linjäranalys och finita elementmetoden (FEM). Jämförelsen har gjorts för numeriska resultat givna för en godtyckligt dimensionerad cisternvägg.

Lasterna på cisternen som togs fram var egenvikt, inre tryck och hydrostatiskt tryck samt vind- och snölast. Lasterna togs fram i enlighet med Eurokoderna. En del antaganden fick göras där standarden var ottydlig eller för att göra handberäkning möjlig, bland annat att beskriva vindlasten som en jämnt fördelad last istället för angulärt varierande. Spänningarna i cisternväggen beräknades sedan genom friläggning och uppställning av kraft- och momentjämvikt. Laster och gränstillstånd bestämdes på liknande sätt i FEM-programmet Ansys som i beräkningsdokumentet för att få jämförbara resultat. Vid jämförelse av resultatet var resultaten från membranteori och FEM ganska lika medan linjäranalys var mycket större. Momenten antogs vara alldeles för stora vilket gör att resultaten från linjäranalys dominerades av momenten. Den godtyckligt dimensionerade cisternen uppfyllde därför inte villkoren när linjäranalys användes medan den uppfyllde villkoren med råge för membranteori och FE-analys.

Eftersom membranteori i de flesta fall var mycket nära FEM, även utan uttryck för lokal buckling, antogs det därför vara en tillräckligt bra metod i denna tillämpning. Det behövs dock förenklade uttryck för lokal buckling för normalspänningen i generatrisled. Slutsatsen av de resultat som erhöles är att membranteori är enkelt att använda och ger tillräckligt bra resultat i de flesta fall. Linjäranalys blir därför överflödigt eftersom den är mer komplicerad och orsakar därför lättare fel, dessutom kan den inte tillämpas vid högre konsekvensklasser än membranteori. FEM, med datorprogram som Ansys, är dock den mest användningsbara beräkningsmetoden eftersom att den kan utföra mer komplicerade beräkningar och får användas för alla konsekvensklasser.

Nyckelord: Cistern, Eurokod, Membranteori, Linjärelastisk skalanalys, Finita elementmetoden

Contents

List of Figures	vi
List of Tables	vii
Nomenclature	viii
1 Introduction	1
1.1 Background	1
1.2 Eurocodes	2
1.3 Purpose, goal and method	4
2 Theory	5
2.1 Membrane theory	5
2.2 Linear elastic shell analysis	5
2.3 Finite element analysis	6
3 Method	7
3.1 Actions	8
3.1.1 Self-weight	8
3.1.2 Internal and hydrostatic pressure	9
3.1.3 Wind load	10
3.1.4 Snow load	11
3.2 Limit states	12
3.2.1 Plastic limit condition	12
3.2.2 Buckling conditions	12
3.3 Free body diagrams and force equilibrium	14
3.4 Stresses calculated by membrane theory	18
3.5 Stresses calculated by linear analysis	18
3.6 Simulation with finite element method (FEM)	19
4 Results	24
4.1 Membrane theory and linear analysis	24
4.2 Finite element analysis	25
4.3 Summary and comparison of results	29
5 Discussion	30
5.1 Limitations of this thesis project	30
5.2 Loads and assumptions	30
5.3 Comparison of obtained results	30
5.4 Comparison against the plastic limit and buckling limit conditions	31
6 Conclusions	33
7 Acknowledgement	34
8 References	35
Appendices	A1
A Geometry of conical roof	A1
B The calculation document	B1

List of Figures

1	A slim tank [5].	1
2	Cross section view of tank [6].	1
3	The inside of a large tank [7].	2
4	The outside of a large tank [7].	2
5	Membrane stresses and bending moments in a shell.	5
6	Transverse shear stresses in a shell.	6
7	Sectioning of a model into finite elements.	6
8	Principal element of finite element method.	6
9	The numerical dimensions of the tank used.	7
10	Numerical values of the stepwise variable shell thickness.	7
11	The internal pressure distribution.	9
12	The hydrostatic pressure distribution.	9
13	The wind distribution around a cylinder [24].	10
14	Wind distribution used.	10
15	The wind load distribution.	11
16	The snow load distribution.	12
17	Transformation of stepwise variable thickness to equivalent uniform thickness.	13
18	Actions on shell wall, seen in xr -plane.	14
19	Actions on the roof.	15
20	Sectioning of shell, seen in xr -plane.	16
21	Meridional stress resultant.	17
22	Meridional bending moment.	17
23	Sectioning of shell, seen in $x\theta$ -plane.	17
24	Circumferential stress resultant.	18
25	Circumferential bending moment.	18
26	The solid model of the tank.	20
27	Close-up on solid model.	20
28	Close-up on shell model.	20
29	Bonded edge contact between sections.	20
30	Symmetry condition limiting displacement in circumferential direction.	21
31	Symmetry condition limiting rotation.	21
32	Boundary condition at the top.	21
33	Boundary condition at the bottom.	21
34	The mesh.	21
35	Close-up on the mesh.	21
36	Self-weight.	22
37	Load from roof.	22
38	Hydrostatic pressure.	22
39	Internal pressure.	23
40	Wind action.	23
41	Meridional path.	23
42	Diagram of the circumferential design stress for the effective cylinder calculated with membrane theory.	25
43	Diagram of the shear design stress for the effective cylinder calculated with membrane theory.	25
44	Diagram of the circumferential design stress for the effective cylinder calculated with linear analysis.	25
45	Diagram of the shear design stress for the effective cylinder calculated with linear analysis.	25
46	Equivalent von Mises stress result	26
47	Equivalent von Mises stress result with exaggerated deformation.	26
48	Deformation of static structural analysis.	26
49	Diagram of the equivalent stress.	27
50	Meridional design stress.	27
51	Diagram of meridional design stress.	27
52	Circumferential design stress for effective cylinder.	27
53	Diagram of circumferential design stress in effective cylinder.	27
54	Shear design stress in effective cylinder.	28
55	Diagram of shear design stress in effective cylinder.	28
A.1	Geometry of a conically shaped roof for a tank.	A1
A.2	Diameter and height of insulation on a conically shaped roof	A1

List of Tables

1	The family of Eurocodes	3
2	The relevant standards for tank shell design	3
3	Thicknesses of roof, insulation and weather protection cover	7
4	Material properties.	7
5	The density of the steels and insulation	8
6	Comparison of equivalent stresses for the three calculation methods	29
7	Comparison of stresses for the three calculation methods	29
8	Comparison of equivalent stresses and meridional stresses with conditions	32
9	Comparison of stresses for effective cylinder with buckling conditions	32
10	Comparison of circumferential and shear stresses with buckling conditions	32

Nomenclature

Factors and other symbols		l_b	Length of section b of the tank wall
γ_F	Partial factor for variable loads (safety factor)	l_c	Length of section c of the tank wall
γ_G	Partial factor for permanent loads (safety factor)	l_{eff}	Effective length
γ_{M0}	Partial factor for resistance to plasticity (safety factor)	l_j	Length of section j of the tank wall
γ_{M1}	Partial factor for resistance to buckling (safety factor)	s_{roof}	Line of the roof of which the line loads are applied
μ_i	Snow load shape coefficient	t_a	Thickness of section a of the tank wall
ψ_{hyd}	Combination factor for hydrostatic load	t_b	Thickness of section b of the tank wall
ψ_{int}	Combination factor for internal pressure	t_c	Thickness of section c of the tank wall
ψ_{snow}	Combination factor for snow load	t_j	Thickness of section j of the tank wall
ψ_{wind}	Combination factor for wind action	t_{ave}	Average thickness of the tank wall
ξ_{weight}	Reduction factor for self-weight	$t_{cover,roof}$	Thickness of the weather protection on the roof
C_e	Exposure coefficient	$t_{cover,shell}$	Thickness of the weather protection around the shell
C_t	Thermal coefficient	$t_{ins,roof}$	Thickness of the insulation on the roof
$c_{pe,roof}$	Pressure coefficient for external wind pressure acting on the roof	$t_{ins,shell}$	Thickness of the insulation around the wall
c_{pe}	Pressure coefficient for external wind pressure	t_{roof}	Thickness of the roof plate
g	Gravitational acceleration	V_{shell}	Volume of the steel plates of the shell
q_p	Peak velocity pressure	z	Height above the ground
s_k	Characteristic value of snow load on ground	z_e	Reference height for the external wind acting on the tank wall
Geometrical dimensions		$z_{e,roof}$	Reference height for the external wind acting on the roof
α_{roof}	Angle of the sloped roof	Loads	
$A_{cover,roof}$	Surface area of the weather protection on the roof	$F_{weight,roof,Ed}$	Design value of force per unit width originating from the total weight of the roof including insulation and weather protection
$A_{ins,roof}$	Surface area of the insulation on the roof	$F_{weight,roof}$	Force per unit width originating from the total weight of the roof including insulation and weather protection
A_{roof}	Surface area of the roof plate	$F_{weight,shell,Ed}$	Design value of force per unit width originating from the total weight of the shell including insulation and weather protection.
D	Diameter of the tank	$F_{weight,shell}$	Force per unit width originating from the total weight of the shell including insulation and weather protection
D_{out}	Outer diameter of the tank including insulation and weather protection cover		
h	Height of the roof		
H_0	Height of the tank wall		
l_a	Length of section a of the tank wall		

P	Internal and hydrostatic pressure combined	$\rho_{liquid,Ed}$	Design value of the density of the liquid
p	Hydrostatic pressure	E	Stiffness of tank steel, Young's modulus
p_i	Internal pressure	f_y	Yield strength of tank steel
p_{Ed}	Design value of the hydrostatic pressure	$f_y k$	Characteristic yield strength of tank steel
$p_{i,Ed}$	Design value of the internal pressure		
$s_{snow,Ed}$	Design value of the snow load		
s_{snow}	Snow load		
$T_{base,r}$	Reaction force from the ground in radial direction		
$T_{base,x}$	Reaction force from the ground in meridional direction		
$T_{roof,r}$	Reaction force from the roof in radial direction		
$T_{roof,x}$	Reaction force from the roof in meridional direction		
$W_{cover,roof}$	Weight of the weather protection on the roof		
$W_{cover,shell}$	Weight of the weather protection around the wall		
$w_{e,Ed}$	Design value of the external wind action acting on the tank wall		
$w_{e,roof,Ed}$	Design value of the external wind action acting on the roof		
$w_{e,roof}$	External wind action acting on the roof		
w_e	External wind action acting on the tank wall		
$W_{ins,roof}$	Weight of the insulation on the roof		
$W_{ins,shell}$	Weight of the insulation around the wall		
W_{roof}	Weight of the roof plates		
W_{shell}	Weight of the wall plates		
Material constants			
γ_{cover}	Density of the weather protection	$\tau_{\theta n,Ed}$	Circumferential transverse shear stress
γ_{ins}	Density of the insulation	$\tau_{x\theta,Ed,eff}$	Design value of shear stress for effective cylinder
γ_{liquid}	Density of the liquid	$\tau_{x\theta,Ed_j}$	Design value of shear stress for section j
γ_{roof}	Density of the roof plate material	$\tau_{x\theta,Ed}$	Design value of shear stress
γ_{shell}	Density of the wall plate material	$\tau_{x\theta,Rcr_j}$	Elastic critical shear buckling stress for section j
ρ_{Ed}	Design value of the density of the steel shell including insulation and weather protection	$\tau_{x\theta,Rd,eff}$	Design buckling shear stress in the direction of circumference for effective cylinder
		$\tau_{xn,Ed}$	Meridional transverse shear stress
		$M_{\theta,Ed}$	Design value of circumferential bending moment per unit width
		M_{θ}	Circumferential bending moment per unit width
		$M_{x,Ed}$	Design value of meridional bending moment per unit width
		$M_{x\theta,Ed}$	Design value of twisting shear moment per unit width

Stresses

$\sigma_{\theta,Ed,eff}$	Circumferential design stress for effective cylinder
σ_{θ,Ed_j}	Circumferential design stress for section j
$\sigma_{\theta,Ed}$	Circumferential design stress
σ_{θ,Rcr_j}	Critical circumferential buckling stress for section j

$\sigma_{\theta,Rd,eff}$	Design buckling stress in circumferential direction for effective cylinder
$\sigma_{eq,Ed}$	Design value of von Mises equivalent stress
σ_{eq}	von Mises equivalent stress

σ_{x,Ed_j}	Meridional design stress for section j
$\sigma_{x,Ed}$	Meridional design stress
σ_{x,Rd_j}	Design buckling stress in generatrix direction for section j

$\tau_{\theta n,Ed}$	Circumferential transverse shear stress
$\tau_{x\theta,Ed,eff}$	Design value of shear stress for effective cylinder
$\tau_{x\theta,Ed_j}$	Design value of shear stress for section j
$\tau_{x\theta,Ed}$	Design value of shear stress
$\tau_{x\theta,Rcr_j}$	Elastic critical shear buckling stress for section j
$\tau_{x\theta,Rd,eff}$	Design buckling shear stress in the direction of circumference for effective cylinder

$\tau_{xn,Ed}$	Meridional transverse shear stress
$M_{\theta,Ed}$	Design value of circumferential bending moment per unit width
M_{θ}	Circumferential bending moment per unit width
$M_{x,Ed}$	Design value of meridional bending moment per unit width
$M_{x\theta,Ed}$	Design value of twisting shear moment per unit width

$M_{x\theta}$	Twisting shear moment per unit width	$N_{x,Ed}$	Design value of meridional membrane stress resultant
M_x	Meridional bending moment per unit width	$N_{x\theta,Ed}$	Design value of maximum membrane shear stress resultant in the shell
$N_{\theta,Ed}$	Design value of circumferential membrane stress resultant	$N_{x\theta,Ed}$	Design value of membrane shear stress resultant
$N_{\theta,max,Ed}$	Design value of maximum circumferential membrane stress resultant in the shell	$N_{x\theta}$	Membrane shear stress resultant
N_{θ}	Circumferential membrane stress resultant	N_x	Meridional membrane stress resultant

1 Introduction

1.1 Background

Tanks are normally used for storing fluids, water or oil for example [1]. Being in possession of a tank leads to the responsibility of ensuring that the tank does not affect the environment, through for example leakage [2]. Tanks that contain flammable fluids have to be inspected regularly by an accredited control organization and have to follow the rules of several actors [2]. The rules are all laws written by the Parliament combined with regulations written by the Government and regulations written by several authorities. They all have to be applied when designing tanks as well as the directives from EU [3].

The research on storage tanks containing oil and fuels has increased significantly the last 20 years [4]. This is due to the huge economic, environmental and social losses caused by failures due to accidents or natural disasters [4]. In Figures 1-4 some examples are shown of what tanks can look like. They come in all sizes and are adapted to the task at hand. Some tanks are tall and slim like the tank in Figure 1 and some are short and wide like the tank in figures Figure 3 and 4. The trend has been the last decade to build fewer tanks with a larger diameter and thus higher capacity than before [4]. Tanks in China have reach a diameter of 100 *m* with a capacity of 100 000 m^3 and in France the tanks have reach a diameter of 80 *m* and volume capacities of 100 000 m^3 , 10 000 m^3 and 1000 m^3 [4].

Vertical aboveground tanks are used in many industries to store water, oil, fuel, chemical and other fluids [4]. The materials used varies depending on the fluid stored and the industry [4]. Metals have been used almost exclusively in the oil industry and are most often short cantilever shells [4]. Silos and pressure vessels tend to be taller than storage tanks [4]. The oil tanks are constructed of curved steel sheets that are welded together to form a cylinder and are prone to fail by buckling due to their slenderness [4].



Figure 1: A slim tank [5].

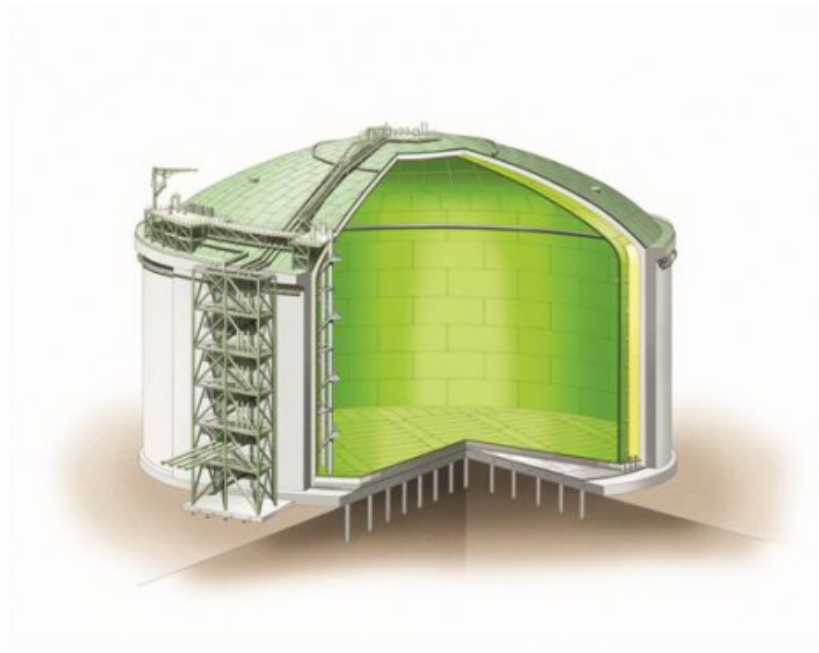


Figure 2: Cross section view of tank [6].

Figure 2 shows a cross-section of a tank with three layers. Tanks usually consists of a cylindrical steel shell of stepwise variable thickness [4] with insulation and some kind of weather protecting layer around the shell. Some tanks are designed with a uniform thickness of the shell but this is not as common as a variable thickness [4]. Tanks are also designed with a circular plate at the base and with a roof [4] which can be conically or spherically shaped where the spherically shaped roofs are better suited for tanks with higher internal pressure above the liquid level [8]. The tank in Figure 3 has poles inside the tank to support the roof while the tank in Figure 2 has a self-supporting roof with no poles inside the tank. It is thus clear that tanks are constructed for the task at hand and can have very different appearances, what they all have in common is that they're used for storing liquids. The liquid they're storing divides the tanks into three different consequence classes, where consequence class 1 is the lowest and least restrictive class and consequence class 3 is the highest and most restrictive class. The governing standard of tanks defines tanks within consequence class 3 as tanks storing toxic or potentially explosive liquids [8]. Consequence class 3 also includes large size tanks, with a volume larger than 50 m^3 [9], containing flammable or water-polluting liquids located in urban areas [8]. Consequence class 2 applies to tanks of medium size with flammable or water-polluting liquids in urban areas and consequence class



Figure 3: The inside of a large tank [7].

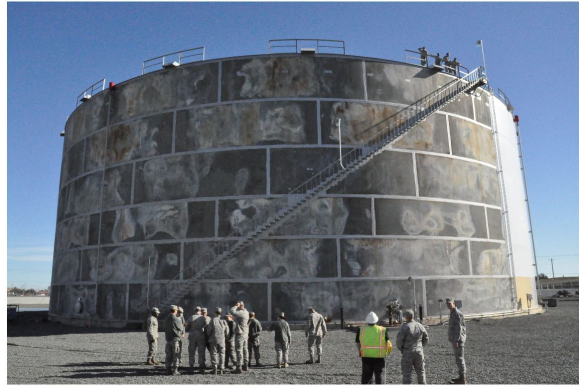


Figure 4: The outside of a large tank [7].

1 applies to agricultural tanks or tanks containing water [8].

Partial vacuum occurring due to operational problems during the discharge of the liquid contents is a common cause of buckling of tanks with uniform external pressure [4]. This type of collapse usually leads to the destruction of the tank [4] and can have catastrophic consequences. A failure analysis of a collapsed tank roof is an example of a failure due to partial vacuum, or under pressure, causing the roof to collapse [10]. The under pressure was caused by an increased discharging of water from the tank and the control system that should have prevented this to happen was not functioning properly [10]. During the failure analysis it was discovered that the tank had some faulty welds, some parts that was not designed correctly and was exposed to corrosion [10]. These factors contributed to the failure of the roof [10].

National Board of Housing, Building and Planning (Boverket) has taken over as one of the authorities that governs the rules controlling construction and inspection of tanks in Sweden after the Swedish Work Environment Authority (Arbetsmiljöverket). This authority change has resulted in that the Eurocodes, the European standards for structural design, now have to be followed. The Eurocodes refers to each other and are therefore more difficult to read than the previous regulations. Sweco Industry AB in Stockholm wants to sort out what this regulatory change means, what rules apply now? This thesis will also make a comparison between three calculation methods described by this new standard to determine which method that is preferred when designing tanks. The Eurocode for tanks suggests membrane theory with factors and simplified expressions for local bending for the lowest consequence class, tanks within consequence class 1 [8]. Membrane theory can be used for the second consequence class if elastic bending theory for local effects is used and as long as the load is axisymmetric, but a numerical analysis such as finite element method (FEM) is also suggested [8]. For the highest consequence class, consequence class 3, a validated analysis like FEM should be used [8]. Linear elastic shell analysis is a method slightly more complex than membrane theory and includes bending moments as well as the membrane stresses [11]. This method can thus be used for the first and second consequence class but is not suggested as much as membrane theory. Of the many research articles written about storage tanks [4, 10, 12] only one attend the topic of comparing calculation methods [12]. This article compares methods based on membrane theory with linear analysis as design methods for cylindrical liquid storage tanks to fulfill the American standard API 650 [12]. The article concludes that membrane theory should be used for tanks with a maximum diameter of 15 m in order to obtain the best solution based on the US standard [12]. For tanks larger than 15 m in diameter both membrane theory and linear analysis can be used [12].

The hypothesis for this project is that the stresses calculated with linear elastic shell analysis will be closer to the result of the finite element analysis conducted with Ansys than the result from membrane theory. The justification to this hypothesis is that the linear elastic shell analysis unlike membrane theory takes the bending moments into account and is thus not as restricted in its application areas.

1.2 Eurocodes

In this thesis project the Eurocodes, a family of standards, are used along with regulations from National Board of Housing, Building and Planning (Boverket) as the sources of information. The Eurocodes are an action program produced by the Commission of the European Community with the goals of eliminating the technical obstacles to trade and to harmonize the technical specifications [8]. When first produced the idea with the program was to eventually replace the national rules in the Member States. Today it is the European Committee for Standardization (CEN) that are preparing and publishing the Eurocodes [8]. The Eurocode programme consists of several standards, Eurocode 0-9 where Eurocode 3 describes design of steel structures, in which tanks are a part [8]. Other important Eurocodes are Eurocode 0 that describes the basis of structural design and Eurocode 1 that describes actions on structures. Eurocode 7 and 8 could also be of interest for tank

design as they describe geotechnical design and design of structures for earthquake resistance, respectively. All the Eurocode groups are listed in Table 1.

Table 1: The family of Eurocodes [13]

Designation	Eurocode	Title
EN 1990	0	Basis of Structural Design
EN 1991	1	Actions on Structures
EN 1992	2	Design of Concrete Structures
EN 1993	3	Design of Steel Structures
EN 1994	4	Design of Composite Steel and Concrete Structures
EN 1995	5	Design of Timber Structures
EN 1996	6	Design of Masonry Structures
EN 1997	7	Geotechnical design
EN 1998	8	Design of Structures for Earthquake Resistance
EN 1999	9	Design of Aluminium Structures

The Eurocodes are used to prove that buildings and plants fulfill the essential requirements of the Council Directive, especially the requirements for mechanical resistance and stability as well as safety in case of fire [8]. The Eurocodes are followed up by a national annex that in some cases changes some equations or variables in the Eurocodes. The national annex is published by the National Board of Housing, Building and Planning (Boverket) and the current governing Swedish annex is called EKS 10 [9].

The most essential Eurocodes for this application, tank shell design, are the Eurocodes in Table 2. These are the ones that will be referred to in this thesis. SS-EN 1990 describes the basis for structural design and will be used to formulate the forces as design forces with their partial and combination factors. It is the design forces that is used to load structures and are therefore relevant for all kinds of structural design, not just tanks or shells. SS-EN 1991-1-1 describes the classification of loads, what loads that are classified as self-weight and imposed loads. It also contains tables of densities for construction materials such as masonry, wood and steel and stored materials such as sand, water, oil and beer. This standard will be used for the density of steel and an arbitrarily chosen liquid.

Table 2: The relevant standards for tank shell design used in this work

Designation	Title	Alternative name
EN 1990	Basis of Structural Design	
EN 1991-1-1	Actions on structures - General actions - Densities, self-weight, imposed loads for buildings	
EN 1991-1-3	Actions on structures - General actions - Snow loads	Snow standard
EN 1991-1-4	Actions on structures - General actions - Wind actions	Wind standard
EN 1991-4	Actions on structures - Silos and tanks	
EN 1993-1-1	Design of steel structures - General rules and rules for buildings	
EN 1993-1-6	Design of steel structures - Strength and Stability of Shell Structures	Shell standard
EN 1993-4-2	Design of steel structures - Tanks	Tank standard
EKS10	Boverkets författningssamling BFS 2015:6, EKS 10	National annex

The snow and wind standards describes how to determine the snow and wind actions acting on structures. These standards are describing the snow and wind actions for different kind of structures and geometries and will in this thesis be used to describe the snow and wind actions on a tank. The standard for actions on silos and tanks has been used to determine the hydrostatic load and the standard for general rules of steel structures has been used to retrieve recommended material properties of the steel. The shell standard describes different calculation methods that can be used for shell design and the conditions that has to be met for the stresses in the shell. This standard will thus be used extensively in this project. The tank standard is obviously very relevant for this thesis but it does not contain much useful information. It most often refers to other parts of the Eurocodes. The tank standard does although describe the consequence classes specific for tanks and what methods that are allowed to use for the different consequence classes. Lastly the national annex of Sweden will be used when any of the Eurocodes makes it possible for each nation to change the Eurocodes and the Swedish national annex has chosen to change a constant, equation or a condition to suit the conditions in Sweden.

1.3 Purpose, goal and method

The purpose of the thesis is to clarify what rules govern tank shell design and to understand the differences between calculation methods for handbook calculations and FEM-calculation. The goals of this thesis project are to:

- Provide a calculation document for the shell of storage tanks according to the Eurocodes with stresses given by both membrane theory analysis and linear elastic shell analysis,
- Provide a comparison of the stresses given by membrane theory analysis, linear elastic shell analysis and a software using finite element method.

In order to accomplish the first goal, provide a calculation document for the shell of storage tanks according to Eurocodes the relevant Eurocodes will be read, i.e. the Eurocodes for tanks, shells and loads. The relevant information from these Eurocodes will be used to create a Mathcad-document for tank shell design where both membrane theory and linear elastic shell analysis will be used. In order to fulfill the second goal a tank shell with arbitrary dimensions will be analyzed in Ansys with the loads described in the Mathcad-document. The result of the analysis will then be compared with the result given by the calculation document for membrane theory and linear elastic shell analysis.

2 Theory

The shell of tanks should be designed after four limit states; plastic limit, cyclic plasticity, buckling and fatigue [11]. In this thesis work calculations will be made for the first and third limit states, plastic limit and buckling. These have been chosen since they are needed in all consequence classes. Cyclic plasticity and fatigue can be neglected for the lowest consequence class, the first consequence class [8]. Among the possible methods for analysis of the plastic limit described by the shell standard are membrane theory and linear elastic analysis [11]. These analysis methods are also among the possible analysis methods for buckling [11]. These two analysis methods can be used for direct design of plastic limit and buckling [11] and have therefore been chosen to be analyzed deeper. FEM is also a possible method to analyze both the plastic limit and buckling limit and can be used for all consequence classes.

2.1 Membrane theory

The description of the methods given by the Eurocodes are very short but concludes that membrane theory can be used as long as the geometry of the shell and the loads vary mildly without any discontinuity or locally concentrated loads [11]. The boundary conditions should be suitable for transfer of stresses in the shell into support reactions without causing significant bending effects if the membrane theory is to be used [11]. A mechanics handbook describes like the Eurocodes that membrane theory can be used if the load is applied without any discontinuities and if the boundary conditions are suitable [14]. A deviation from the membrane state is represented by bending state, which is always linked to membrane state in the general shell equations [14]. The mechanics handbook remarks that only normal forces, N_x and N_θ , are allowed to be transferred at the boundary if membrane state should reign [14], see Figure 5. The bending moments can be neglected if the flexural stiffness is very low or if the changes in the curvature and twist of the middle surface are very small [15]. The flexural stiffness depends on the stiffness of the material and the second moment of inertia [14], i.e. the geometry of the shell. A thinner shell and/or a lower stiffness material results in a lower flexural stiffness [14].

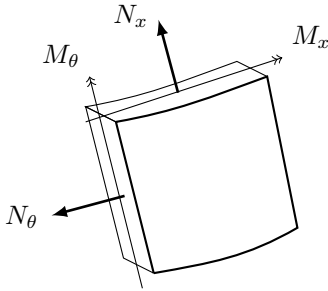


Figure 5: Membrane stresses, N_x and N_θ , and bending moments, M_x and M_θ , in a shell.

If the membrane theory is used for plastic limit design the two dimensional field of stress resultants $N_{x,Ed}$, $N_{\theta,Ed}$ and $N_{x\theta,Ed}$ are represented by an equivalent design stress $\sigma_{eq,Ed}$ given by Equation 1 [11]. t is the thickness of the wall.

$$\sigma_{eq,Ed} = \frac{1}{t} \cdot \sqrt{N_{x,Ed}^2 + N_{\theta,Ed}^2 - N_{x,Ed} \cdot N_{\theta,Ed} + 3N_{x\theta,Ed}^2} \quad (1)$$

2.2 Linear elastic shell analysis

The shell standard of the Eurocodes concludes that linear elastic shell analysis is based on the assumption of a linear elastic material and that the deformations are small [11]. If the linear elastic shell analysis is used for plastic limit design Equation 2 should be used to calculate the equivalent design stress [11]. The transverse stresses, $\tau_{xn,Ed}$ and $\tau_{\theta n,Ed}$, can in most cases be neglected [11] and a simplified equivalent design stress, Equation 4, can therefore be used. The negligible transverse shear stresses can be seen in Figure 6. The design stresses in meridional and circumferential direction should be calculated using Equation 3 [11].

$$\sigma_{eq,Ed} = \frac{1}{t} \cdot \sqrt{\sigma_{x,Ed}^2 + \sigma_{\theta,Ed}^2 - \sigma_{x,Ed} \cdot \sigma_{\theta,Ed} + 3 \left(\tau_{x\theta,Ed}^2 + \tau_{xn,Ed}^2 + \tau_{\theta n,Ed}^2 \right)} \quad (2)$$

$$\sigma_{x,Ed} = \frac{N_{x,Ed}}{t} \pm \frac{M_{x,Ed}}{t^2/4} \quad \sigma_{\theta,Ed} = \frac{N_{\theta,Ed}}{t} \pm \frac{M_{\theta,Ed}}{t^2/4} \quad \tau_{x\theta,Ed} = \frac{N_{x\theta,Ed}}{t} \pm \frac{M_{x\theta,Ed}}{t^2/4} \quad (3)$$



$$\sigma_{eq,Ed} = \sqrt{\sigma_{x,Ed}^2 + \sigma_{\theta,Ed}^2 + \sigma_{x,Ed} \cdot \sigma_{\theta,Ed} + 3\tau_{x\theta,Ed}^2} \quad (4)$$

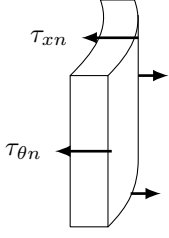


Figure 6: Transverse shear stresses in a shell.

2.3 Finite element analysis

Engineering simulation softwares such as Ansys enables a quick and easy way to solve complex structural engineering problems. Ansys uses tools for finite element analysis [16]. The finite element method (FEM) is a numerical technique for the approximate solution of partial differential equations [17]. The method were introduced as early as 1943 but was forgotten and not rediscovered until the early 1950's [17]. The development of the method came through the generalization of known calculation methods within the structural mechanics for constructions composed by simple beam elements [18]. The method is based on the sectioning of the model into finite elements [18], see Figure 7. Shell elements combine the properties of the 2D-solid elements that handle membrane or in-plane effects with plate elements that handle bending or off-plane effects [19]. The plate and shell elements are more tedious to solve than 2D-solid elements since they involve more degrees of freedom [19]. There are six degrees of freedom for a shell element; three translational displacements in x-, y-, z-direction and three rotational deformations with respect to x-, y-, z-axis [19]. In a 2D-solid element there are only two translational displacements corresponding to displacement in x- and y-direction and thus only two degrees of freedom [19]. But with computer software executing these tedious calculations even shell elements can be calculated fast. With FEM it is possible to solve complex problems, even non-linear problems, numerically and has been used extensively to simulate collisions between vehicles [18]. Conventional experimental testing has in many cases been replaced by computerized simulation and has thus decreased cost and time spent on testing [18].

The principle of FEM is to solve Equation 5 where Ω is an area in the plane with the edge Γ [18], see Figure 8. f is a given function and u is the sought after solution [18]. Equation 5 should be solved for the u that minimizes the total potential energy in Equation 6 over the volume V of functions with finite energy $a(v, v)$ that is zero on Γ [18]. The static structural analysis in Ansys uses FEM to determine the stresses in the model but does this under the assumption of steady loading and response [20].

$$-\Delta u = f \text{ in } \Omega \quad u = 0 \text{ at } \Gamma \quad (5)$$

$$F(u) = \frac{1}{2} a(u, u) - L(u) \text{ where} \quad a(v, w) = \int_{\Omega} \sum_{j=1}^3 \frac{\partial v}{\partial x_j} \frac{\partial w}{\partial x_j} dx \quad L(v) = \int_{\Omega} f v dx \quad (6)$$

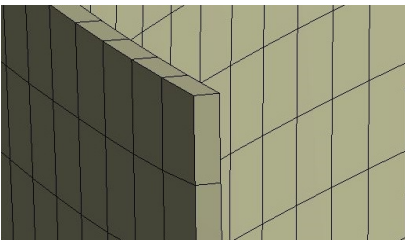


Figure 7: Sectioning of a model into finite elements.

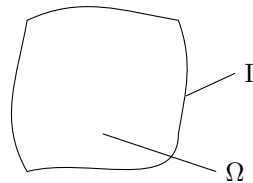


Figure 8: Principal element of finite element method.

3 Method

In this section of the thesis the procedure of creating a Mathcad-document for tank shell design and the calculation of the stresses with membrane theory and linear elastic shell analysis will be described. Since tanks consists of many parts when a closer study of them is made this thesis will only focus on the tank shell and leave the design of the roof or manhole etc for potential future thesis projects or projects within the company. The project is further limited by the standards it follows; the tank shell design will only be applicable to tanks that are vertical, cylindrical and axisymmetric tanks. The calculation document is also only applicable to tanks made of steel that are placed above ground and that serves as a container for storage of liquid products. Further delimitations have been set and they can be seen in the calculation document in Appendix B. These delimitations have been made in order to keep the Mathcad-sheet in the framework of the tank, wind and snow standard of the Eurocodes.

The calculation document is also limited to tanks with conical roofs but will not be limited in other dimensions. Arbitrary dimensions will although have to be set in order to determine the loads and retrieve numerical results from the calculations that can be compared. The dimensions of the tank used for the numerical calculations and comparisons can be seen in Figure 9 and 10. The thickness of the tank shell is stepwise variable and have been divided into six sections in this work. Note that Figure 10 is not made to scale. The thicknesses of the roof plate, the insulation and weather protection layer can be seen in Table 3. They have been arbitrarily set in order to obtain numerical results. The material properties used are stiffness, transverse contraction and yield strength which can be seen in Table 4. The stiffness and transverse contraction was set as the recommended values given by the standard for general rules of steel constructions [21], the yield strength was set at the value of one of the materials recommended by the same standard [21].

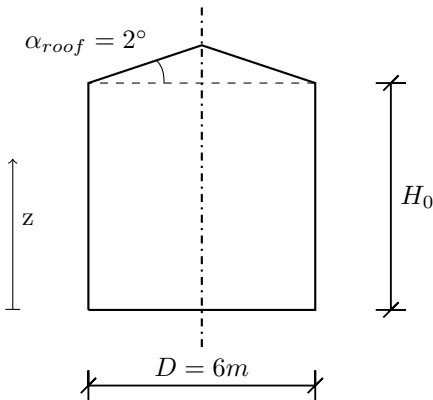


Figure 9: The numerical dimensions of the tank used.

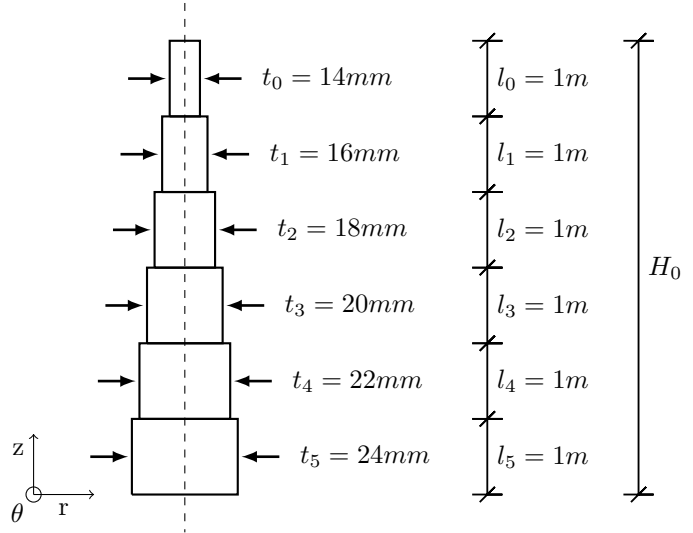


Figure 10: Numerical values of the stepwise variable shell thickness of the tank used.

Table 3: Thicknesses of roof, insulation and weather protection cover

Designation	Thickness [mm]	Description
t_{roof}	10	The thickness of the roof plate
$t_{ins,roof}$	140	The thickness of the insulation on the roof
$t_{ins,shell}$	140	The thickness of the insulation on the shell
$t_{cover,roof}$	3	The thickness of the cover on the roof
$t_{cover,shell}$	3	The thickness of the cover on the shell

Table 4: Material properties.

Designation	Value	Description
E	210 GPa	Stiffness, Young's modulus
ν	0.3	Transverse contraction, Poisson's ratio
f_y	235 MPa	Yield strength

The procedure of the FEM-analysis with Ansys has been conducted to give a comparable result to the result

of membrane theory and linear analysis. This procedure will be described more thoroughly in Section 3.6 after the limit conditions and stress calculations by hand have been described. The stress results calculated with the calculations by hand and by Ansys will be presented in the result section before they are compared with the limit conditions.

3.1 Actions

A description of the actions is needed for all analysis methods. There are many possible actions that can act on the tank shell, but only self-weight, internal pressure, hydrostatic pressure, wind load and snow load have been included in the calculation document. Other loads that can act on tanks are for example thermal loads, accidental loads and seismic loads.

3.1.1 Self-weight

The shell wall of the tank constitutes a self-weight but it also carries the weight of the roof. In addition the tank is covered by insulation and a layer of weather protection, which add to the weight of the whole construction. The self-weight of the roof was calculated by multiplying the volume of the roof plate with the density measured in force per volume, see Equation 7. The weight of the insulation on the roof and the weather protection cover was calculated in the same way and added to the total weight of the roof, see Equation 8, 9 and 10. The force $F_{weight,roof}$ was calculated adding the weights of the roof plates, insulation and weather protection per circumferential unit. The areas of the roof, insulation and cover can be seen in Appendix A and the densities can be seen in Table 5. The density of the steel was taken from Appendix A of SS-EN 1991-1-1 as the tank standard described that one should [8]. The density of the insulation was although not taken from SS-EN 1991-1-1 since the density of insulation materials were not present. The density of the insulation was assumed to be the value of Table 5 and the cover was assumed to be of the same steel that the shell of the tank. The design value of the self-weight of the roof adds a reduction factor, ξ_{weight} , and a partial factor for permanent loads, γ_G , to the load, see Equation 11 [13]. The reduction factor is a user defined constant which was set to 1 and the partial factor, which works as a safety factor, is 1.35 [9].

Table 5: The density of the steels and insulation

Designation	Value [kN/m^3]	Value [kg/m^3]	Description
γ_{shell}	77.75 [22]	7 930	The density of the shell plates
γ_{roof}	77.75 [22]	7 930	The density of the roof plates
γ_{ins}	1.3	133	The density of the insulation (assumed)
γ_{cover}	77.75	7 930	The density of the cover plates (assumed)

$$W_{roof} = \gamma_{roof} A_{roof} t_{roof} \quad (7)$$

$$W_{ins,roof} = \gamma_{ins} A_{ins,roof} t_{ins,roof} \quad (8)$$

$$W_{cover,roof} = \gamma_{cover} A_{cover,roof} t_{cover,roof} \quad (9)$$

$$F_{weight,roof} = \frac{1}{s_{roof}} (W_{roof} + W_{ins,roof} + W_{cover,roof}) = 3.68 \frac{kN}{m} \quad (10)$$

$$F_{weight,roof,Ed} = \gamma_G \cdot \xi_{weight} \cdot F_{weight,roof} = 4.97 \frac{kN}{m} \quad (11)$$

The weight of the shell was calculated through multiplying the density of the steel with the volume of the shell, see Equation 12. The volume of the shell was calculated with the average thickness t_{ave} which was determined to 19 mm. The weight of the insulation and cover around the shell was calculated in the same way, see Equation 13 and Equation 14. Since it is unknown how the insulation and cover are attached to the shell it was assumed that the weight of the insulation and the cover could be added to the weight of the steel in order

to simplify the problem, see Equation 15. The design value of the self-weight of the shell was calculated the same way as the roof, with the same reduction and partial factor.

$$W_{shell} = \gamma_{shell} H_0 \pi D \cdot t_{ave} \quad (12)$$

$$W_{ins,shell} = \gamma_{ins} H_0 \pi (D + t_{ave} + t_{ins,shell}) t_{ins,shell} \quad (13)$$

$$W_{cover,shell} = \gamma_{cover} H_0 \pi (D + t_{ave} + 2t_{ins,shell} + t_{cover}) t_{cover} \quad (14)$$

$$F_{weight,shell} = \frac{1}{\pi D} (W_{shell} + W_{ins,shell} + W_{cover,shell}) = 10.5 \frac{kN}{m} \quad (15)$$

$$F_{weight,shell,Ed} = \gamma_G \cdot \xi_{weight} \cdot F_{weight,shell} = 14.1 \frac{kN}{m} \quad (16)$$

3.1.2 Internal and hydrostatic pressure

The internal pressure was designed to be an input variable given by the user of the calculation document. The pressure should be given relative the atmospheric pressure and positive for overpressure, see Figure 11. The internal pressure was set on 0.001 bar, which is a small overpressure relative atmospheric pressure. The hydrostatic pressure was however calculated through Equation 17 which was given by the Eurocode for loads on silos and tanks [23]. The density of the was set to $10.0 \frac{kN}{m^3}$, or $1\ 020 \frac{kg}{m^3}$, which is the density of water [22]. The maximum design height of the hydrostatic pressure is at the top of the shell [8], the hydrostatic pressure has therefore been limited to only act on the shell, not the roof.

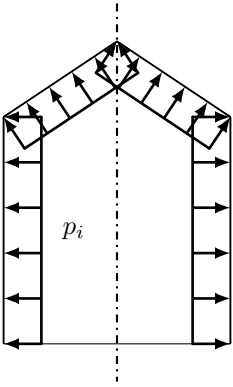


Figure 11: The internal pressure relative atmospheric pressure is equal all around and has a positive direction outwards.

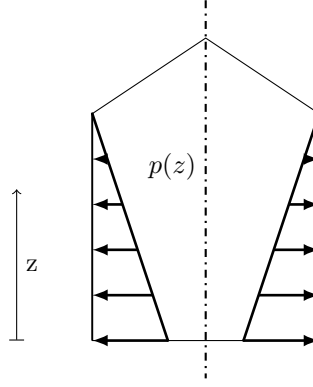


Figure 12: The hydrostatic pressure acting positively outwards. The pressure caused by the liquid increases further down the tank, with the highest pressure at the bottom.

$$p(z) = \gamma_{liquid} (H_0 - z) = 10.0 \frac{kN}{m^3} \cdot (6m - z) \quad (17)$$

The internal and hydrostatic pressure have in some figures been combined into $P(z)$, see Equation 18, in order to make the figures easier to interpret. In the calculations the pressures have although been separated. The pressures need to be separated in order to have different combination factors. The combination factors, ψ_{int} and ψ_{hyd} , are user defined constants that was set to 1 for both the internal and hydrostatic pressure, this in order to include both loads at their full value in the calculation of the stresses in the shell. The partial factor γ_F , which works as a safety factor, is 1.4 [9]. See the design value of the loads in Equation 19 and 20.

$$P(z) = p(z) + p_i \quad (18)$$

$$p_{i,Ed} = \gamma_F \cdot \psi_{int} \cdot p_i = 140 \text{ Pa} \quad (19)$$

$$p_{Ed}(z) = \gamma_F \cdot \psi_{hyd} \cdot \gamma_{liquid}(H_0 - z) = 14.0 \frac{kN}{m^3} (6 \text{ m} - z) \quad (20)$$

3.1.3 Wind load

The wind pressure acting on the external surfaces was calculated through Equation 21 given by the wind standard [24]. The external wind pressure consists of two constants, the first one is the peak velocity pressure, $q_p(z)$, given by the national annex. The peak velocity pressure was determined through several factors which are described by Appendix B but can be shortly described as factors determined for the terrain type and the basic wind velocity. The terrain type was chosen as a terrain with regular cover of vegetation or buildings, for example a forest or village. The basic wind velocity depends on the geographical location where the coastal areas generally have a higher basic wind velocity than further in the country [9]. The location was in this case set in the area of Stockholm. The height of which the external pressure should be calculated at, z_e , is the reference height given by the wind standard [24], see Equation 22. The other constant in Equation 21, c_{pe} , is the pressure coefficient for the external pressure given by the wind standard [24]. This constant is also described by Appendix B but can be shortly described as a factor determined for the Reynold's number and the geometry and slenderness of the tank. This constant varies with the angle around the tank as can be seen in Figure 13. It was although problematic to describe this wind load distribution with hand-calculations with no available guidance from the standard. The wind load was therefore calculated at the angle around the tank that would lead to the wind load adding to the other loads, in this case the hydrostatic load and internal overpressure. The angle of which the wind load was calculated was thus 75° which gave the largest outward wind load, see Figure 14. The design value of the wind load with this simplified distribution can be seen in Equation 23.

$$w_e = q_p(z_e) \cdot c_{pe} = -493 \text{ Pa} \quad (21)$$

$$z_e = 0.6 \cdot H_0 = 3.6 \text{ m} \quad (22)$$

$$w_{e,Ed} = \gamma_F \cdot \psi_{wind} \cdot q_p(z_e) \cdot c_{pe} = -690 \text{ Pa} \quad (23)$$

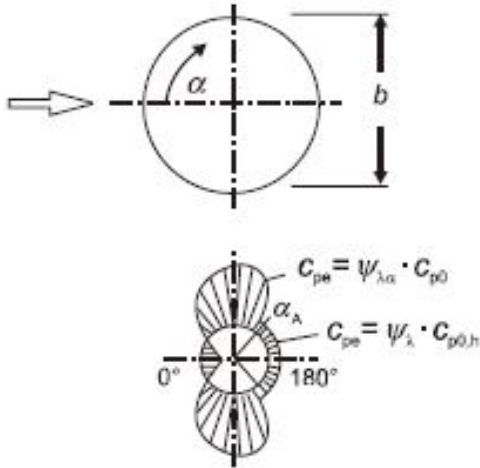


Figure 13: The wind distribution around a cylinder [24].

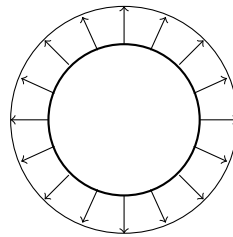


Figure 14: Wind distribution used was set to act outwards to add to the other loads, giving c_{pe} and w_e a negative value. The positive direction is inwards.

The external wind acting on the roof was calculated with Equation 24 where the peak velocity pressure was calculated at height $z_{e,roof}$, see Equation 25, given by the wind standard [24]. $c_{pe,roof}$ is the pressure coefficient determined by the height of the roof, the height of the shell and the diameter of the tank, see and Appendix B. The wind standard does not describe the pressure coefficient for conical roof, but it does for a dome. It was therefore assumed that the pressure coefficient for a conical roof could be approximated by the pressure coefficient of a dome.

$$w_{e,roof} = q_p(z_{e,roof}) \cdot c_{pe,roof} = -227 \text{ Pa} \quad (24)$$

$$z_{e,roof} = H_0 + h = 6.11 \text{ m} \quad (25)$$

$$w_{e,roof,Ed} = \gamma_F \cdot \psi_{wind} \cdot q_p(z_{e,roof}) \cdot c_{pe,roof} = -317 \text{ Pa} \quad (26)$$

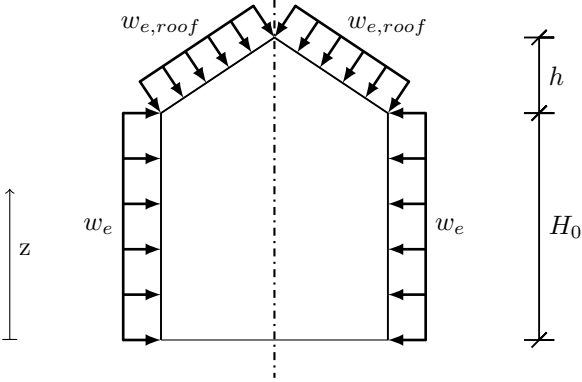


Figure 15: The wind load axisymmetrically distributed with positive values in inward direction.

3.1.4 Snow load

The snow load was given by the snow standard [25] as described by Equation 27. μ_i is the snow load shape coefficient given by the snow standard for the slope of the roof. C_e is the exposure coefficient determined for the topography; windswept, normal or sheltered, where the sheltered topography leads to a larger exposure coefficient [25]. A normal topography was chosen. C_t is the thermal coefficient given by a handbook on snow and wind load by the Swedish National Board of Housing, Building and Planning (Boverket) [26]. The thermal coefficient depends on heat transfer coefficient, temperatures in the surroundings and whether or not the roof has a snow guard, i.e. the probability of the snow staying on the roof. s_k is the characteristic value of snow load on the ground which was determined by the national annex for the geographical location of the tank [9]. The location was chosen as Stockholm and s_k . A closer description of the calculations can be seen in Appendix B. The snow load was then assumed to act vertically to the horizontal plane, at an angle for a roof with a slope, see Figure 16.

$$s_{snow} = \mu_i \cdot C_e \cdot C_t \cdot s_k = 749 \text{ Pa} \quad (27)$$

$$s_{snow,Ed} = \gamma_F \cdot \psi_{snow} \cdot \mu_i \cdot C_e \cdot C_t \cdot s_k = 1\,050 \text{ Pa} \quad (28)$$

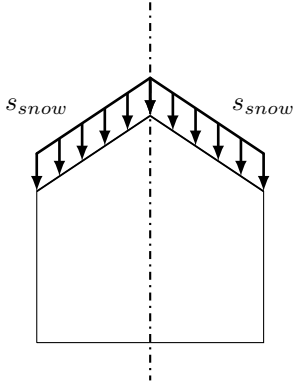


Figure 16: The snow load has been assumed to act vertically, at an angle of a sloped roof.

3.2 Limit states

There are four limit states; plastic limit (LS1), cyclic plasticity (LS2), buckling (LS3) and fatigue (LS4) [11]. All of these should be used when designing the shell of a tank of the higher consequence classes but for the lower one, consequence class 1, cyclic plasticity and fatigue can be neglected [11]. This thesis have been limited to the limit states needed for all consequence classes, plastic limit and buckling.

3.2.1 Plastic limit condition

The condition that has to be met for the plastic limit can be seen in Equation 29 where the equivalent design stress should be lower than the characteristic value of the yield strength divided by the partial factor for plastic limit γ_{M0} [11]. The characteristic value of the yield strength was assumed to be equal to the yield strength, which was set arbitrary to 235 MPa according to the material properties set in Table 4. The partial factor was given by the national annex and set to 1 [9].

$$\sigma_{eq,Ed} \leq \frac{f_{yk}}{\gamma_{M0}} = 235 \text{ MPa} \quad (29)$$

3.2.2 Buckling conditions

For buckling there are several conditions that has to be met. Since the tank has a stepwise variable shell thickness verifications have to be made for an equivalent cylinder as well as every section of the shell. The equivalent cylinder with an effective length and thickness can be seen in Figure 17. The equivalent thickness, t_a , was calculated to 15 mm, which equals the average thickness of the two top sections of the wall. The effective length, l_{eff} , was calculated to 3.636 m which is more than half the wall height of 6 m. The calculations can be seen in Appendix B. The verifications that has to be met for this equivalent cylinder can be seen in Equation 30 and 31, where the design stress, $\sigma_{Ed,eff}$, has to be lower than the design buckling stress, $\sigma_{Rd,eff}$ [11]. The design buckling stresses were determined for geometrical dimensions, yield strength, f_y , stiffness, E , and the partial factor for stability, γ_{M1} . The stiffness was set arbitrary to 210 GPa and the partial factor was given by the national annex as 1. The calculations of the design buckling stress can be seen in Appendix B.

$$\sigma_{\theta,Ed,eff} \leq \sigma_{\theta,Rd,eff} = 28.2 \text{ MPa} \quad (30)$$

$$\tau_{x\theta,Ed,eff} \leq \tau_{x\theta,Rd,eff} = 85.3 \text{ MPa} \quad (31)$$

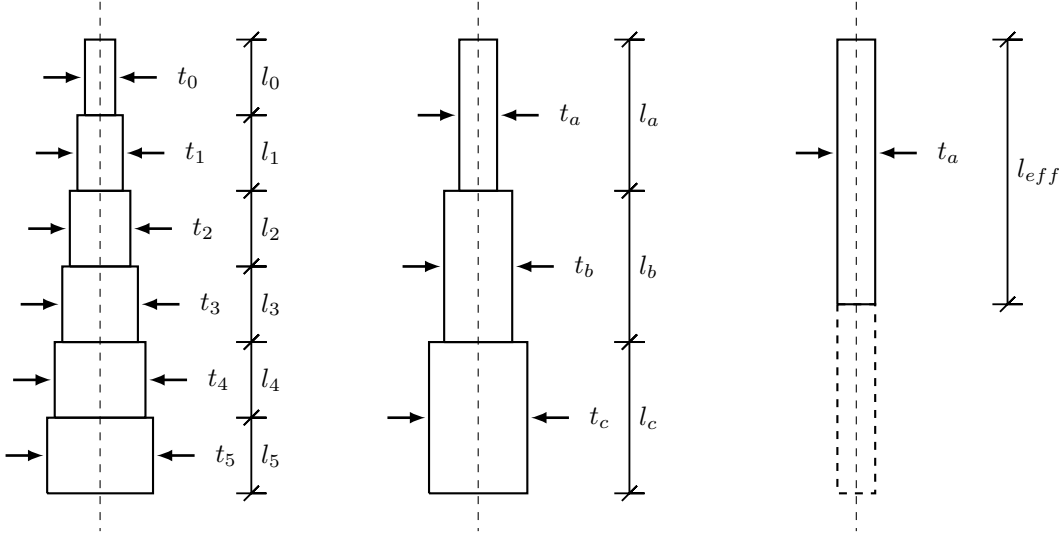


Figure 17: Transformation of stepwise variable thickness to equivalent uniform thickness. The transformation is done in two steps where the stepwise variable thickness, left, is transformed to an equivalent cylinder with three sections, middle, before transformed again to an equivalent cylinder with uniform wall thickness, right.

The verifications that have to be made for every section of the wall can be seen in Equation 32, 33 and 34. The design stresses cannot exceed the design buckling stress, σ_{x,Rd_j} or the critical buckling stresses, σ_{θ,Rcr_j} and $\tau_{x\theta,Rcr_j}$ [11]. The design buckling stresses were calculated for geometrical dimensions, the stiffness, yield strength as well as the partial factor for stability. The critical buckling stresses were calculated for geometrical dimensions and the stiffness, see Appendix B. The design stress in the circumferential direction, σ_{θ,Ed_j} , and the design shear stress, $\tau_{x\theta,Ed_j}$, in Equation 33 and 34 should be calculated with Equation 35 [11] and is thus not linked to the calculation methods compared in this document. These should be calculated for the largest circumferential membrane stress resultant and membrane shear stress resultant in the shell. The membrane stresses and membrane shear stress will be calculated in the next section, see Section 3.3.

$$\sigma_{x,Ed_j} \leq \sigma_{x,Rd_j} = \begin{bmatrix} 154 \\ 153 \\ 152 \\ 151 \\ 150 \\ 150 \end{bmatrix} MPa \quad < \quad (\quad) \quad (32)$$

$$\sigma_{\theta,Ed_j} \leq \sigma_{\theta,Rcr_j} = \begin{bmatrix} 60.3 \\ 52.8 \\ 46.9 \\ 42.2 \\ 38.4 \\ 35.2 \end{bmatrix} MPa \quad < \quad (\quad) \quad (33)$$

$$\tau_{x\theta,Ed_j} \leq \tau_{x\theta,Rcr_j} = \begin{bmatrix} 203 \\ 178 \\ 158 \\ 142 \\ 129 \\ 118 \end{bmatrix} MPa \quad (34)$$

$$\sigma_{\theta,Ed} = \frac{N_{\theta,max,Ed}}{t} \quad \tau_{x\theta,Ed} = \frac{N_{x\theta,max,Ed}}{t} \quad (35)$$

3.3 Free body diagrams and force equilibrium

The force equilibrium was used in order to determine the unknown forces acting on the shell wall and sectioning was used to determine the stresses in the wall. A free body diagram was created for the wall, displaying it in the xr -plane, see Figure 18. The equations for the case of axisymmetric condition in a cylinder shell get the same form as beams [14] and this was used to create the free body diagram in Figure 18. Observe that the bottom of the wall does not have a reaction moment. For an anchored tank the bottom should be free to move in an angular direction but not in radial or axial direction [11]. The base will thus not absorb moment. The internal and hydrostatic pressure as well as the wind load has already been determined but the reaction forces from the roof, $T_{roof,r}$ and $T_{roof,x}$, have not. In order to determine $T_{roof,r}$ a moment equilibrium was established around point A at the bottom of the shell wall, see Figure 18 and Equation 36. The equation for $T_{roof,r}$ can be seen in Equation 37 and the design value of it can be seen in Equation 38.

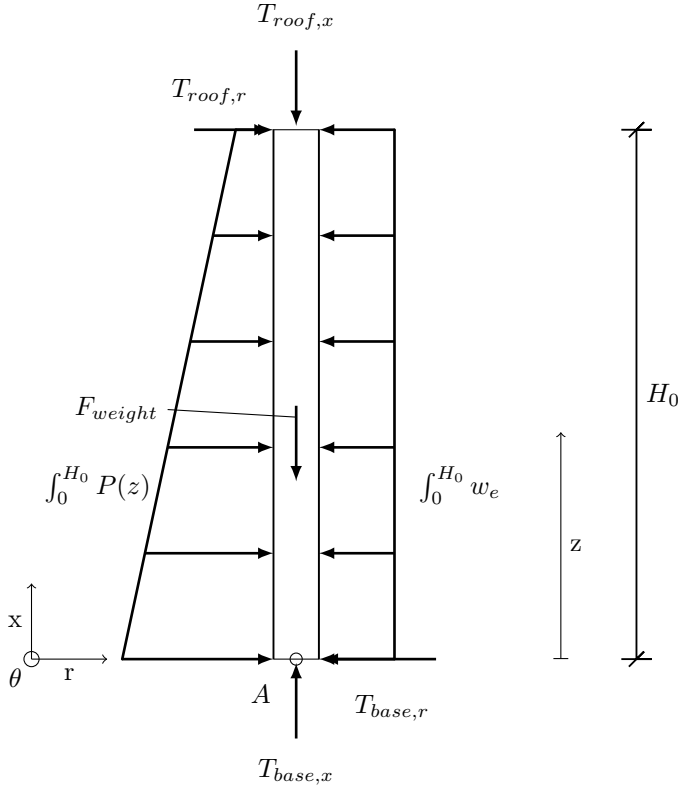


Figure 18: Actions on shell wall, seen in the xr -plane. The left side, with the combined internal and hydrostatic pressure $P(z)$, is the inside of the tank and the right side, with the wind load w_e , is the outside of the tank. $T_{roof,x}$ is the load from the roof in the direction of the generatrix and $T_{roof,r}$ is the load from the roof in the radial direction. F_{weight} is the self weight of the shell and $T_{base,x}$ and $T_{base,r}$ are reaction forces from the base.

$$\widehat{A} : \int_0^{H_0} p(z) dz \cdot \frac{1}{3} H_0 + \int_0^{H_0} p_i dz \cdot \frac{1}{2} H_0 + T_{roof,r} \cdot H_0 - \int_0^{H_0} w_e dz \cdot \frac{1}{2} H_0 = 0 \quad (36)$$

$$T_{roof,r} = \int_0^{H_0} w_e dz \cdot \frac{1}{2} - \int_0^{H_0} p(z) dz \cdot \frac{1}{3} - \int_0^{H_0} p_i dz \cdot \frac{1}{2} = -59.2 \frac{kN}{m} \quad (37)$$

$$T_{roof,r,Ed} = \gamma_F \psi_{wind} \int_0^{H_0} w_e dz \cdot \frac{1}{2} - \gamma_F \psi_{hyd} \int_0^{H_0} p(z) dz \cdot \frac{1}{3} - \gamma_F \psi_{int} \int_0^{H_0} p_i dz \cdot \frac{1}{2} = -82.9 \frac{kN}{m} \quad (38)$$

The vertical force from the roof, $T_{roof,x}$, was determined by creating a free body diagram of the roof, see Figure 19. The loads in the radial direction cancels each other out so a force equilibrium was only written for vertical loads, see Equation 39. The force equilibrium was used to create an expression for the last unknown force $T_{roof,x}$ and its design value, see Equation 40 and 41. The line surface of which the wind and snow loads as well as the internal pressure are applied to, s_{roof} , was calculated through the known diameter and height of the roof, see Equation 42.

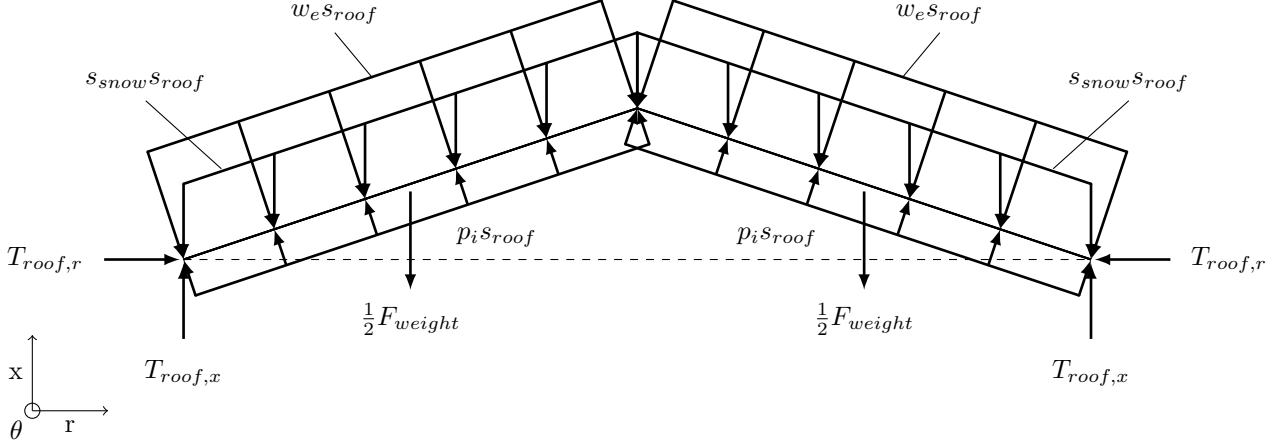


Figure 19: Actions on the roof. Wind and snow load as well as the self weight from both the roof as well as the insulation and cover have been taken into account. $T_{x,roof}$ and $T_{r,roof}$ are counter forces from the tank shell that carries the loads of the roof. s_{roof} is the line of the roof of which the lineloads are applied.

$$\uparrow: -2w_e s_{roof} \cos(\alpha_{roof}) - 2s_{snow} s_{roof} + 2p_i s_{roof} \cos(\alpha_{roof}) - 2\frac{1}{2}F_{weight,roof} + 2T_{roof,x} = 0 \quad (39)$$

$$T_{roof,x} = w_e s_{roof} \cos(\alpha_{roof}) + s_{snow} s_{roof} - p_i s_{roof} \cos(\alpha_{roof}) + \frac{1}{2}F_{weight,roof} = 3.11 \frac{kN}{m} \quad (40)$$

$$T_{roof,x,Ed} = w_{e,Ed} s_{roof} \cos(\alpha_{roof}) + s_{snow,Ed} s_{roof} - p_{i,Ed} s_{roof} \cos(\alpha_{roof}) + \frac{1}{2}F_{weight,roof,Ed} = 4.26 \frac{kN}{m} \quad (41)$$

$$s_{roof} = \sqrt{\left(\frac{D}{2}\right)^2 + h^2} \quad (42)$$

In order to determine the stresses in the shell the wall was sectioned at height z , see Figure 20. The force and moment of interest, N_x and M_x , were determined by force equilibrium and moment equilibrium around the point A, see Equation 43 and 45. The stress resultant N_x and bending moment M_x has been written as dependent of the height z since the weight depends on this height and the lever of the moment decreases just like the hydrostatic load with height, see Figure 21 and 22 as well as Equation 44 and 46. As Figure 21 displays the absolute value of the meridional stress resultant decreases with height above ground. The maximum value is thus at the very bottom of the tank. The meridional bending moment is although not highest at the bottom but at 2.545 m above ground as can be seen in Figure 22. The index Ed indicates that the stress resultant and bending moment are the design values including the combination and partial factors.

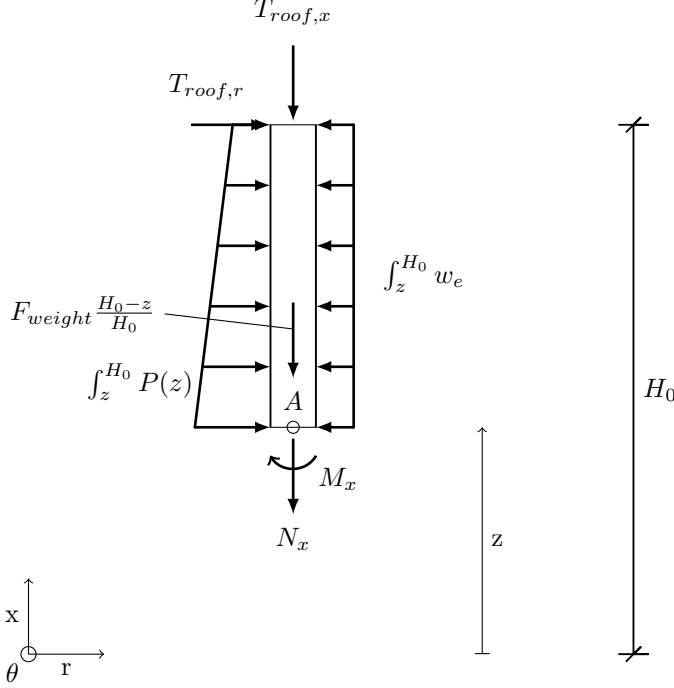


Figure 20: Sectioning of the shell, seen in the xr -plane. The normal force N_x and the moment M_x at the surface of the cut at height z .

$$\uparrow: -N_x - T_{roof,x} - F_{weight,shell} \frac{H_0 - z}{H_0} = 0 \quad (43)$$

$$N_{x,Ed}(z) = -T_{roof,x,Ed} - F_{weight,shell,Ed} \frac{H_0 - z}{H_0} \quad (44)$$

$$\tilde{A}: M_x + \int_z^{H_0} p(z) dz \frac{1}{3} (H_0 - z) + \int_z^{H_0} p_i \frac{1}{2} (H_0 - z) + T_{roof,r} (H_0 - z) - \int_z^{H_0} w_e \frac{1}{2} (H_0 - z) = 0 \quad (45)$$

$$M_{x,Ed}(z) = \int_z^{H_0} w_{e,Ed} \frac{1}{2} (H_0 - z) - \int_z^{H_0} p_{Ed}(z) dz \frac{1}{3} (H_0 - z) - \int_z^{H_0} p_{i,Ed} \frac{1}{2} (H_0 - z) - T_{roof,r,Ed} (H_0 - z) \quad (46)$$

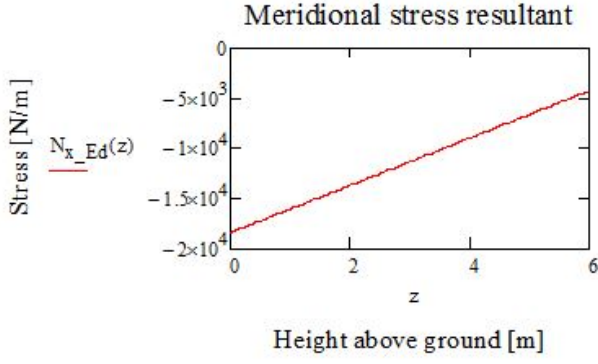


Figure 21: Meridional stress resultant as a function of height above ground.

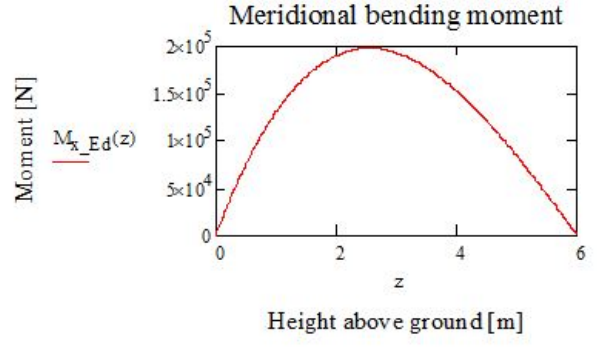


Figure 22: Meridional bending moment as a function of height above ground.

N_θ was taken forth by sectioning the shell in the $x\theta$ -plane, see Figure 23. The load acting on the shell due to wind has been assumed to act on an area as wide as the outer diameter, i.e. the width of the shell with insulation and cover, but absorbed only by the shell. The outer diameter can be seen in Equation 49. This wind force was then used when an equation for force equilibrium was written to determine N_θ , see Equation 47 and 48. The moment, M_θ was determined through multiplying Poisson's ratio with M_x , see Equation 50. This description of M_θ is based on the assumption that the material obeys Hooke's generalized law [14]. The circumferential membrane stress resultant is the highest at the bottom of the tank and decreases with height above ground as can be seen in Figure 24. The bending moment increases with height until it reaches $z = 2.545 \text{ m}$ where it reaches its maximum value and then decreases to zero at the top of the tank, see Figure 25.

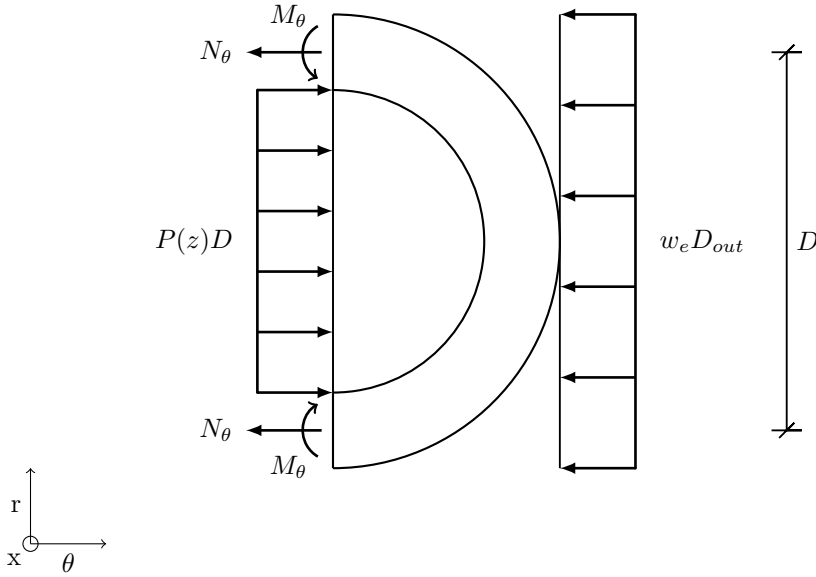


Figure 23: Sectioning of the shell, seen in $r\theta$ -plane. The normal force N_θ and the moment M_θ at the surface of the cut. The structure is thin walled, but the walls have been thickened in this figure in order to see the surface of the cut.

$$\rightarrow: p(z)D + p_i D - 2N_\theta - w_e D_{out} = 0 \quad (47)$$

$$N_{\theta,Ed}(z) = \frac{1}{2}((p_{Ed}(z) + p_{i,Ed})D - w_{e,Ed}D_{out}) \quad (48)$$

$$D_{out} = D + t_{shell} + 2t_{ins} + t_{cover} \quad (49)$$

$$M_{\theta,Ed}(z) = \nu M_{x,Ed}(z) \quad (50)$$

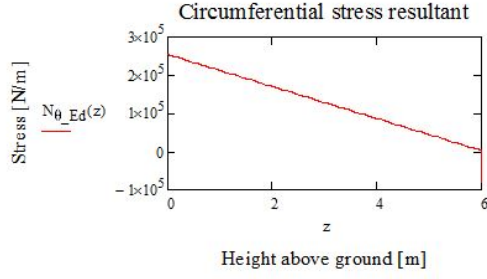


Figure 24: Circumferential stress resultant as a function of height above ground.

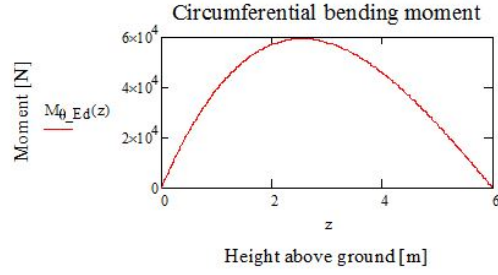


Figure 25: Circumferential bending moment as a function of height above ground.

3.4 Stresses calculated by membrane theory

The absolute value of the membrane stress resultants increases further down the wall of the tank, see Figure 21 and 24. The membrane stresses at the bottom of each section were therefore retrieved in order to obtain the highest equivalent design stress for every section. The value of the membrane stresses at each section can be seen in Equation 51 where section 0, the top section, is the top value in Equation 51 and the bottom value is the membrane stress at the very bottom. These membrane stresses were then be used to calculate the equivalent stress in Equation 52 for every section with the sections' thickness given in Table 3. The membrane shear stress resultant, $N_{x\theta}$, was set to zero since there's no torsion of the cylinder. The design stresses, $\sigma_{\theta,Ed,eff}$ and $\tau_{x\theta,Ed,eff}$, were calculated as described by Equation 54.

$$N_{x,Ed} = \begin{bmatrix} -6.61 \\ -8.97 \\ -11.3 \\ -13.7 \\ -16.0 \\ -18.4 \end{bmatrix} \frac{kN}{m} \quad N_{\theta,Ed} = \begin{bmatrix} 44.6 \\ 86.6 \\ 129 \\ 171 \\ 213 \\ 255 \end{bmatrix} \frac{kN}{m} \quad N_{x\theta,Ed} = 0 \frac{kN}{m} \quad (51)$$

$$\sigma_{eq,Ed} = \frac{1}{t} \cdot \sqrt{N_{x,Ed}^2 + N_{\theta,Ed}^2 - N_{x,Ed} \cdot N_{\theta,Ed} + 3N_{x\theta,Ed}^2} \quad (52)$$

$$\sigma_{x,Ed} = \frac{N_{x,Ed}}{t} \quad (53)$$

$$\sigma_{\theta,Ed,eff} = \frac{N_{\theta,Ed}}{t_a} \quad \tau_{x\theta,Ed,eff} = \frac{N_{x\theta,Ed}}{t_a} \quad (54)$$

3.5 Stresses calculated by linear analysis

The equations of the moments $M_{x,Ed}$ and $M_{\theta,Ed}$ calculated in Equation 46 and 50 resulted in the largest moments of each section as described by Equation 55. The largest moment was retrieved at the bottom of the three uppermost section, at approximately the middle of the section 3 (at $z = 2.545 \text{ m}$) and at the top of the two bottommost sections, see the diagrams of the moments in Figure 22 and 25. There is no torsion acting on the cylinder so the twisting shear moment is thus zero. The membrane stress resultants, $N_{x,Ed}$ and $N_{\theta,Ed}$ had to be retrieved at the same heights as the bending moments and the values of these can be seen in Equation 56. The stress, $\sigma_{x,Ed}$ was calculated through subtracting the moment from the membrane stress resultant. This gave a larger stress than if the moment would be added to the membrane stress resultant. The stress $\sigma_{\theta,Ed}$ was calculated by subtracting the moment to the membrane stress resultant for the use in the equivalent stress Equation 58 to avoid irrational numbers and to obtain the largest possible equivalent stress. For $\sigma_{\theta,Ed,eff}$ the moment was added to the membrane stress resultant in order to obtain the largest stress possible, see Equation 59. For $\tau_{x\theta,Ed}$ and $\tau_{x\theta,Ed,eff}$ the choice between adding or subtracting did not matter

since the moment is zero due to that no twisting act on the tank shell.

$$M_{x,Ed} = \begin{bmatrix} 83.7 \\ 153 \\ 193 \\ 198 \\ 190 \\ 130 \end{bmatrix} m \frac{kN}{m} \quad M_{\theta,Ed} = \begin{bmatrix} 25.1 \\ 45.8 \\ 57.8 \\ 59.3 \\ 57.0 \\ 39.1 \end{bmatrix} m \frac{kN}{m} \quad M_{x\theta,Ed} = 0 m \frac{kN}{m} \quad (55)$$

$$N_{x,Ed} = \begin{bmatrix} -6.61 \\ -8.97 \\ -11.3 \\ -12.4 \\ -13.7 \\ -16.0 \end{bmatrix} \frac{kN}{m} \quad N_{\theta,Ed} = \begin{bmatrix} 44.6 \\ 86.6 \\ 129 \\ 148 \\ 171 \\ 213 \end{bmatrix} \frac{kN}{m} \quad (56)$$

$$\sigma_{x,Ed} = \frac{N_{x,Ed}}{t} (\pm) \frac{M_{x,Ed}}{t^2/4} \quad \sigma_{\theta,Ed} = \frac{N_{\theta,Ed}}{t} (\pm) \frac{M_{\theta,Ed}}{t^2/4} \quad \tau_{x\theta,Ed} = \frac{N_{x\theta,Ed}}{t} \pm \frac{M_{x\theta,Ed}}{t^2/4} \quad (57)$$

$$\sigma_{eq,Ed} = \sqrt{\sigma_{x,Ed}^2 + \sigma_{\theta,Ed}^2 + \sigma_{x,Ed} \cdot \sigma_{\theta,Ed} + 3\tau_{x,\theta,Ed}^2} \quad (58)$$

$$\sigma_{\theta,Ed,eff} = \frac{N_{\theta,Ed}}{t_a} (\pm) \frac{M_{\theta,Ed}}{t_a^2/4} \quad \tau_{x\theta,Ed,eff} = \frac{N_{x\theta,Ed}}{t_a} \pm \frac{M_{x\theta,Ed}}{t_a^2/4} \quad (59)$$

3.6 Simulation with finite element method (FEM)

The tank shell was modeled as a solid with the arbitrary dimensions in Figure 9 and 10. The solid model can be seen in Figure 26 where the stepwise variable thickness was modeled with the midsurfaces of the sections alined, see Figure 27. The solid was then converted into a shell model using the midsurfaces of the sections, see Figure 28. Every section of the tank has a thickness but they are not visible in the shell model. Since the model was converted into a shell it was easy to adjust the shell's thickness which had to be done in order to obtain the effective stresses corresponding to the ones in Equation 54 and 59. When the tank was modeled it was given the material properties in Table 4 and the density was set to $12\,620 \frac{kg}{m^3}$. Note that the density set in Ansys is far higher than the density of the steel plate. The density set in Ansys was calculated through adding the weight of the insulation and weather protection cover to the density of the shell. The gravitational acceleration used was the one preselected by Mathcad, $g = 9.807 \frac{m}{s^2}$. This acceleration constant has been used for all calculations including the gravitational acceleration. The density was also multiplied with the partial and reduction factor in order to obtain the design value of the density, see Equation 60.

$$\rho_{Ed} = \gamma_G \cdot \xi_{weight} \frac{1}{g} \left(\frac{W_{shell} + W_{ins,shell} + W_{cover,shell}}{V_{shell}} \right) = 12\,620 \frac{kg}{m^3} \quad (60)$$

With the sections of the tank modeled and given material properties the tank had to be given boundary conditions. The boundary conditions that had to be set were;

- Contact conditions for the sections,
- Symmetry conditions since only half the shell was modeled,
- Boundary conditions at the top and bottom for the contact with the roof and the ground.

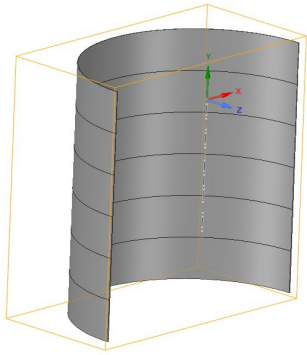


Figure 26: The solid model of the tank with stepwise variable shell thickness.

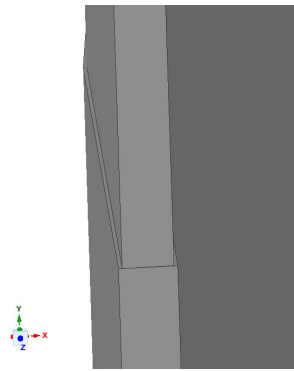


Figure 27: Close-up on solid model. The sections are placed on top of each other with the midsurfaces aligned.

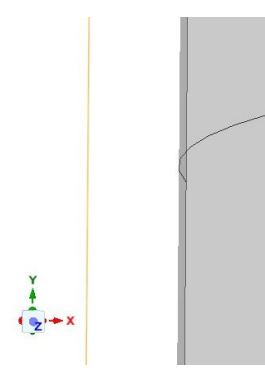


Figure 28: Close-up on shell model where the midsurfaces are aligned. Every section has a thickness but they are not visible in the shell model.

The sections were bonded together using the bonded contact condition at the edges, see Figure 29. This contact resembles a weld. Since only half of the tank was modeled the symmetry conditions were described as a displacement condition with zero displacement in the circumferential direction, see Figure 30, and a rotation condition. Fixed rotation was set at the circumferential edges, see Figure 31. The boundary conditions given by the Eurocodes for anchored tanks with roofs were set to the model, i.e. zero displacement in radial direction at the top and zero displacement in radial and axial direction and the bottom [11], see Figure 32 and 33. Rotation should be allowed at both the top and the bottom according to the Eurocodes [11]. When all the boundary conditions were set a fine mesh was created with an element size of 50 mm and mostly rectangular elements, see Figure 34. A closer view of the mesh can be seen in Figure 35.

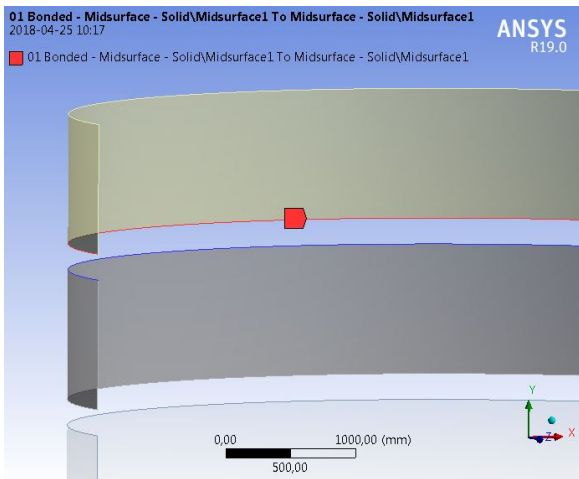


Figure 29: Bonded edge contact between sections. The figure shows the contact setting between the two topmost sections.

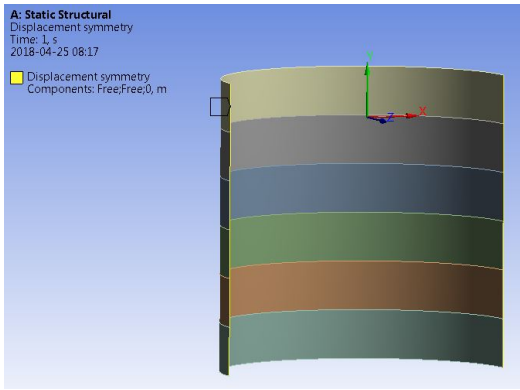


Figure 30: Symmetry condition limiting displacement in circumferential direction, the models z-axis, at the circumferential edges.

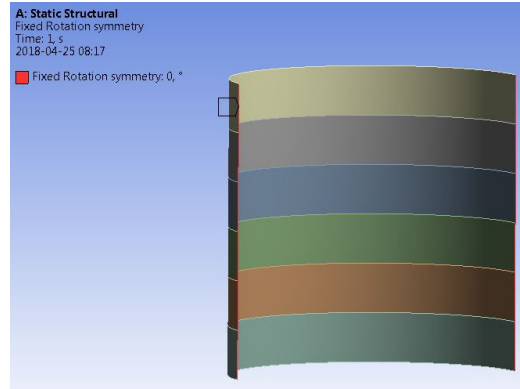


Figure 31: Symmetry condition limiting rotation at the circumferential edges.

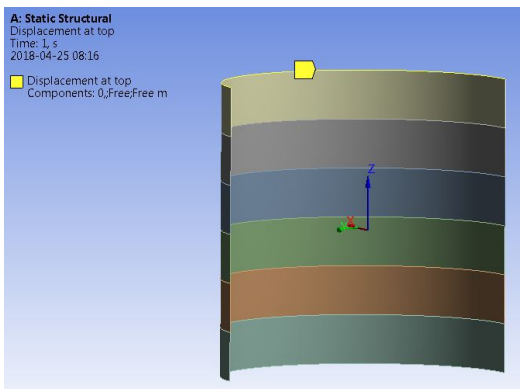


Figure 32: Boundary condition at the top was set as zero displacement in radial direction.

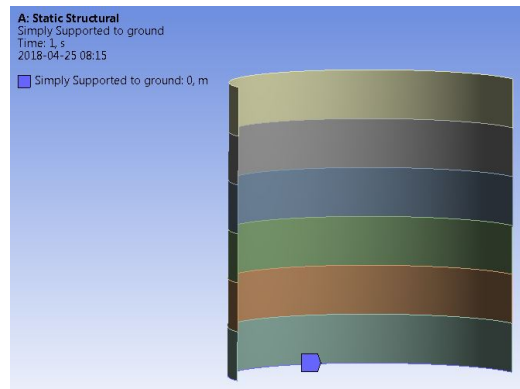


Figure 33: Boundary condition at the bottom was set as zero displacement in radial and axial direction.

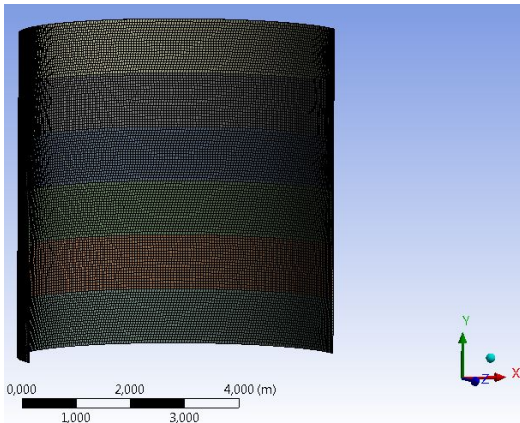


Figure 34: The mesh with an element size of 50 mm.

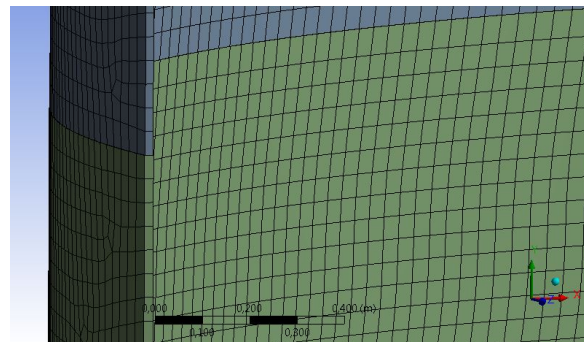


Figure 35: Close-up on the mesh with an element size of 50 mm and mostly rectangular elements.

The loads were set as line loads and pressures, except the self-weight of the shell which was added simply by defining the acceleration constant $g = 9.807 \frac{m}{s^2}$ since the density of the shell already had been specified. The self-weight can be seen in Figure 36. The load from the roof was added as a line load and represents the resulting load of self-weight of the roof, the internal pressure, wind action and snow load acting on the roof. The load from the roof was set at the top edge, in the negative axial direction, at a magnitude of $4\,262 \frac{N}{m}$, see Figure 37. The hydrostatic load was set as a hydrostatic pressure with the design density of the liquid, see Equation 61,

and the gravitational acceleration used for the self-weight.

$$\rho_{liquid,Ed} = \gamma_F \cdot \psi_{hyd} \cdot \frac{\gamma_{liquid}}{g} = 1428 \frac{kg}{m^3} \quad (61)$$

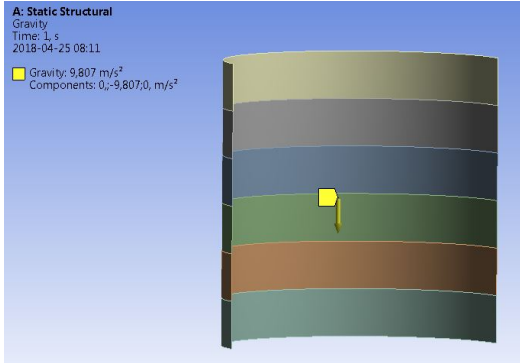


Figure 36: Self-weight of the shell including the weight of the insulation and weather protection cover.

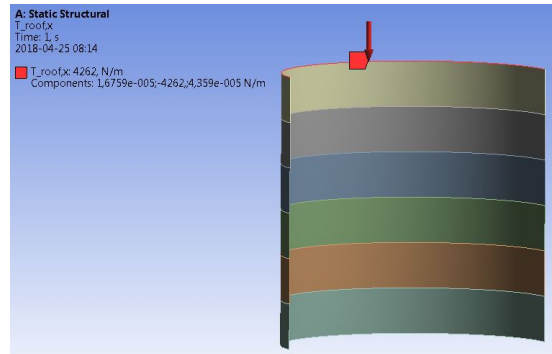


Figure 37: Load from roof in the axial direction combined self-weight of the roof with internal pressure, wind action and snow load acting on the roof.

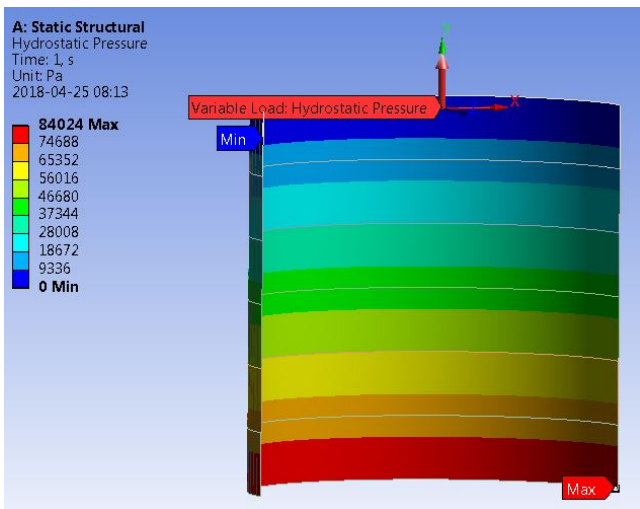


Figure 38: Hydrostatic pressure acting outwards on the shell. The hydrostatic load decreases with height, being zero at the top of the shell.

The internal pressure was added as a pressure in the radial direction with magnitude of $140 Pa$, which equals the design value of the internal pressure determined by Equation 19. The wind action was set as a pressure acting on the shell in the radial direction with a magnitude of $690 Pa$ determined by Equation 23 as the design value of the external wind action. A static structural analysis was then run in order to obtain the von Mises equivalent stress and the stresses were plotted along a meridional path, see Figure 41 in order to see how the stresses vary with height. The path starts at the top of the shell and will thus create graphs plotting stresses as a function of the distance from the top.

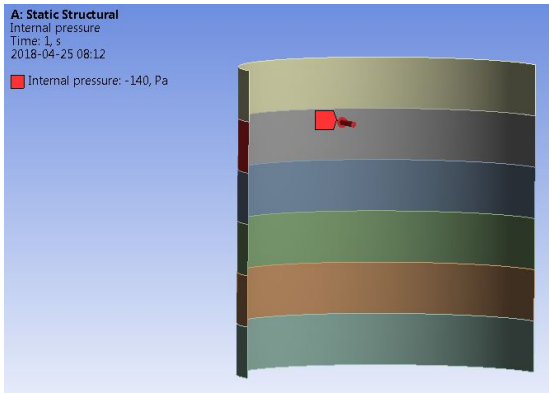


Figure 39: Internal pressure set to the inside of the tank shell as an overpressure relative atmospheric pressure.

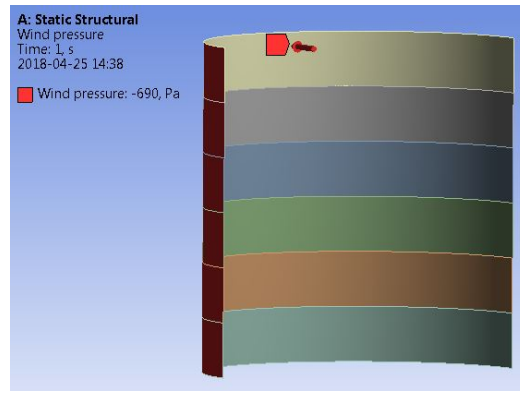


Figure 40: Wind action as a pressure acting on the shell outwards.

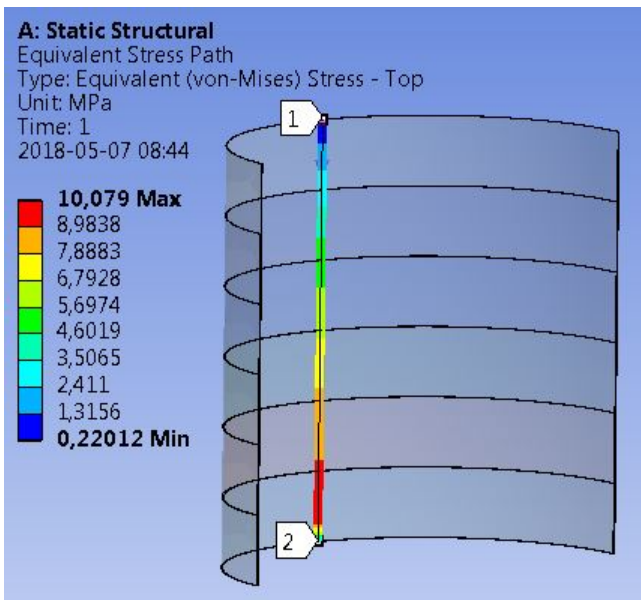


Figure 41: Meridional path used to plot stresses against the distance from the top of the shell.

4 Results

This chapter has been divided into three sections, the first for the result of the calculations by hand with membrane theory and linear analysis, the second for the result of the FEM-calculations in Ansys and the third section for a summary of the results and comparison of the calculation methods.

4.1 Membrane theory and linear analysis

The equivalent stress used to check the plastic limit conditions, calculated with membrane theory using Equation 52, resulted in the stresses seen in Equation 62 where the first number, 3.45 MPa , is the stress at the bottom part of the top section. The second value, 5.71 MPa , is the stress at the bottom of the second top section etc. This equivalent stress is thus the largest stress for membrane theory since the membrane stress resultants are largest at the bottom of each section. The equivalent stress for linear elastic analysis was calculated with Equation 58 at the height where the moment was largest in each section in order to obtain the largest value of the equivalent stress, see Equation 63. The stresses were largest at the bottom of the three topmost sections, in approximately the middle of the lower middle section and at the top of the two bottommost sections.

$$\sigma_{eq,Ed,MT} = \begin{bmatrix} 3.45 \\ 5.71 \\ 7.45 \\ 8.89 \\ 10.0 \\ 11.0 \end{bmatrix} \text{ MPa} \quad (62)$$

$$\sigma_{eq,Ed,LA} = \begin{bmatrix} 1520 \\ 2120 \\ 2120 \\ 1760 \\ 1400 \\ 808 \end{bmatrix} \text{ MPa} \quad (63)$$

The values of the design stresses in axial and circumferential direction used for validation against the buckling conditions can be seen in Equation 64 for membrane theory and in Equation 65 for linear analysis. The stresses calculated with membrane theory decreased with height above ground, having the maximum at the bottom of the tank, while the stresses calculated with linear analysis show highest stresses at the middle of the tank. The stresses were therefore retrieved at the different heights for membrane theory and linear analysis as described earlier. The design stresses for the effective cylinder could be plotted against the height above ground and can be seen in Figure 42 and 43 for membrane theory and in Figure 44 and 45 for linear analysis. These figures shows the same things as Equation 64 and 65, that the stress varies linearly for membrane theory with maximum stress at the bottom and with a maximum at about half the tank for linear analysis. The shear stress, shown in Figure 43 and 45, is zero for both membrane theory and linear analysis since there is no torsion acting on the tank.

$$\sigma_{x,Ed,MT} = \begin{bmatrix} -0.472 \\ -0.560 \\ -0.629 \\ -0.683 \\ -0.728 \\ -0.765 \end{bmatrix} \text{ MPa} \quad \sigma_{\theta,Ed,eff,MT} = \begin{bmatrix} 2.97 \\ 5.77 \\ 8.57 \\ 11.37 \\ 14.17 \\ 16.97 \end{bmatrix} \text{ MPa} \quad \tau_{x\theta,Ed,eff,MT} = \begin{bmatrix} 0 \\ 0 \\ 0 \\ 0 \\ 0 \\ 0 \end{bmatrix} \text{ MPa} \quad (64)$$

$$\sigma_{x,Ed,LA} = \begin{bmatrix} -1710 \\ -2390 \\ -2380 \\ -1980 \\ -1570 \\ -906 \end{bmatrix} \text{ MPa} \quad \sigma_{\theta,Ed,eff,LA} = \begin{bmatrix} 450 \\ 820 \\ 1040 \\ 1020 \\ 707 \\ 14.2 \end{bmatrix} \text{ MPa} \quad \tau_{x\theta,Ed,eff,LA} = \begin{bmatrix} 0 \\ 0 \\ 0 \\ 0 \\ 0 \\ 0 \end{bmatrix} \text{ MPa} \quad (65)$$

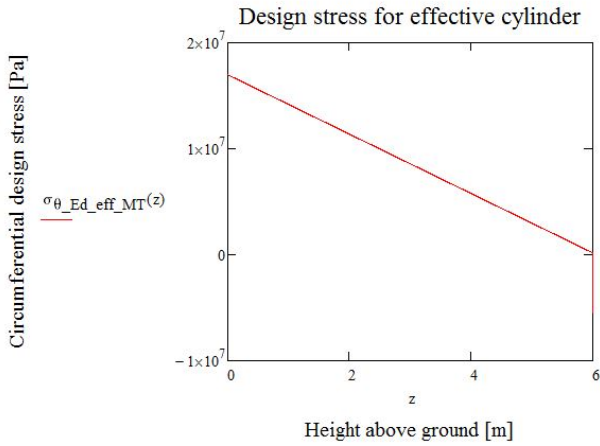


Figure 42: Diagram of the circumferential design stress for the effective cylinder as a function of height above ground calculated with membrane theory.

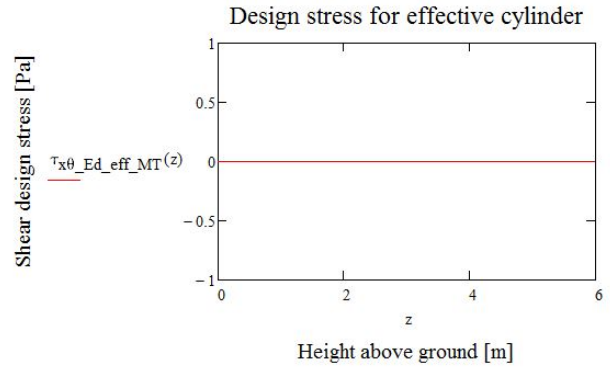


Figure 43: Diagram of the shear design stress for the effective cylinder as a function of height above ground calculated with membrane theory.

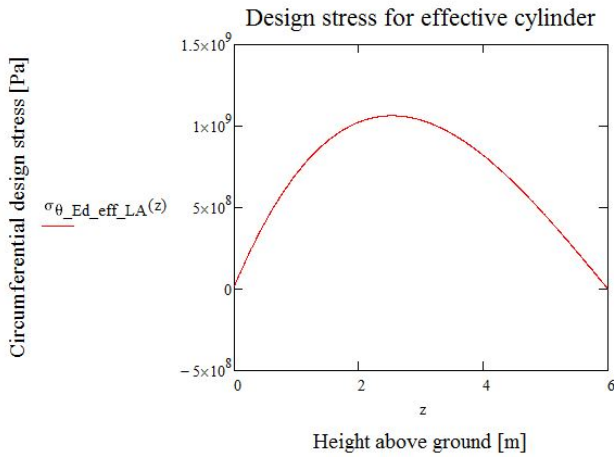


Figure 44: Diagram of the circumferential design stress for the effective cylinder as a function of height above ground calculated with linear analysis.

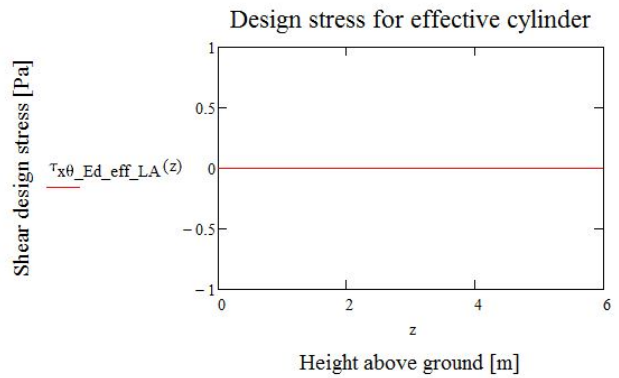


Figure 45: Diagram of the shear design stress for the effective cylinder as a function of height above ground calculated with linear analysis.

4.2 Finite element analysis

The result of the static structural finite element analysis can be seen in Figures 46 - 48 for the equivalent stress. Note that the deformation is heavily exaggerated in Figure 47 and 48 and shows a deformation scaled 3000 times the true deformation. The von Mises equivalent stress increases further down the tank wall to reach a maximum of 11.1 MPa at the middle of the lowest section, see Figure 49. The deformation of the tank is negligible relative the size of the 6 m-diameter tank, with a maximum at the bottom of the tank wall with 0.148 mm .

The meridional design stress obtained from Ansys can be seen in Figures 50 and 51. In Figure 50 the blue area shows compressive stresses of 5.73 MPa at the most on the inside of the tank and the red area shows tensile stresses at the outside of the tank at 6.45 MPa . The green area corresponds to stresses close to zero. At the meridional path the meridional stress reaches 5.98 MPa at the highest but is close to zero otherwise. The lowest, most negative, values has been chosen in each section for comparison since it's the compressive stresses that cause buckling. The values of the circumferential design stress and shear stress for the effective cylinder used for validation against buckling can be seen in Figures 52-55. The circumferential stress increases towards the bottom of the tank, which can be seen in Figure 52 as colors changing from blue to green to yellow and red. It can also be seen in Figure 53 as a steady increase towards the bottom until it drops drastically at the lower part of the bottom section. The shear design stress for the effective cylinder displayed in Figure 54 as a consistent yellow stress which in this case is the color closest to zero. The maximum shear reaches only 0.108 MPa and the minimum shear is -0.246 MPa . The shear along the meridional path can be seen in

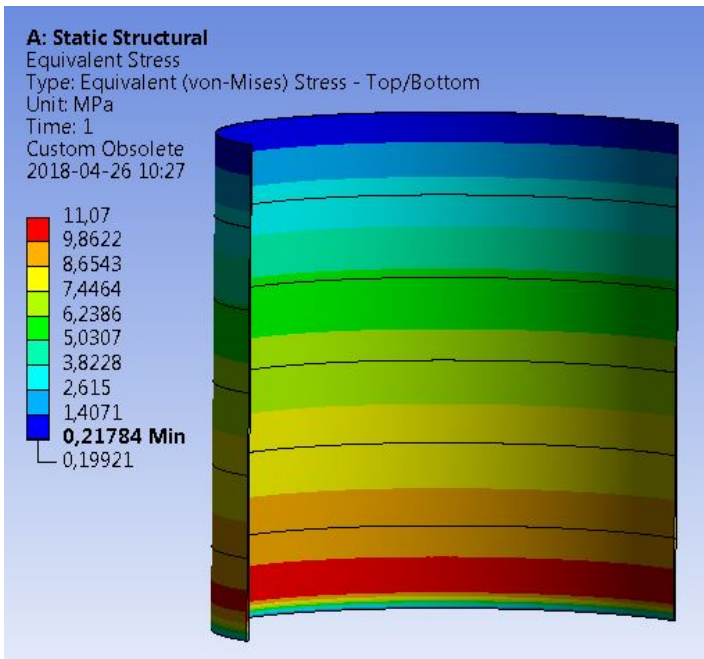


Figure 46: Equivalent von Mises stress result for static structural analysis with true deformation.

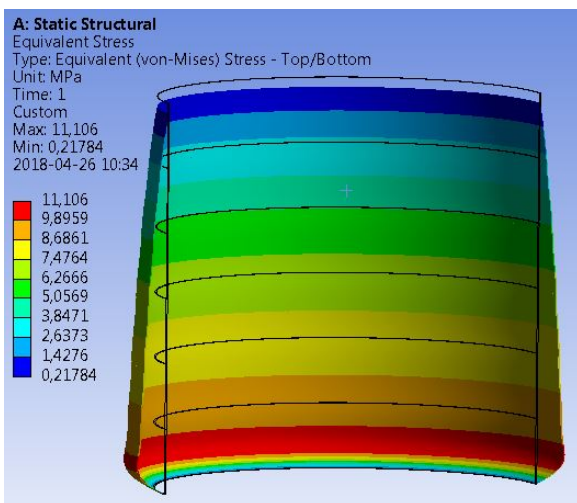


Figure 47: Equivalent von Mises stress result for static structural analysis with scaled deformation.

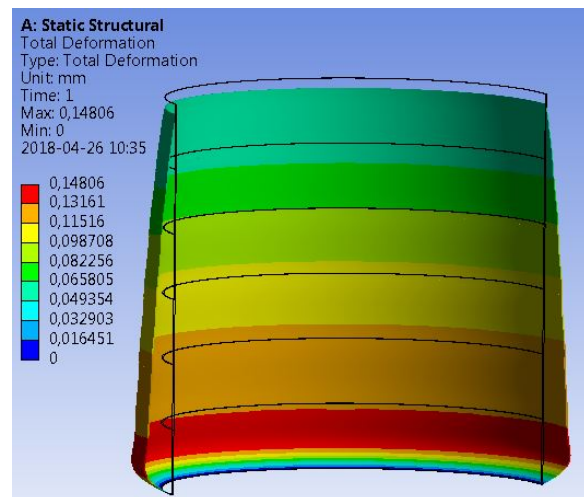


Figure 48: Deformation of static structural analysis. Note that the deformation is scaled by a factor of 3000.

Figure 55, which shows stresses close to zero with peaks at the welds connecting the sections.

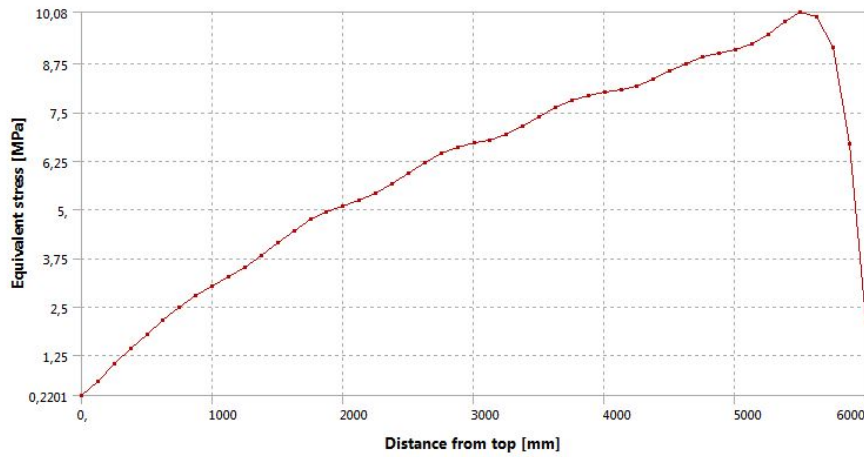


Figure 49: Diagram of the equivalent stress calculated with FEM along an axial path where 0 mm is at the top of the tank shell and 6000 mm is at the bottom of the tank.

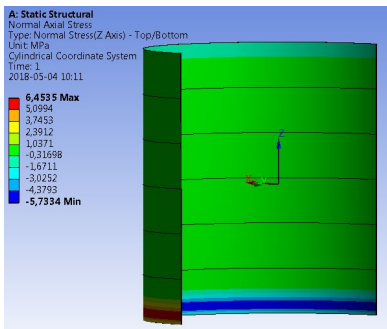


Figure 50: Meridional design stress.

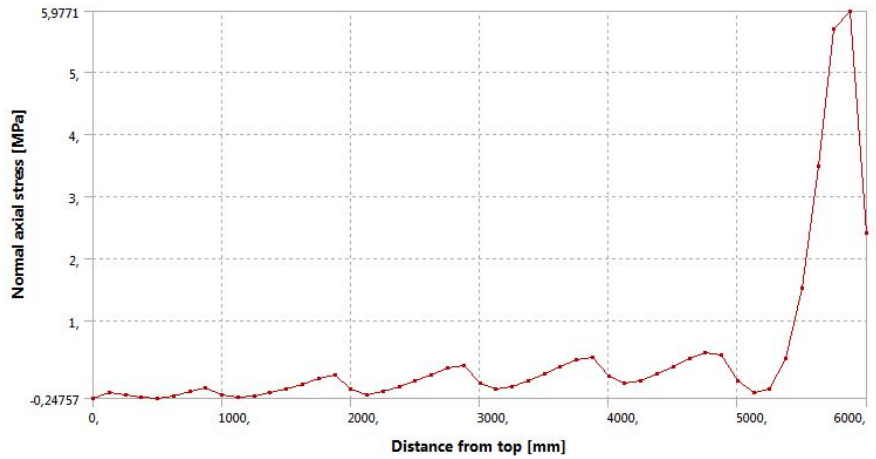


Figure 51: Diagram of meridional design stress along an axial path where 0 mm is at the top of the tank shell and 6000 mm is at the bottom of the tank.

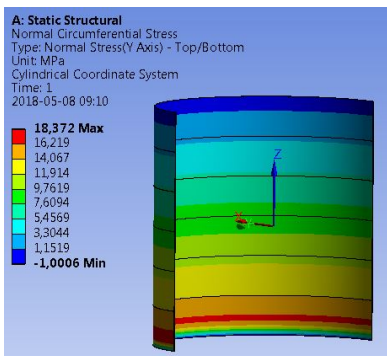


Figure 52: Circumferential design stress for effective cylinder.

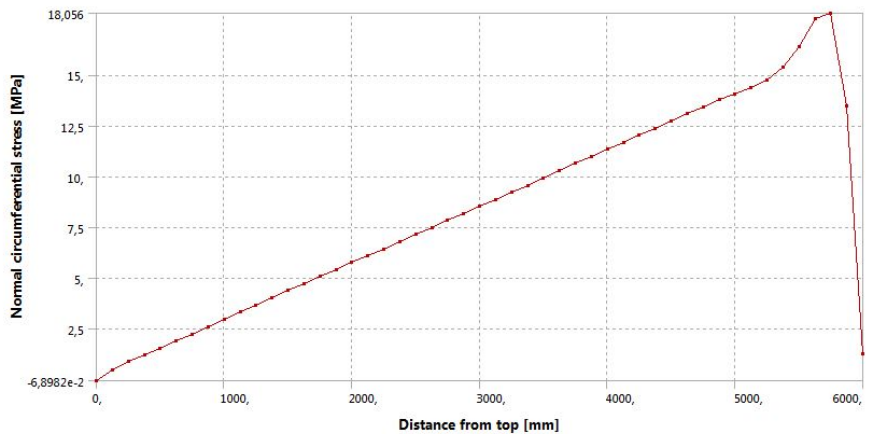


Figure 53: Diagram of circumferential design stress in effective cylinder along an axial path where 0 mm is at the top of the tank shell and 6000 mm is at the bottom of the tank.

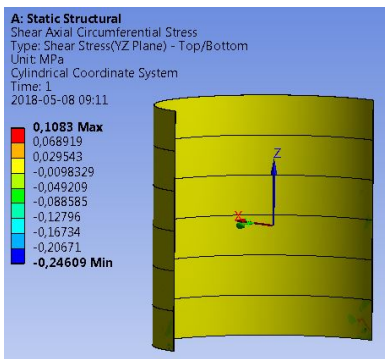


Figure 54: Shear design stress in effective cylinder.

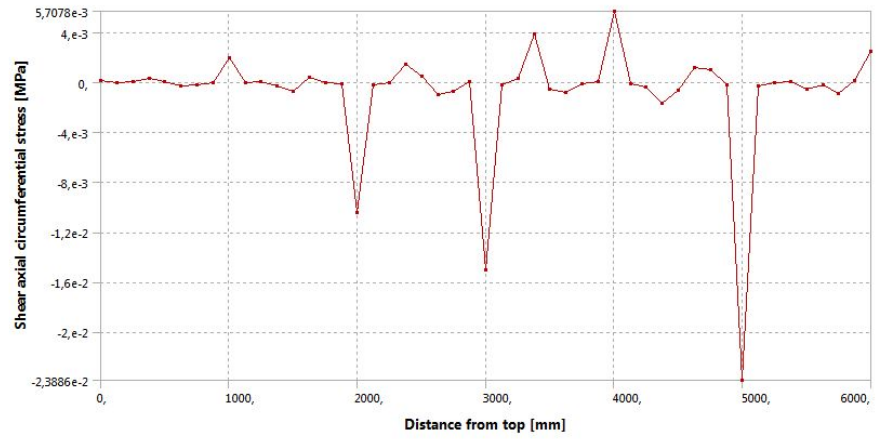


Figure 55: Diagram of shear design stress in effective cylinder along an axial path where 0 mm is at the top of the tank shell and 6000 mm is at the bottom of the tank.

4.3 Summary and comparison of results

The highest von Mises equivalent stress of each section calculated with FEM in Ansys can be seen in Table 6 where the von Mises stresses calculated with the handbook formulas can be seen as well for comparison between the calculation methods. Note that the equivalent stresses calculated with the three methods are not necessarily at the same height of each section. The result of the membrane theory locates the maximum at the bottom of each section whilst the linear analysis and FEM not necessarily locates the maximum at the bottom for every section. The result of the stresses for comparison against the buckling conditions can be seen in Table 7 for all calculation methods. The result of the calculations for $\sigma_{\theta,Ed}$ and $\tau_{x\theta,Ed}$ that were calculated with a special method can be seen in Equation 66. Tables 6 and 7 shows that the membrane theory and FEM produce similar results whilst the linear analysis results in much larger stresses, except for the shear stress. The assumption of no shear due to no torsion produces the same result for linear analysis as membrane theory, which is similar to that of FE-analysis.

Table 6: Comparison of plastic limit results for the three calculation methods; membrane theory (MT), linear elastic shell analysis (LA) and finite element method (FEM). The equivalent stresses are the largest in each section

Section	Equivalent stress [MPa]		
	MT	LA	FEM
0	3.45	1520	3.06
1	5.71	2120	5.11
2	7.48	2120	6.71
3	8.89	1760	8.04
4	10.0	1400	9.09
5	11.0	808	11.1

Table 7: Comparison of buckling results for the three calculation methods; membrane theory (MT), linear elastic shell analysis (LA) and finite element method (FEM)

Section	$\sigma_{x,Ed}$ [MPa]			$\sigma_{\theta,Ed,eff}$ [MPa]			$\tau_{x\theta,Ed,eff}$ [MPa]		
	MT	LA	FEM	MT	LA	FEM	MT	LA	FEM
0	-0.472	-1710	-0.248	2.97	450	2.95	0	0	0.00197
1	-0.560	-2390	-0.235	5.77	820	5.75	0	0	-0.0104
2	-0.629	-2380	0.281	8.57	1040	8.54	0	0	-0.0150
3	-0.683	-1980	0.408	11.4	102	11.3	0	0	0.00571
4	-0.728	-1570	0.483	14.2	707	14.1	0	0	-0.0239
5	-0.765	-906	5.98	17.0	14.2	18.1	0	0	0.00245

$$\sigma_{\theta,Ed} = \begin{bmatrix} 18.2 \\ 15.9 \\ 14.1 \\ 12.7 \\ 11.6 \\ 10.6 \end{bmatrix} MPa \quad \tau_{x\theta,Ed} = \begin{bmatrix} 0 \\ 0 \\ 0 \\ 0 \\ 0 \\ 0 \end{bmatrix} MPa \quad (66)$$

5 Discussion

The discussion has been divided into a few sections discussing limitations of this project, the description of the loads and the assumptions made. The loads and assumptions effect all calculation methods and will thus not be seen in the comparison of the calculation methods. They will therefore be in need of discussion instead. With the conditions discussed the results from the three calculation methods will be analyzed and then compared with the plastic limit and buckling limit conditions.

5.1 Limitations of this thesis project

The project was limited to only evaluating one tank with a certain wall thickness, height and diameter. The thickness of the wall was set quite thick, with a highest thickness of 24 *mm*. The thickness was set quite thick since it was first thought that the tank would not hold without any stiffeners. The thickness could although not be set too thick if the steel plates were to be manufacturable. The thickness of the sections can be adjusted in order to fulfill the conditions without over dimensioning. If stiffeners are introduced the thickness can be reduced further and less material can be used. This although requires recalculations, for example in Ansys, since the calculation document produced in this thesis work does not contain calculations for stiffened walls.

The thesis work was further limited in the number of loads accounted for. Only the most common loads; self-weight, hydrostatic load and internal pressure as well as wind and snow load have been used in the calculation document. Other loads that have not been accounted for are temperature loads, accidental loads, geotechnical loads and seismic loads etc. There are one or several standards describing each of these loads, if they all would have been accounted for this thesis work would not be completed in four months. Some assumptions that have been made in this project have been made in order to complete some kind of comparison in the available time given the project. In order to complete a fully usable calculation document that accounts for the whole tank further work has to be put in. Calculations should be done to the roof of the tank, the circular bottom plate and stiffeners. Rafters should be introduced as well. The question is if the work is worth while? A calculation document for hand calculations is only applicable for tanks within the first consequence class or the second consequence class as long as they do not exceed a size of 50 m^3 [8]. It has been reported that tanks have increased in size the past decades [4] and the trend might continue. The tank in this project is not very large but still reaches a volume of 170 m^3 . It would therefore be classed as either the first or the third consequence class, depending on its contents. The tank in this project can therefore only be calculated with the calculation document if it is designed to store water or another non-hazardous liquid.

5.2 Loads and assumptions

Possible faulty assumptions that will not be apparent in the comparison of the calculation methods are the description of the loads that has been used for all calculation methods. The Eurocodes are difficult to interpret in some cases and some assumptions have been made along the way. The snow load was assumed to act vertical to the horizontal plane and not vertically to the roof as the wind load. This is an assumption that was easy to make but was not described by the Eurocodes. Other assumptions that had to be made was how to apply the wind load to the shell when performing hand calculations. It did not seem possible to make a calculation by hand with a wind load that varied around the shell since the loads already varied with height above ground. It was therefore assumed that the wind load could be applied with its most unfavorable value. The wind load was applied in the same way for the FEM-calculations made in Ansys even if more complex calculations are possible to do with a FEM-software compared to by hand. Further assumptions had to be made for both the wind and snow load on the roof since the Eurocodes are insufficient in their description of roof types. Coefficients used in the calculations of wind and snow load are not described for conical roofs and it therefore had to be assumed that coefficients for spherical roofs could be used.

5.3 Comparison of obtained results

The results from the membrane theory and the FE-analysis are very similar for the equivalent stress and the stresses for the effective cylinder as can be seen in Table 6 and 7. The results for the meridional stress, $\sigma_{x,Ed}$, is although of different signs and in some sections doubled in the absolute value. The stress calculated with membrane theory is easy to follow. The stress becomes negative since the meridional membrane stress resultant becomes negative and thus compressive due to the load case. The result of the FE-analysis on the other hand starts off negative and increases further down the tank. At the bottom section of the tank the meridional stress increases significantly and then drops. A possible reason for the difference between the result of the membrane theory and FEM is that the FE-analysis most likely take the moments into account while the membrane theory does not. As can be seen in Figure 50 there is compressive stresses on the inside of the tank and tensile stresses on the outside of the tank. These stresses can be explained by a moment that is not taken into account by the

membrane theory. At the bottom of the tank the shell is forced to a certain line by the boundary conditions probably causing larger moments and thus a larger meridional stress. The membrane theory is thus not sufficient to describe the bending effect that occurs in meridional direction. Membrane theory does although describe the other stresses very well without factors and expressions for local buckling effects.

The results of the linear analysis are a lot larger compared with membrane theory and FEM. Since the difference between membrane theory and linear elastic analysis is that the bending moments are taken into account for the linear elastic analysis and the result of membrane theory comes very close to that of FEM it is assumed that the bending moments calculated for linear analysis are too large. The calculation method used for the bending moments is probably not usable for cylinders, even though available expertise could not see where the calculation is wrong and cannot come up with a better calculation method. As can be seen by comparing the bending moments in Equation 55 with Equation 56, $M_{x,Ed}$ is more than ten times larger than $N_{x,Ed}$ and $M_{\theta,Ed}$ not much smaller than $N_{\theta,Ed}$. This leads to the bending moments being the major part of the σ stresses in both the meridional and circumferential direction. Since the standard proposes membrane theory as the method to use when it is valid the faulty bending moments in the linear analysis was not given more attention. Especially since an article [12] comparing the two methods concluded that membrane theory was better to use for tanks with a maximum diameter of 15 m. If this conclusion is assumed to be suitable for the Eurocodes as well as the American standard it would mean that the linear analysis is redundant. Membrane theory is recommended for the lowest consequence class by the Eurocodes and can be used for the second consequence class as well. A FE-analysis, or an equivalent method, should be used when the tanks in the second consequence class exceeds a volume of 50 m³ and thus becomes classified as tanks in the third consequence class. A tank with a diameter of 15 m exceeds a volume of 50 m³ at only 3 dm height. This means that all tanks in the second consequence class exceeding 15 m and is thus not a part of the tanks where the membrane theory is can be used, should not be calculated by hand either way. The linear analysis thus appear to be redundant. The hypothesis states in the beginning of this thesis thus appear to be wrong, membrane theory seems to be better than linear analysis rather than the opposite.

The stresses in the sections have been taken at the location where the stresses are the highest. This location varies depending on the calculation method. For membrane theory it is very easy to conclude that the stresses are the highest at the bottom of each section just by analyzing the diagrams of the membrane stress resultants in Figure 21 and 24. The location of the maximum stress calculated with linear analysis is although at the top of the bottom sections and at the bottom of the top sections. In section 3 the stress is the highest at the lower middle of the section. This is due to that linear analysis combines the membrane stress resultant and the bending moments resulting in higher stresses closer to the middle of the tank shell due to the large bending moment. The FE-analysis locates the maximum in the lower part of each section, but not necessarily at the very bottom of the section. This can most easily be seen in the diagram of the equivalent stress in Figure 49 and in the diagram of the meridional stress in Figure 51. In the diagram of the meridional stress there is a clear peak just before the bottom of the section. This is probably due to the bending moment that pushes the location of the maximum towards the middle of the section. The bending moment seems, by comparing the diagrams of the meridional and the circumferential stress, to be larger in the meridional direction. The diagram of the circumferential stress shows that the stress is largest at the bottom of each section, except the bottom section, and is not offset by the bending moment to a significant degree. The circumferential bending moment thus seems to be less than the meridional bending moment relative their membrane stress resultants. This corresponds to the bending moments calculated for linear elastic analysis; the meridional bending moment is larger than the circumferential bending relative their membrane stress resultants. For the equivalent stress where the meridional, circumferential and shear stresses are combined the maximum is thus at the bottom of each section, except the bottom section, but does not show the straight line as the membrane theory does nor the maximum at the middle of the tank shell. This corresponds to the theory that there are bending moments in the shell but not as large as calculated by the linear analysis.

The shear stress is very close to zero even with FE-analysis. There are although a few positive and negative peaks as can be seen in Figure 55. The larger peaks are at the heights where the sections are bonded together with a weld-like constraint and the amplitude of the peaks increases further down the tank. The load on the shell increases further down the tank and is most likely the reason why the shear stress peaks are larger at the bottom compared to the top. The peaks are located at the heights of which the sections are bonded probably due to that the bonded constraint forces the sections together causing shear stresses. These shear stress peaks are although very small, not even a hundredth of the equivalent stress. To apply zero to $\tau_{x\theta}$ does thus seem reasonable.

5.4 Comparison against the plastic limit and buckling limit conditions

The shell standard provides six conditions that had to be met for the tank. The condition for the plastic limit is that the equivalent stress should not exceed the yield strength of the material, as described by Equation 29. As can be seen in Table 8 the yield strength is far from exceeded for the result from membrane theory and

FEM. FE-analysis which results in slightly larger stresses at the bottom and top compared to membrane theory reaches 5 % of the maximum allowed stress at the most. The result from the linear analysis does although not meet the condition, it exceeds it with a factor of nine. The buckling condition for the meridional stress $\sigma_{x,Ed}$, described in Equation 32, is also met for membrane theory and FEM, but not for linear analysis, see Table 8. For linear analysis the condition is exceeded by a factor 16. The stresses calculated with membrane theory is slightly larger than those calculated with FEM, except at the bottom section where the FEM gives a much larger meridional stress than membrane theory. The stresses does although not reach higher than 0.5 % and 4 % of the maximum allowed stress for membrane theory and FEM respectively. The same trend can be seen for the effective cylinder with the conditions for the circumferential stress $\sigma_{\theta,Ed,eff}$ in Table 9. The condition is met for membrane theory and FEM but the margin is not as large as for $\sigma_{eq,Ed}$ and $\sigma_{x,Ed}$. Membrane theory reaches to 60 % of the maximum allowed value and FEM to 64 %. The tank shell thickness is although still over dimensioned. The shear stress $\tau_{x\theta,Ed,eff}$ is equal for both membrane theory and linear analysis since both the shear stress resultant and the torsion moment was set to zero. Since the FE-analysis showed the same result the condition is easily met, reaching only 0.03 % for the shear stress of the effective cylinder.

Table 8: Comparison of equivalent stresses and meridional stresses with plastic limit (P) condition and buckling limit (B) condition. The stresses are results from membrane theory (MT), linear elastic shell analysis (LA) and finite element method (FEM)

Section	$\sigma_{eq,Ed}$ [MPa]				$\sigma_{x,Ed}$ [MPa]			
	MT	LA	FEM	P Condition	MT	LA	FEM	B Condition
0	3.45	1520	3.06	≤ 235	-0.472	-1710	-0.248	≤ 155
1	5.71	2120	5.11	≤ 235	-0.560	-2390	-0.235	≤ 153
2	7.48	2120	6.71	≤ 235	-0.629	-2380	0.281	≤ 152
3	8.89	1760	8.04	≤ 235	-0.683	-1980	0.408	≤ 151
4	10.1	1400	9.09	≤ 235	-0.728	-1570	0.483	≤ 151
5	11.0	808	11.1	≤ 235	-0.765	-906	5.98	≤ 151

Table 9: Comparison of stresses for effective cylinder with buckling conditions. The stresses are results from membrane theory (MT), linear elastic shell analysis (LA) and finite element method (FEM)

Section	$\sigma_{\theta,Ed,eff}$ [MPa]				$\tau_{x\theta,Ed,eff}$ [MPa]			
	MT	LA	FEM	Condition	MT	LA	FEM	Condition
0	2.97	450	2.95	≤ 28.2	0	0	0.00197	≤ 85.3
1	5.77	820	5.75	≤ 28.2	0	0	-0.0104	≤ 85.3
2	8.57	1040	8.54	≤ 28.2	0	0	-0.0150	≤ 85.3
3	11.4	1020	11.3	≤ 28.2	0	0	0.00571	≤ 85.3
4	14.2	707	14.1	≤ 28.2	0	0	-0.0239	≤ 85.3
5	17.0	14.2	18.1	≤ 28.2	0	0	0.00245	≤ 85.3

The stresses $\sigma_{\theta,Ed}$ and $\tau_{\theta,Ed}$ that were not calculated with neither membrane theory, linear analysis nor FEM but with an equation given by the shell standard also met the conditions as can be seen in Table 10. The circumferential stress reaches only 30 % of the maximum allowed stress, which demonstrates that the tank shell is over dimensioned.

Table 10: Comparison of circumferential and shear stresses with buckling conditions

Section	$\sigma_{\theta,Ed}$ [MPa]		$\tau_{x\theta,Ed}$ [MPa]	
	Stress	Condition	Stress	Condition
0	18.2	≤ 60.4	0	≤ 204
1	15.9	≤ 52.8	0	≤ 178
2	14.1	≤ 47.0	0	≤ 159
3	12.7	≤ 42.3	0	≤ 143
4	11.6	≤ 38.4	0	≤ 130
5	10.6	≤ 35.2	0	≤ 119

It is evident that the tank meets both the plastic limit and buckling limit conditions and will hold for the applied loads, at least when comparing with the results from the membrane theory and FE-analysis. The stress that comes closest to its condition is $\sigma_{\theta,Ed,eff}$ at 60 % and 64 %, which is a buckling condition. The stress that comes second closest to its condition is $\sigma_{\theta,Ed}$ which also is a buckling condition. It thus appears as if buckling is the most limiting condition. This corresponds with the statement that tanks tend to fail through buckling due to their slenderness explained in the introduction.

6 Conclusions

Three calculations methods have been used to calculate the stresses in a tank and comparison of the results have been made. The comparison of the stresses show that membrane theory gives similar results to FEM and that linear analysis give stresses much larger than FEM and membrane theory. The conclusions of the comparison of the calculation methods are that;

- Membrane theory is a simple and acceptable method that can be used for tanks in the first consequence class and small tanks within the second consequence class. In some cases it might although need factors or simplifications for local buckling effects.
- Linear elastic shell analysis is redundant, it is more complicated and faults are more easily made. It cannot be used in more application areas than membrane theory either.
- FE-analysis can make complex calculations and is a valid method for all consequence classes. With new tanks growing larger this will become the only approved method when liquids that can potentially damage the environment are stored.

7 Acknowledgement

This is a master thesis that has been written as the last project within the master of science in mechanical engineering program at Karlstad University. I would like to thank my supervisor Jens Bergström at Karlstad University for the input on the thesis. You have asked questions much like an opponent, giving me valuable input on where my thesis has not been fully elucidative.

The project has been performed in collaboration with Sweco Industry AB with supervisors from the Stockholm office. Many thanks to the supervisors Joakim Nyman and Marko Nikolic for the help during the project, you have helped me move on when I have been stuck at a problem and helped me keep the project going forward in the right direction. Though the project has been conducted in collaboration with the Stockholm office the project has been executed at the office in Karlstad. I would like to thank those of you at the office that have helped me during the project and to all of you that have given me a pleasant four months at Sweco. It would have been much more difficult to complete the project without the pleasant and supporting environment.

Last but not least I would like to thank my fellow student and partner Christopher Ekängen. You have been of great help with the calculations and helped me during the tough times of the project. Without the support from home the project would have been difficult to complete.

Yours sincerely,
Malin Pluto

8 References

- [1] Nationalencyklopedin. *Cistern*. URL: <https://www.ne.se/uppslagsverk/encyklopedi/l%C3%A5ng/cistern> (visited on 01-02-2018).
- [2] Swedac. *Cisterner*. URL: <https://www.swedac.se/amnesomraden/cisterner/> (visited on 01-02-2018).
- [3] Boverket. *Regelhierarki - från lag till allmänt råd*. URL: <http://www.boverket.se/sv/lag--ratt/forfattningssamling/regelhierarki/> (visited on 26-01-2018).
- [4] Luis A. Godoy. "Buckling of vertical oil storage steel tanks: Review of static buckling studies". In: *Thin-Walled Structures* 103 (Jan. 2016), pp. 1–21.
- [5] Samuel King Jr. *Life cycle of AF fuel: onto base and into storage*. Dec. 2011. URL: <http://www.eglin.af.mil/News/Article/391484/life-cycle-of-af-fuel-onto-base-and-into-storage/> (visited on 12-04-2018).
- [6] LNG World News. *NSSMC Provides Nickel Steel for Soma LNG Storage Tank*. June 2014. URL: <https://www.lngworldnews.com/nssmc-provides-nickel-steel-for-soma-lng-storage-tank/> (visited on 09-05-2018).
- [7] Travis Air Force Base. *New fuel tanks offer larger, safer storage*. Dec. 2011. URL: <http://www.travis.af.mil/News/Article/150869/new-fuel-tanks-offer-larger-safer-storage/> (visited on 12-04-2018).
- [8] CEN. "Eurokod 3: Dimensionering av stålkonstruktioner – Del 4-2: Cisterner". In: (2009).
- [9] Boverket. "Boverkets författningssamling BFS 2015:6 EKS 10". In: (2015).
- [10] F. Trebuna, F. Simcak, and J. Bocko. "Failure analysis of storage tank". In: *Engineering Failure Analysis* 16 (Dec. 2007), pp. 26–38.
- [11] CEN. "Eurokod 3: Dimensionering av stålkonstruktioner – Del 1-6: Skal". In: (2015).
- [12] Eyas Azzuni and Sukru Guzey. "Comparison of the shell design methods for cylindrical liquid storage tanks". In: *Engineering Structures* 101 (July 2015), pp. 621–630.
- [13] CEN. "Eurokod - Grundläggande dimensioneringsregler för bärverk". In: (2010).
- [14] Bengt Sundström, ed. *Handbok och formelsamling i Hållfasthetslära*. 8th ed. Stockholm: Instant Book AB, 2013.
- [15] Eduard Ventsel and Theodor Krauthammer. *Thin Plates and Shells*. 1st ed. New York, NY: Marcel Dekker, Inc., 2001.
- [16] Ansys Inc. *Structures*. URL: <https://www.ansys.com/products/structures> (visited on 11-05-2018).
- [17] Endre Süli. *Lecture notes on finite element methods for differential equations*. Mathematical institute at the University of Oxford. Dec. 2012.
- [18] Nationalencyklopedin. *finita elementmetoden*. URL: <https://www.ne.se/uppslagsverk/encyklopedi/l%C3%A5ng/finita-elementmetoden> (visited on 14-05-2018).
- [19] G.R. Liu and S.S. Quek. *Finite Element Method*. 1st ed. Oxford: Butterworth-Heinemann, 2003.
- [20] SAS IP Inc. *Static Structural Analysis*. URL: https://www.sharcnet.ca/Software/Ansys/17.2/en-us/help/wb_sim/ds_static_mechanical_analysis_type.html (visited on 11-05-2018).
- [21] CEN. "Eurokod 3: Dimensionering av stålkonstruktioner – Del 1-1: Allmänna regler och regler för byggnader". In: (2008).
- [22] CEN. "Eurokod 1: Laster på bärverk – Del 1-3: Allmänna laster - Tunghet, egyptyngd, nyttig last för byggnader". In: (2011).
- [23] CEN. "Eurokod 1: Laster på bärverk – Del 4: Silor och behållare". In: (2014).
- [24] CEN. "Eurokod 1: Laster på bärverk – Del 1-3: Allmänna laster - Vindlast". In: (2008).
- [25] CEN. "Eurokod 1: Laster på bärverk – Del 1-3: Allmänna laster - Snölast". In: (2005).
- [26] Kjell Nero and Sture Åkerlund, eds. *Boverkets handbok om snö- och vindlast, utgåva 2*. 1:1. Karlskrona: Boverket, 1997.

Appendices

A Geometry of conical roof

To fully describe the geometry of the tank, the shape of the roof has to be described. In order to determine the geometry of the conical roof some geometrical expressions can be taken forth. For a conically shaped roof, see Figure A.1, the slope of the roof, α_{roof} , is expressed by the user of the Mathcad-sheet, along with the diameter D of the tank. The height of the roof can then be determined as described by Equation A.1 and the area of the roof can be described by Equation A.2, which is a reformulation of the equation for surface area of a circular cone given by Physics Handbook for Science and Engineering by Carl Nordling and Jonny Österman.

$$h = \frac{D}{2} \tan(\alpha_{roof}) \quad (A.1)$$

$$A_{roof} = \pi \frac{D}{2} \sqrt{\left(\frac{D}{2}\right)^2 + h^2} \quad (A.2)$$

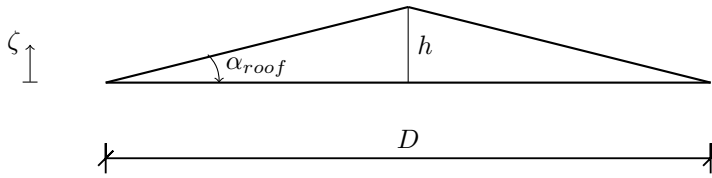


Figure A.1: Geometry of a conically shaped roof for a tank. The diameter of the tank, D , as well as the angle of the roof, α_{roof} , are known variables while the height of the roof, h , can be calculated through D and α_{roof} .

The surface area of the insulation placed on a conical roof can be described with the height of the insulation above the top of the shell, h_{ins} , see Figure A.2, as well as the diameter of the insulation, D_{ins} . These variables can be determined through the input variables t_{roof} , $t_{ins,roof}$ (thickness of roof insulation) and D , see Equation A.3 and Equation A.4. The surface area of the insulation can thereby be calculated as described by A.5.

$$h_{ins} \approx h + \frac{1}{2} t_{roof} + \frac{1}{2} t_{ins,roof} \quad (A.3)$$

$$D_{ins} \approx D + t_{roof} + t_{ins,roof} \quad (A.4)$$

$$A_{roof} = \pi \frac{D_{ins}}{2} \sqrt{\left(\frac{D_{ins}}{2}\right)^2 + h_{ins}^2} \quad (A.5)$$

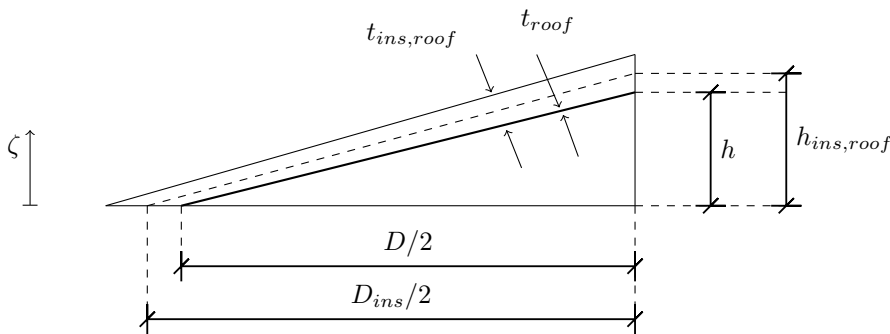


Figure A.2: The diameter, D_{ins} , and height, h_{ins} , of insulation on a conically shaped roof. The diameter of the roof, D , the thickness of the roof, t_{roof} , and the thickness of the insulation, t_{ins} , are input variables.

B The calculation document

Dimensioning of Tanks According to Eurocode

Contents

- Limitations of this document
- Note
- Geometry of the tank
 - Stepwise variable shell thickness
 - The roof
- Material properties
- Calculation of loads
 - Self-weight
 - Internal pressure
 - Hydrostatic load
 - Wind load
 - Snow load
- Partial factors and combination of actions
- Calculation of stresses
 - Active force diagram of the roof
 - Active force diagram of the shell
 - Limit states
 - Plastic limit (LS1)
 - Buckling (LS3)

Limitations of this document

This document calculates only the stresses in the shell wall of the tank when the following loads are applied;

- self-weight,
- internal pressure,
- hydrostatic load,
- wind load and/or
- snow load.

This calculation document does not take accidental loads, loads occurring due to depletion etc into account, but can be altered in order to add these loads. The document does not treat cyclic plasticity or fatigue. This calculation document is also only applicable to tanks that;

- are anchored at the bottom (clamped boundary condition),
- have a roof (pinned boundary condition at the top) and
- have conically shaped roof.

This calculation document is further limited by the standards that has been followed. In order to follow the tank standard, SS-EN 1993-4-2, this calculation document is only applicable to tanks that;

- are vertical, cylindrical and axisymmetric,
- are constructed in steel,
- are placed above ground,
- are used for storing liquids,
- have a characteristic internal pressure above the liquid between -100 and 500 mbar,
- have a maximum design liquid level not higher than the shell and
- have a design metal temperature of -165 - 300 degrees Celcius if not fatigue loaded, then the upper limit should be 150 degrees Celcius

In order to follow the wind standard, SS-EN 1991-1-4, and the snow standard, SS-EN 1991-1-3, this document is only applicable to tanks that;

- have a maximum height of 200 m and
- are placed not higher than 1500 m

Note

The Eurocodes that have been used to create this document are;

- SS-EN 1991-1-1 (edition 1, approved 2002-06-28, published 2011-01-26),
- SS-EN 1991-1-3 (edition 1, approved 2003-08-29, published 2015-10),
- SS-EN 1991-1-4: 2005 (edition 1, approved 2005-04-22, published 2008-10-16),
- SS-EN 1991-4: 2006 (edition 1, approved 2006-06-01, published 2014-10-21),
- SS-EN 1993-1-6: 2007 (edition 1, approved 2007-03-07, published 2015-10-28) and
- SS-EN 1993-4-2: 2007 (edition 1, approved 2007-03-07, published 2015-06-10)

They are in this document simply referred to as;

- SS-EN 1991-1-1,
- SS-EN 1991-1-3,
- SS-EN 1991-1-4,
- SS-EN 1991-4,
- SS-EN 1993-1-6 and
- SS-EN 1993-4-2

This calculation document is conformed to Swedish conditions, following the Swedish national annex EKS 10. The equations and values chosen by the Swedish annex have been marked in order to make it possible to change back to the original equations and values of the Eurocodes or adapt the document for another national annex.

Some simplifications and assumptions have been made in order to produce this calculation document. These simplifications and assumptions have been marked with N.B., make sure to read these notes in order to control that they are applicable to your situation.

This calculation document should only be used for tanks of consequence class 1 or 2 when dimensioning a tank. For consequence class 3 a validated analysis, for example finite element shell analysis, should be used in order to follow the demands given by SS-EN 1993-4-2 for consequence class 3 (SS-EN 1993-4-2 4.2.2.4(1)).

Note: The consequence classes as described by SS-EN 1993-4-2 2.2(3):

"Consequence class 3: Tanks storing liquids or liquefied gases with toxic or explosive potential and large size tanks with flammable or water-polluting liquids in urban areas. Emergency loadings should be taken into account for these structures where necessary, see annex A.2.14.

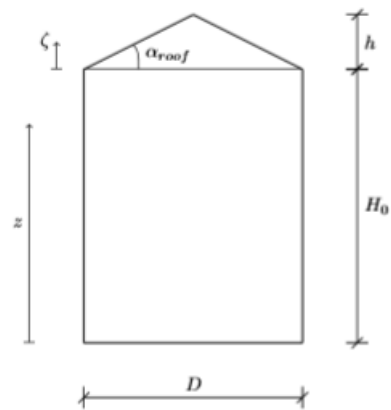
Consequence class 2: Medium size tanks with flammable or water-polluting liquids in urban areas.

Consequence class 1: Agricultural tanks or tanks containing water"

EKS 10 chapter 3.4.2 part 2.2(3) 3§ adds a size limit of the tanks for the third consequence class. Consequence class 3 applies only to tanks with a volume of 50 m³ or larger.

Geometry of tank

Insert	$D := 6\text{m}$	Diameter of tank
Variable	$0 \leq \zeta \leq h$	Height above the shell
Variable	$0 \leq z \leq H_0 + h$	Height above ground



Stepwise variable shell thickness

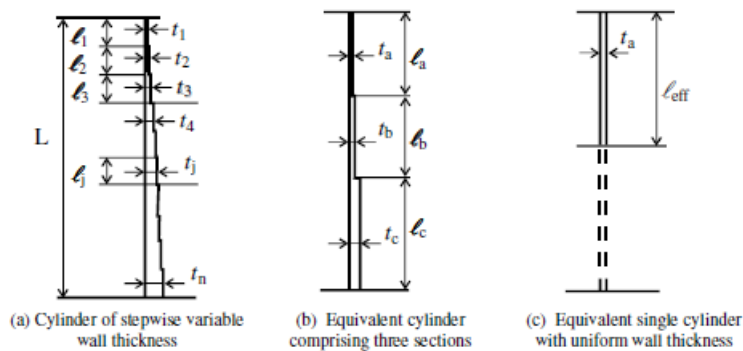


Figure D.5: Transformation of stepped cylinder into equivalent cylinder

Note: L in Figure D.5 is the shell height H_0 . Figure D.5 has been taken from SS-EN 1993-1-6.

Insert	$\underline{l} :=$	$\begin{pmatrix} 1\text{m} \\ 1\text{m} \\ 1\text{m} \\ 1\text{m} \\ 1\text{m} \\ 1\text{m} \end{pmatrix}$	
--------	--------------------	--	--

The lengths of the plates that the shell consists of, see Figure D.5 above.

Note: The number of input variables in \underline{l} , the number of rows, can be changed to suit the number of plates used but then there are some vectors further down the document that have to be updated.

Insert	$n := 6$	The number of rows in \underline{l}
--------	----------	---------------------------------------

$$j := 0..n - 1$$

	$H_0 := \sum_j l_j = 6\text{m}$	The shell height
--	---------------------------------	------------------

	$\text{Volume} := \pi \cdot \left(\frac{D}{2}\right)^2 \cdot H_0 = 169.646 \cdot \text{m}^3$	The volume of the tank
--	--	------------------------

An iterative process has to be done for the plate thicknesses, insert probable thicknesses:

$$\text{Insert } t := \begin{pmatrix} 14\text{mm} \\ 16\text{mm} \\ 18\text{mm} \\ 20\text{mm} \\ 22\text{mm} \\ 24\text{mm} \end{pmatrix}$$

The thicknesses of the plates that the shell consists of, see Figure D.5 above.

$$\text{Insert } n_a := 2$$

The number of plates, or rows in l, for the upper part, a, see Figure D.5 above.

$$j := 0..n_a - 1$$

$$l_a := \sum_j l_j = 2\text{m}$$

The length of the upper part. This length should be from the top of the shell to the top of the plate that exceeds a thickness 1.5 times the smallest thickness as long as this length does not exceed half of the shell height H_0 . See description in D.2.3.1(4) of SS-EN 1993-1-6 and Figure D.5 if not clear.

$$t_a := \frac{1}{l_a} \left[\sum_j (l_j \cdot t_j) \right] = 15\text{-mm}$$

The equivalent thickness for the upper part, a (equation D.58 of SS-EN 1993-1-6).



$$l_b = 2\text{m}$$

The length of the middle part (equations D.56 and D.57 of SS-EN 1993-1-6)

$$l_c = 2\text{m}$$

The length of the lower part (equations D.56 and D.57 of SS-EN 1993-1-6)

$$\text{Insert } n_b := 2$$

The number of plates used for the middle part, b, see Figure D.5 above.

$$j := n_a..n_a + n_b - 1$$

$$t_b := \frac{1}{l_b} \left[\sum_j (l_j \cdot t_j) \right] = 19\text{-mm}$$

The equivalent thickness for the middle part, b (equation D.59 of SS-EN 1993-1-6).

$$\text{Insert } n_c := 2$$

The number of plates used for the lower part, c, see Figure D.5 above.

$$j := n_a + n_b..n_a + n_b + n_c - 1$$

$$t_c := \frac{1}{l_c} \left[\sum_j (l_j \cdot t_j) \right] = 23\text{-mm}$$

The equivalent thickness for the lower part, c (equation D.60 of SS-EN 1993-1-6).

$t_{\text{shell}} := t_a = 15 \cdot \text{mm}$ The equivalent shell thickness

$j := 0..n - 1$

$t_{\text{ave}} := \frac{1}{H_0} \cdot \left[\sum_j (l_j \cdot t_j) \right] = 19 \cdot \text{mm}$ The average shell thickness

Note: This t_{ave} will only be used for calculating the weight of the shell.

The roof

Insert $t_{\text{roof}} := 10 \text{mm}$ Probable roof plate thickness. The thickness needs to be iterated when roof plate thickness has been given at the end of the document.

Insert $\alpha_{\text{roof}} := 2^\circ$ The roof angle for a conical roof

$h = 0.105 \text{m}$ The height of the roof

$H_{\text{tot}} := H_0 + h = 6.105 \text{m}$ The height of the tank

$\text{Height_requirement_of_1991_1_4} = \text{"Met"}$

Material properties

Insert	$E := 210000 \frac{\text{N}}{\text{mm}^2}$	Young's modulus, stiffness of the steel
Insert	$\nu := 0.3$	Poisson's ratio
Insert	$f_y := 235\text{MPa}$	Yield strength of steel

Partial factors and combination factors for actions

$\gamma_F := 1.4$	The partial factor for variable actions from liquids (EKS 10 chapter 3.4.2 part 2.9.1(1)P 4§ and chapter 1.4 part B.3(2) 4§)
$\gamma_G := 1.35$	The partial factor for permanent loads (EKS 10 chapter 3.4.2 part 2.9.1(1)P 4§)
$\gamma_{M0} := 1.0$	The partial factor for resistance of welded or bolted shell wall to plastic limit state, cross-sectional resistance (EKS 10 chapter 3.4.2 part 2.9.2.2(3)P 6§)
$\gamma_{M1} := 1.0$	The partial factor for resistance of shell wall to stability (EKS 10 chapter 3.4.2 part 2.9.2.2(3)P 6§)

Insert reduction factor and combination factors for relevant combination of actions. If a combination factor is set to 0 the load will not be applied, if set to 1 the whole load will be applied without any reduction.

Insert	$\xi_{\text{weight}} := 1$	Reduction factor for self-weight
Insert	$\psi_{\text{int}} := 1$	Combination factor for the internal pressure above liquid level
Insert	$\psi_{\text{hyd}} := 1$	Combination factor for the hydrostatic pressure caused by the liquid
Insert	$\psi_{\text{snow}} := 1$	Combination factor for the snow load
Insert	$\psi_{\text{wind}} := 1$	Combination factor for the wind load

Note: SS-EN 1993-4-2 2.10, 1990 6.4-6.5 and 1991-4 A.4 might be useful.

Calculation of loads

Self-weight

Insert $\gamma_{\text{shell}} := 77.75 \frac{\text{kN}}{\text{m}^3}$ The density of the shell steel, see Annex A of SS-EN 1991-1-1

$V_{\text{shell}} := H_0 \cdot \pi \cdot D \cdot t_{\text{ave}} = 2.149 \cdot \text{m}^3$ The volume of shell

$W_{\text{shell}} := \gamma_{\text{shell}} \cdot V_{\text{shell}} = 167.073 \cdot \text{kN}$ Weight of tank shell

Insert $\gamma_{\text{roof}} := 77.75 \frac{\text{kN}}{\text{m}^3}$ The density of the roof plate, see Annex A of SS-EN 1991-1-1



$V_{\text{roof}} := A_{\text{roof}} \cdot t_{\text{roof}} = 0.283 \cdot \text{m}^3$ The volume of the roof plate

$W_{\text{roof}} := \gamma_{\text{roof}} \cdot V_{\text{roof}} = 21.997 \cdot \text{kN}$ Weight of roof

Insert $\gamma_{\text{ins}} := 1.3 \frac{\text{kN}}{\text{m}^3}$ The density of the insulation

Insert $t_{\text{ins_shell}} := 140 \text{mm}$ The thickness of the insulation around the shell

Insert $t_{\text{ins_roof}} := 140 \text{mm}$ The thickness of the insulation on the roof



The volume of the insulation around the shell:

$V_{\text{ins_shell}} := H_0 \cdot \pi \cdot t_{\text{ins_shell}} \cdot (D + t_{\text{shell}} + t_{\text{ins_shell}}) = 16.243 \cdot \text{m}^3$

$W_{\text{ins_shell}} := \gamma_{\text{ins}} \cdot V_{\text{ins_shell}} = 21.115 \cdot \text{kN}$ The weight of the insulation around the shell

The volume of the insulation on the roof:

$V_{\text{ins_roof}} := A_{\text{roof_ins}} \cdot t_{\text{ins_roof}} = 4.173 \cdot \text{m}^3$

$W_{\text{ins_roof}} := \gamma_{\text{ins}} \cdot V_{\text{ins_roof}} = 5.425 \cdot \text{kN}$ The weight of the insulation on the roof

Insert $\gamma_{\text{cover}} := 77.75 \frac{\text{kN}}{\text{m}^3}$ The density of the weather protection cover

Insert $t_{\text{cover}} := 3 \text{mm}$ The thickness of the weather protection cover



The volume of the weather protection cover around the shell:

$$V_{\text{cover_shell}} := H_0 \cdot t_{\text{cover}} \cdot (D + t_{\text{shell}} + 2 \cdot t_{\text{ins_shell}} + t_{\text{cover}}) = 0.113 \cdot \text{m}^3$$

The weight of the cover around the shell:

$$W_{\text{cover_shell}} := \gamma_{\text{cover}} \cdot V_{\text{cover_shell}} = 8.814 \cdot \text{kN}$$

The volume of the weather protection cover around the shell:

$$V_{\text{cover_roof}} := t_{\text{cover}} \cdot A_{\text{roof_cover}} = 0.094 \cdot \text{m}^3$$

The weight of the cover on the roof:

$$W_{\text{cover_roof}} := \gamma_{\text{cover}} \cdot V_{\text{cover_roof}} = 7.29 \cdot \text{kN}$$

The force occurring due to the combined weight of the shell, insulation and weather protection around the shell:

$$F_{\text{weight_shell}} := \frac{1}{\pi D} (W_{\text{shell}} + W_{\text{ins_shell}} + W_{\text{cover_shell}}) = 10.451 \cdot \frac{\text{kN}}{\text{m}}$$

N.B: It has been assumed that the shell carries the entire weight of the shell, insulation and cover around the shell.

The design value of the force occurring due to the combined weight of the shell, insulation and weather protection around the shell:

$$F_{\text{weight_shell_Ed}} := \xi_{\text{weight}} \cdot \gamma_G \cdot F_{\text{weight_shell}} = 14.109 \cdot \frac{\text{kN}}{\text{m}}$$

$$s_{\text{roof}} := \sqrt{\frac{D^2}{4} + h^2} = 3.002 \text{ m}$$

The line of which the wind and snow load as well as internal pressure is applied

Note: See free body diagram of the conical roof in chapter for calculation of stresses.

The force occurring due to the combined weight of the roof, insulation and weather protection on the roof:

$$F_{\text{weight_roof}} := \frac{1}{\frac{A_{\text{roof}}}{s_{\text{roof}}}} (W_{\text{roof}} + W_{\text{ins_roof}} + W_{\text{cover_roof}}) = 3.683 \cdot \frac{\text{kN}}{\text{m}}$$

The design value of the force occurring due to the combined weight of the roof, insulation and weather protection on the roof:

$$F_{\text{weight_roof_Ed}} := \gamma_G \cdot \xi_{\text{weight}} \cdot F_{\text{weight_roof}} = 4.972 \cdot \frac{\text{kN}}{\text{m}}$$

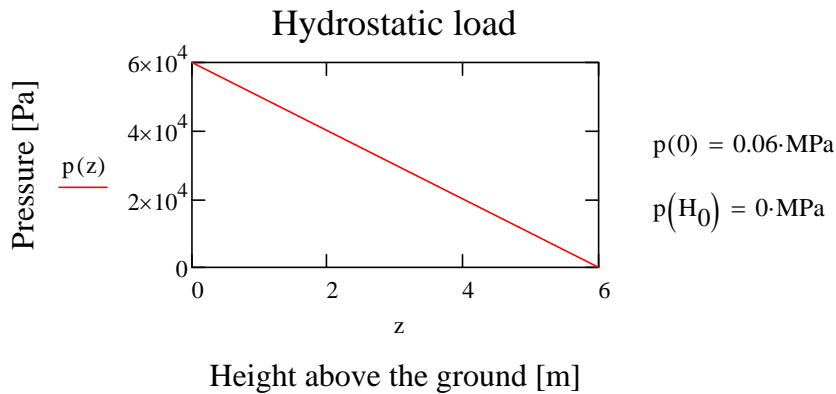
Hydrostatic load

Insert $\gamma_{\text{liquid}} := 10.0 \frac{\text{kN}}{\text{m}^3}$

The density of the liquid, densities in Annex A of SS-EN 1991-1-1 should be used.

$p(z) := \gamma_{\text{liquid}} \cdot (H_0 - z)$

The hydrostatic pressure (SS-EN 1991-4 equation 7.1)



$p_{\text{Ed}}(z) := \gamma_F \cdot \psi_{\text{hyd}} \cdot p(z)$

The design value of the hydrostatic pressure

Wind load

$z_e := 0.6 \cdot H_0 = 3.6 \text{ m}$

The reference height for the external pressure (SS-EN 1991-1-4 7.9.1(1), figure 6.1)

$z_i := H_0 = 6 \text{ m}$

The reference height for the internal pressure (SS-EN 1991-1-4 7.2.9(8))

N.B. An assumption has been made that the height of the structure is equal to the height of the shell, see SS-EN 1991-1-4 figure 6.1 and 7.2.9(8).

$z_{e_roof} := H_0 + h = 6.105 \text{ m}$

The reference height for the external pressure on the roof (SS-EN 1991-1-4 7.2.8(1)ANM)

The roughness length, determined by the terrain type 0-IV (SS-EN 1991-1-4 Table 4.1):

Insert $z_0 :=$

Description of the terrain categories of SS-EN 1991-1-4 Table 4.1:

"0 Sea or coastal area exposed to the open sea

I Lakes or flat and horizontal area with negligible vegetation and without obstacles

II Area with low vegetation such as grass and isolated obstacles (trees, buildings) with separations of at least 20 obstacle heights

III Area with regular cover of vegetation or buildings or with isolated obstacles with separations of maximum 20 obstacle heights (such as villages, suburban terrain, permanent forest)

IV Area in which at least 15 % of the surface is covered with buildings and their average heights exceeds 15 m"

Illustrations of the terrain categories can be seen in A.1 of SS-EN 1991-1-4.



$z_0 = 0.3 \text{ m}$

Insert $c_0(z) := 1$ The orography factor, determine it through annex A.3 of SS-EN 1991-1-4

$I_v(z) := \frac{1}{\left(c_0(z) \cdot \ln\left(\frac{z}{z_0}\right)\right)}$ The turbulence intensity (EKS 10 chapter 1.1.4 part 4.5(1) Anm.1 7§)

$z_{0II} := 0.05\text{m}$ The roughness length of terrain category II (SS-EN 1991-1-4 4.3.2(1)note)

$k_r := 0.19 \cdot \left(\frac{z_0}{z_{0II}}\right)^{0.07} = 0.215$ The terrain factor (SS-EN 1991-1-4 equation 4.5)

Insert $v_b := 24 \frac{\text{m}}{\text{s}}$ The basic wind velocity, determine it through figure C-4 of EKS 10

$\rho := 1.25 \frac{\text{kg}}{\text{m}^3}$ The air density (SS-EN 1991-1-4 4.5(1) note 2)

$q_b := \frac{1}{2} \cdot \rho \cdot v_b^2 = 360\text{Pa}$ The basic velocity pressure (SS-EN 1991-1-4 equation 4.10)

The peak velocity pressure (EKS 10 chapter 1.1.4 part 4.5(1) Anm.1 7§ replaces equation 4.8 of SS-EN 1991-1-4 with this):

$$q_p(z) := \left(1 + 6 \cdot I_v(z)\right) \cdot \left(k_r \cdot \ln\left(\frac{z}{z_0}\right) \cdot c_0(z)\right)^2 \cdot q_b$$

Insert $c_{p0} := -1.4$ The external pressure coefficient without free-end flow, determine it through Figure 7.27 of SS-EN 1991-1-4 for the following Reynolds number.



$$Re_{air} := D \cdot \frac{v(z_e)}{\nu_{air}} = 9.495 \times 10^6$$

The Reynolds number (SS-EN 1991-1-4 equation 7.15)

Insert $\alpha := 75^\circ$ Choose an angle between 0 and 180, see Figure 7.27 of SS-EN 1991-1-4.

Insert $\alpha_{min} := 75^\circ$ Determine through Figure 7.27 of SS-EN 1991-1-4 for the Reynolds number above.

Insert $\alpha_A := 105^\circ$ The position of the flow separation, determine it through Figure 7.27 of SS-EN 1991-1-4 for the Reynolds number above.

Insert $\psi_\lambda := 0.92$ The end-effect factor, determine it through Figure 7.36 of SS-EN 1991-1-4 with solidity ratio and slenderness given below



$\lambda = 70$ The slenderness given by table 7.16 of SS-EN 1991-1-4 for circular cylinders

$\varphi := 1$ The solidity ratio (SS-EN 1991-1-4 equation 7.28)



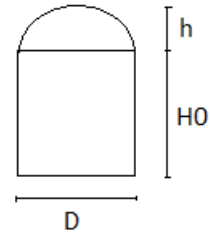
$\psi_{\lambda\alpha} = 1$ The end-effect factor, determined by equation 7.17 of SS-EN 1991-1-4

$c_{pe} := c_{p0} \cdot \psi_{\lambda\alpha} = -1.4$ The pressure coefficient for the external pressure (SS-EN 1991-1-4 equation 7.16)

Insert $c_{pe_roof} := -0.5$ The pressure coefficient for the external pressure acting on the roof, determine it through Figure 7.12 of SS-EN 1991-1-4 for f/d and h/d below.

X-axis, f/d $\frac{h}{D} = 0.017$

Curve, h/d $\frac{H_0}{D} = 1$



N.B: An assumption has been made that the pressure coefficient for the external pressure acting on the roof can be determined by figure 7.12 of SS-EN 1991-1-4, even if the shape of the roof is not a dome. The pressure coefficient for a conically shaped roof is not described by SS-EN 1991-1-4.

Insert $c_{pi} := -0.40$ The pressure coefficient for the internal pressure acting on vented tanks with small openings (SS-EN 1993-4-2 A.2.9(2)b)

Note: The pressure coefficient for the internal pressure acting on vented tanks with small openings applies to both the shell and the roof (SS-EN 1993-4-2 figure A.1b)

The external wind pressure acting on the shell:

$w_e := q_p(z_e) \cdot c_{pe} = -492.988 \cdot \text{Pa}$ The wind pressure acting on the external surfaces (SS-EN 1991-1-4 equation 5.1)

$w_{e_Ed} := \gamma_F \cdot \psi_{wind} \cdot w_e = -690.183 \text{ Pa}$ The design value of the wind pressure acting on the external surfaces

The external wind pressure acting on the roof:

$w_{e_roof} := q_p(z_{e_roof}) \cdot c_{pe_roof}$ The wind pressure acting on the external surfaces of the roof

$w_{e_roof} = -226.776 \cdot \text{Pa}$

$w_{e_roof_Ed} := \gamma_F \cdot \psi_{wind} \cdot w_{e_roof}$ The design value of the wind pressure acting on the external surfaces of the roof

$w_{e_roof_Ed} = -317.487 \text{ Pa}$

The internal wind pressure:

$$w_i := q_p(z_i) \cdot c_{pi} = -180.032 \cdot \text{Pa}$$

The wind pressure acting on the internal surfaces of a structure (SS-EN 1991-1-4 equation 5.2)

$$w_{i_Ed} := \gamma_F \cdot \psi_{wind} \cdot w_i = -252.045 \cdot \text{Pa}$$

The design value of the wind pressure acting on the internal surfaces of a structure.

Internal pressure

Insert Vented_tank :=

Insert whether or not the tank is vented.

The internal pressure above the maximum liquid level, relative atmospheric pressure if tank not vented. Over pressure is positive and under pressure is negative.

Insert $p_{int} := 0.001 \text{ bar} = 100 \cdot \text{Pa}$

Note: The maximum allowed characteristic internal pressure above the liquid level is between -0.1 bar and 0.5 bar or -0.01 - 0.05 MPa.

$$P_{int_Ed} := \gamma_F \cdot \psi_{int} \cdot p_{int} = 140 \cdot \text{Pa}$$

The design value of the internal pressure for tanks that are not vented.



$$p_i = 100 \cdot \text{Pa}$$

The internal pressure

$$P_{i_Ed} = 140 \cdot \text{Pa}$$

The design value of the internal pressure

N.B: It has been assumed that the wind pressure acting on the internal surfaces acts when the tank is vented and that there are not any other internal pressure in the tank then. For a tank that is not vented the internal pressure becomes the user defined internal pressure p_{int} .

Snow load

Note: The exceptional cases in Annex A of SS-EN 1991-1-3 have not been considered since exceptional cases are not relevant for Swedish conditions (EKS 10 chapter 1.1.3 part 1.1(3) 3§)

Insert $s_k := 2 \frac{\text{kN}}{\text{m}^2}$

The characteristic value of snow load on the ground, determine it through Figure C-2 of EKS 10.

Insert Snowguard :=

Does the roof have a snowguard?

Insert $U := 1 \frac{\text{W}}{\text{m}^2 \cdot \text{K}}$

Heat transfer coefficient of the roof

Insert $R_e := 0$

External thermal transition resistance

Insert $T_{winter} := -8 \text{ } ^\circ\text{C}$

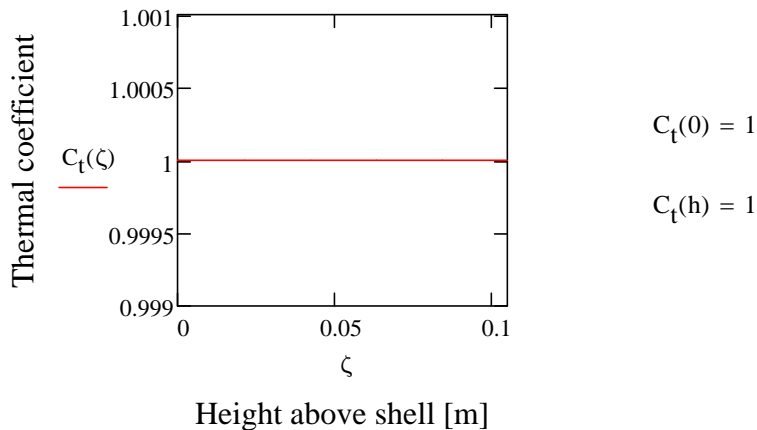
Lowest expected inner temperature during winter

Insert $T_{m_winter} := -5\text{ °C}$

The mean temperature of the coldest month of the year



The thermal coefficient, determined through BSV 97 2:nd edition on command of EKS 10 (chapter 1.1.3 part 5.2(8) 12§).



Note: The thermal coefficient depends on the slope of the roof among other things. For conical roofs the angle of the slope is constant and the thermal coefficient will therefore always be constant, but for spherical roofs the slope changes with height above the shell and the thermal coefficient might therefore change with height above the shell.



$$A_{\text{snow}} = 28.292\text{ m}^2$$

The size of the area on which the snow stays on the roof and causes a snow load, determined with the conditions for C_t given by BSV 97 2:nd edition and EKS 10 and μ_i given by SS-EN 1991-1-3.

$$\frac{A_{\text{snow}}}{A_{\text{roof}}} = 100\%$$

The proportion of the roof that the snow stays on.

Insert $C_e :=$

The exposure coefficient (Table 5.1 of SS-EN 1991-1-3. This value cannot be less than 1 according to EKS 10 chapter 1.1.3 part 5.2(7) 11a§).

SS-EN 1991-1-3 Table 5.1:

"Windswept topography: flat unobstructed areas on all sides without, or little shelter afforded by terrain, higher construction works or trees.

Normal topography: areas where there is no significant removal of snow by wind on construction work, because of terrain, other construction works or trees.

Sheltered topography: areas in which the construction work being considered is considerably lower than the surrounding terrain or surrounded by high trees and/or surrounded by higher construction works."

$$C_e = 1$$



$$\mu_1 = 0.375$$

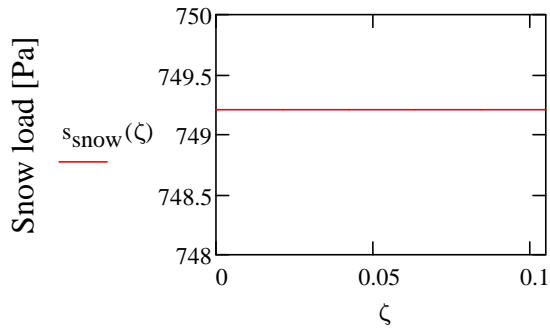
The snow load shape coefficient (SS-EN 1991-1-3 equation 5.5)

N.B An assumption has been made that the shape coefficient for a conically shaped roof can be calculated in the same way as dome shaped roof as described by SS-EN 1991-1-3 5.3.5. The shape coefficient for a conically shaped roof is not described by SS-EN 1991-1-3.

Snow load on roof:

$$s_{\text{snow}}(\zeta) := \mu_i \cdot C_e \cdot C_t(\zeta) \cdot s_k$$

The snow load on the roof (SS-EN 1991-1-3 equation 5.1)



$$s_{\text{snow}}(0) = 749.208 \cdot \text{Pa}$$

$$s_{\text{snow}}(h) = 749.208 \cdot \text{Pa}$$

Note: The snow load depends on the slope of the roof among other things. For conical roofs the angle of the slope is constant and the snow load will therefore always be constant, but for spherical roofs the slope changes with height above the shell and the snow load might therefore change with height above the shell.

$$s_{\text{snow_Ed}}(\zeta) := \gamma_F \cdot \psi_{\text{snow}} \cdot s_{\text{snow}}(\zeta)$$

The design value of the snow load on the roof

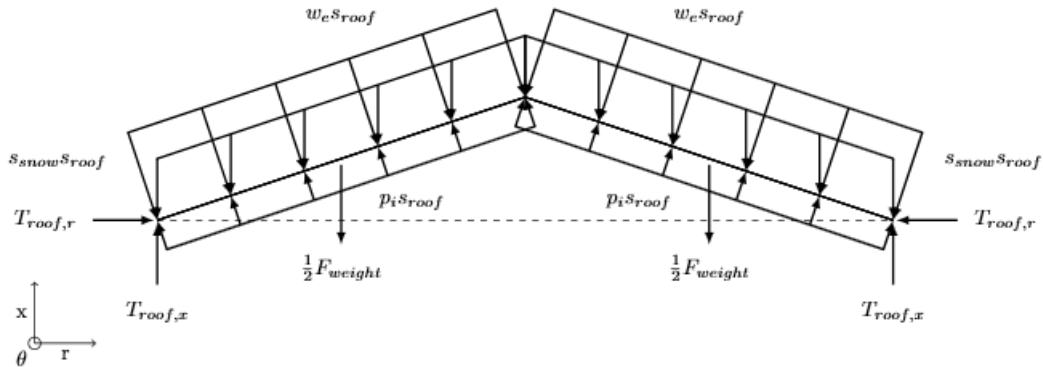
$$A_{\text{snow}} = 28.292 \text{ m}^2$$

The area on which the snow is applied (see calculation above)



Calculation of stresses

Free body diagram of a conical roof



▶

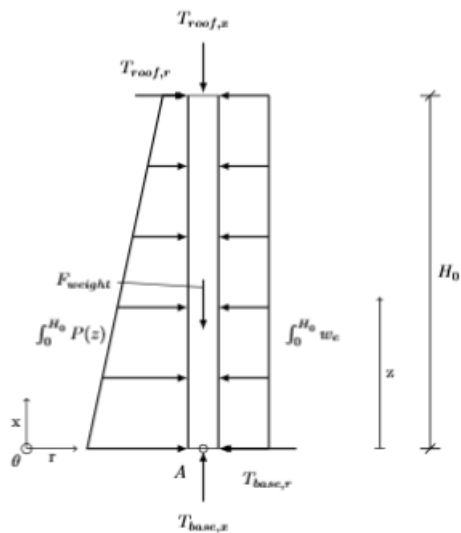
$$T_{\text{roof}_x} := \frac{1}{2} F_{\text{weight_roof}} + \frac{1}{2} F_{\text{snow}} + \frac{1}{2} F_{\text{wind_roof}} \cdot \cos(\alpha_{\text{roof}}) - \frac{1}{2} F_{\text{int}} \cdot \cos(\alpha_{\text{roof}}) = 3.11 \cdot \frac{\text{kN}}{\text{m}}$$

N.B: It has been assumed that the roof is well jointed together at the top so that it supports itself in the radial direction.

$$T_{\text{roof}_x_Ed} := \frac{1}{2} (F_{\text{weight_roof_Ed}} + F_{\text{snow_Ed}} + F_{\text{wind_roof_Ed}} \cdot \cos(\alpha_{\text{roof}}) - F_{\text{int_Ed}} \cdot \cos(\alpha_{\text{roof}}))$$

$$T_{\text{roof}_x_Ed} = 4.262 \cdot \frac{\text{kN}}{\text{m}}$$

Free body diagram of the shell



$$P(z) := p(z) + p_i$$

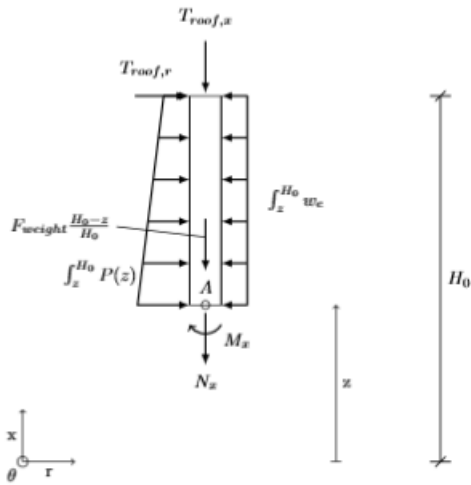
▶

The reaction force from the roof in radial direction:

$$T_{\text{roof}_r} := \frac{1}{H_0} \left(\int_0^{H_0} w_e dz \cdot \frac{1}{2} H_0 - \int_0^{H_0} p(z) dz \cdot \frac{1}{3} H_0 - \int_0^{H_0} p_i dz \cdot \frac{1}{2} H_0 \right) = -61.779 \cdot \frac{\text{kN}}{\text{m}}$$

The design value of the reaction force from the roof in radial direction:

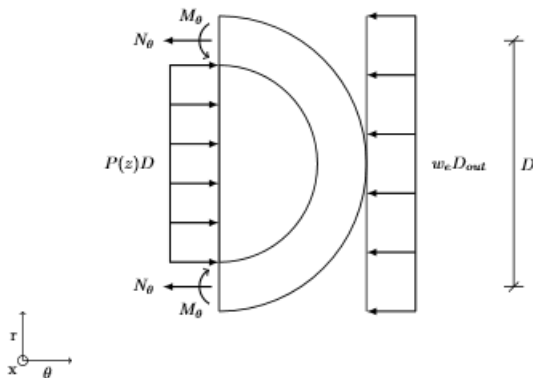
$$T_{\text{roof}_r_Ed} := \frac{1}{H_0} \left(\int_0^{H_0} w_{e_Ed} dz \cdot \frac{1}{2} H_0 - \int_0^{H_0} p_{Ed}(z) dz \cdot \frac{1}{3} H_0 - \int_0^{H_0} p_{i_Ed} dz \cdot \frac{1}{2} H_0 \right) = -86.491 \cdot \frac{\text{kN}}{\text{m}}$$



$$N_x(z) := -T_{\text{roof}_x} - F_{\text{weight_shell}} \cdot \frac{(H_0 - z)}{H_0}$$

Note: The weight of the shell is described as the weight per circumferential unit at the height z. The weight of the shell decreases with height above the ground.

$$M_x(z) := \left[\frac{w_e}{2} (H_0 - z)^2 - \frac{p_i}{2} (H_0 - z)^2 - \frac{1}{3} \int_z^{H_0} p(z) dz (H_0 - z) - T_{\text{roof}_r} \cdot (H_0 - z) \right]$$



$$D_{\text{out}} := D_{\text{cover}} + t_{\text{cover}} = 6.301 \text{ m}$$

$$N_{\theta}(z) := \text{if} \left[z < H_0, \frac{1}{2} (P(z) \cdot D - w_e \cdot D_{\text{out}}), \frac{1}{2} (P(H_0) \cdot D - w_e \cdot D_{\text{out}}) + T_{\text{roof}_r} \right]$$

$$M_{\theta}(z) := \nu \cdot M_x(z)$$

$$N_{x\theta}(z) := 0 \quad \text{The membrane shear stress resultant}$$

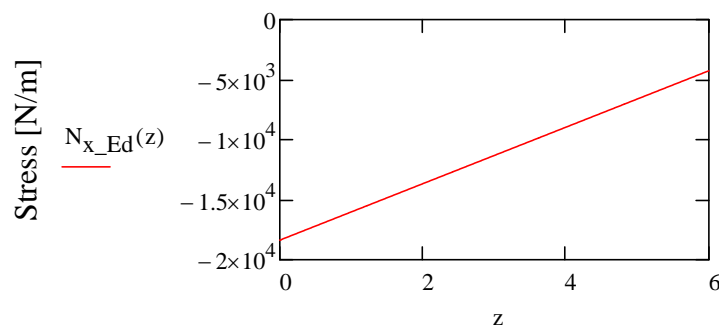
$$N_{x\theta_{\text{max_Ed}}} := 0 \quad \text{The maximum value of the membrane shear stress resultant}$$

$$M_{x\theta}(z) := 0 \quad \text{Twisting shear moment per unit width}$$

N.B: $N_{x\theta}=0$, $M_{x\theta}=0$ assuming that there's no torsion acting on the shell.



Meridional stress resultant



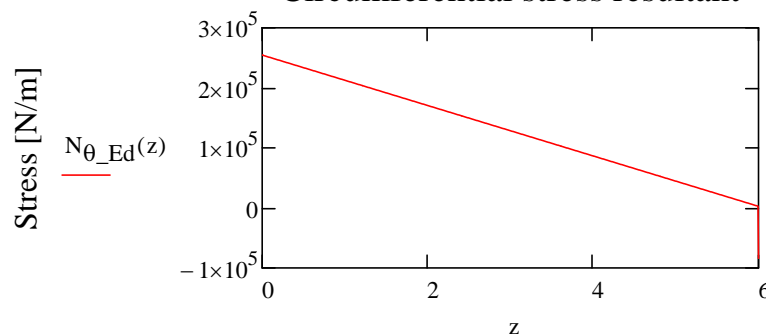
$$N_{x_Ed}(0) = -18.371 \cdot \frac{\text{kN}}{\text{m}}$$

$$N_{x_Ed}(H_0) = -4.262 \cdot \frac{\text{kN}}{\text{m}}$$

Note: A negative sign of N_x implies compression and buckling as a possible failure cause.

Height above ground [m]

Circumferential stress resultant

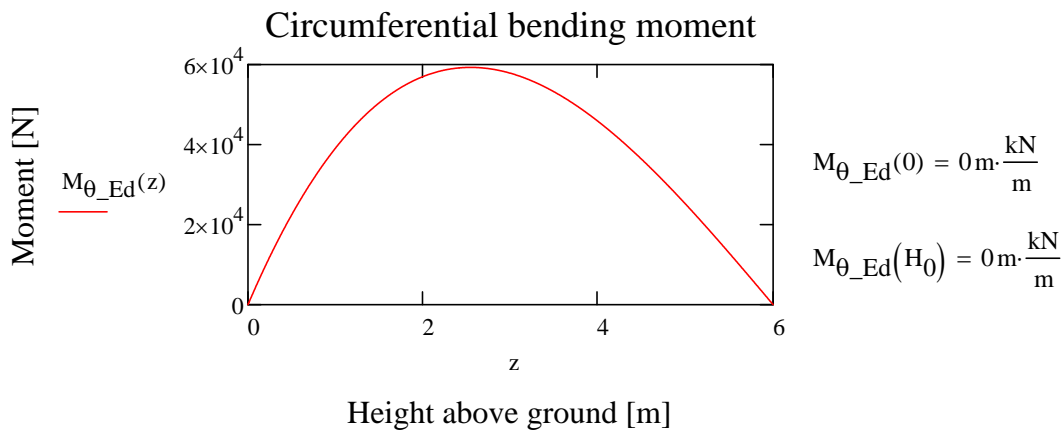
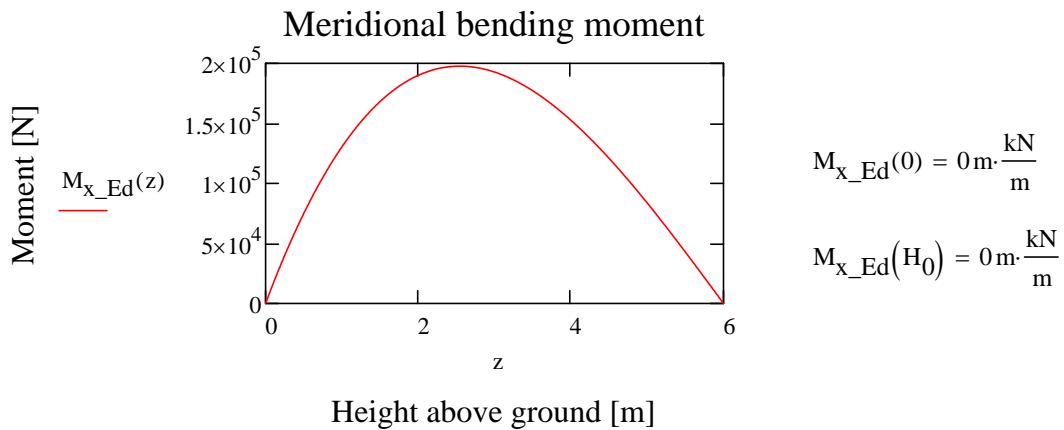


$$N_{\theta_Ed}(0) = 254.594 \cdot \frac{\text{kN}}{\text{m}}$$

$$N_{\theta_Ed}(H_0) = -83.896 \cdot \frac{\text{kN}}{\text{m}}$$

Height above ground [m]

Insert $N_{\theta_{\text{max_Ed}}} := N_{\theta_Ed}(0)$ The maximum value of the circumferential stress resultant



Limit states

Plastic limit (LS1)

$$\sigma_{eq_Ed} \leq \frac{f_{yk}}{\gamma_{M0}}$$

The condition of the design stress (SS-EN 1993-1-6 equations 6.5 and 6.6)

$$f_{yk} := f_y = 235 \cdot \text{MPa}$$

The characteristic value of the yield strength

N.B: It is assumed that the characteristic value of the yield strength equals the yield strength.



$$\sigma_{eq_Ed_mt} = \begin{pmatrix} 3.446 \\ 5.713 \\ 7.478 \\ 8.891 \\ 10.047 \\ 11.011 \end{pmatrix} \cdot \text{MPa}$$

The equivalent design stress according to membrane theory analysis (equation 6.1 of SS-EN 1993-1-6)

N.B: If the stresses are not highest at the bottom of each section the location of which the stresses are calculated needs to be changed. This is done in the hidden area above.

The extent of which the design stress fulfills the plastic limit for membrane theory analysis:

$$\text{ratio_plastic_limit_mt} := \frac{\sigma_{\text{eq_Ed_mt}}}{\frac{f_{yk}}{\gamma_{M0}}} = \begin{pmatrix} 1.466 \\ 2.431 \\ 3.182 \\ 3.783 \\ 4.275 \\ 4.685 \end{pmatrix} \cdot \%$$

Note: If ratio_plastic_limit exceeds 100 % the plastic limit has been exceeded and the thickness of the plate where the plastic limit has been exceeded has to be increased.



The equivalent design stress according to linear elastic shell analysis (equation 6.2 of SS-EN 1993-1-6):

$$\sigma_{\text{eq_Ed_la1}} = \begin{pmatrix} 1.518 \times 10^3 \\ 2.118 \times 10^3 \\ 2.113 \times 10^3 \\ 1.754 \times 10^3 \\ 1.393 \times 10^3 \\ 802.347 \end{pmatrix} \cdot \text{MPa} \quad \sigma_{\text{eq_Ed_la2}} = \begin{pmatrix} 1.52 \times 10^3 \\ 2.122 \times 10^3 \\ 2.117 \times 10^3 \\ 1.759 \times 10^3 \\ 1.398 \times 10^3 \\ 807.609 \end{pmatrix} \cdot \text{MPa}$$

The extent of which the design stress fulfills the plastic limit:

$$\text{ratio_plastic_limit_la1} := \frac{\sigma_{\text{eq_Ed_la1}}}{\frac{f_{yk}}{\gamma_{M0}}} = \begin{pmatrix} 645.893 \\ 901.397 \\ 899.025 \\ 746.554 \\ 592.875 \\ 341.424 \end{pmatrix} \cdot \%$$

$$\text{ratio_plastic_limit_la2} := \frac{\sigma_{\text{eq_Ed_la2}}}{\frac{f_{yk}}{\gamma_{M0}}} = \begin{pmatrix} 646.887 \\ 902.89 \\ 900.905 \\ 748.473 \\ 594.866 \\ 343.664 \end{pmatrix} \cdot \%$$

Note: If ratio_plastic_limit exceeds 100 % the plastic limit has been exceeded and the thickness of the plate where the plastic limit has been exceeded has to be increased.

Buckling (LS3)

Note: In order to determine the design buckling stress there are many factors that has to be determined. The following line gives a hint of how the factors relate to each other and will hopefully give an understanding of what has to be determined in order to reach the design buckling stress.

$$\sigma_{Rd}(Y_{M1}, \sigma_{Rk}) \rightarrow \sigma_{Rk}(\chi f_{yk}) \rightarrow \chi(\lambda, \lambda_0, \lambda_p, \alpha, \beta, \eta) \rightarrow \alpha(\text{Tolerance_class}), \lambda(f_{yk}, \sigma_{Rcr}) \rightarrow \sigma_{Rcr}(\omega)$$

$$\omega := \frac{1}{\sqrt{\frac{D}{2t}}} = \begin{pmatrix} 4.88 \\ 4.564 \\ 4.303 \\ 4.082 \\ 3.892 \\ 3.727 \end{pmatrix}$$

The length parameter for each section j of the shell
(SS-EN 1993-1-6 equation D.1)

$$\beta := 0.60$$

The plastic range factor (SS-EN 1993-1-6 equation D.16, D.26, D.39)

$$\eta := 1.0$$

The interaction exponent (SS-EN 1993-1-6 equation D.16, D.26, D.39)

Insert $\kappa := 0.55$

Determine from Figure D.6 of SS-EN 1993-1-6 for the following variables:

$$l_a = 2 \text{ m} \quad l_b = 2 \text{ m} \quad l_c = 2 \text{ m}$$
$$\frac{l_a}{H_0} = 0.333 \quad \frac{t_b}{t_a} = 1.267 \quad \frac{t_c}{t_a} = 1.533$$

Note: κ is dependent on the thicknesses and has therefore to be updated if the thicknesses, or lengths, are changed.

$$l_{\text{eff}} := \frac{l_a}{\kappa} = 3.636 \text{ m}$$

The effective length for the stepwise variable wall thickness shell (equation D.61 of SS-EN 1993-1-6)

$$\omega_{\text{eff}} := \frac{l_{\text{eff}}}{\sqrt{\frac{D}{2} t_a}} = 17.142$$

The length parameter for the effective length

Insert Tolerance_class :=

Note: Geometrical tolerances relevant for buckling are described by SS-EN 1993-1-6 8.4.



$$Q = 16$$

The fabrication quality parameter (SS-EN 1993-1-6 Table D.2)

First condition:

$$\sigma_{x_Ed_j} \leq \sigma_{x_Rd_j}$$

The buckling strength verification in the generatrix direction (SS-EN 1993-1-6 equation 8.18 with modification according to D.2.2(1))



$$C_x = \begin{pmatrix} 1 \\ 1 \\ 1 \\ 1 \\ 1 \\ 1 \end{pmatrix}$$

A factor depending on the height of the tank (equations D.3-D.10 of SS-EN 1993-1-6)

$$\sigma_{x_Rcr_j} := 0.605 \cdot E \cdot C_{x_j} \cdot \frac{t_j}{\frac{D}{2}}$$

The elastic critical meridional buckling stress (SS-EN 1993-1-6 equation D.2 with corrections for stepwise variable wall thickness according to D.2.2(1))

$$\sigma_{x_Rcr} = \begin{pmatrix} 592.9 \\ 677.6 \\ 762.3 \\ 847 \\ 931.7 \\ 1.016 \times 10^3 \end{pmatrix} \cdot \text{MPa}$$

$$\lambda_x := \sqrt{\frac{f_{yk}}{\sigma_{x_Rcr}}} = \begin{pmatrix} 0.63 \\ 0.589 \\ 0.555 \\ 0.527 \\ 0.502 \\ 0.481 \end{pmatrix}$$

The relative slenderness parameter in generatrix direction (SS-EN 1993-1-6 equation 8.17)



$$\alpha_x = \begin{pmatrix} 0.363 \\ 0.303 \\ 0.259 \\ 0.226 \\ 0.2 \\ 0.179 \end{pmatrix}$$

The unpressurised elastic imperfection reduction factor

Note: The calculation of the unpressurised elastic imperfection reduction factor is very long and has therefore been hidden in the area above.

$$\lambda_{x0} := 0.20$$

The meridional squash limit slenderness determined from equatio D.16 of SS-EN 1993-1-6

N.B: An assumption has been made that none of the wall sections is seen as a long cylinder. To varify that this assumption is valid please look in the hidden area below.



$$\lambda_{xp} := \sqrt{\frac{\alpha_x}{1 - \beta}} = \begin{pmatrix} 0.953 \\ 0.87 \\ 0.805 \\ 0.751 \\ 0.707 \\ 0.669 \end{pmatrix}$$

The plastic limit relative slenderness (SS-EN 1993-1-6 equation 8.16)



$$\chi_x = \begin{pmatrix} 0.658 \\ 0.652 \\ 0.648 \\ 0.644 \\ 0.642 \\ 0.641 \end{pmatrix}$$

The buckling reduction factor in generatrix direction
(calculated from equations 8.13-8.15 of SS-EN
1993-1-6)

$$\sigma_{x_Rk} := \chi_x \cdot f_{yk} = \begin{pmatrix} 154.574 \\ 153.209 \\ 152.189 \\ 151.437 \\ 150.895 \\ 150.526 \end{pmatrix} \cdot \text{MPa}$$

The characteristic buckling stress in the generatrix
direction (SS-EN 1993-1-6 equation 8.12)

$$\sigma_{x_Rd} := \frac{\sigma_{x_Rk}}{\gamma_{M1}} = \begin{pmatrix} 154.574 \\ 153.209 \\ 152.189 \\ 151.437 \\ 150.895 \\ 150.526 \end{pmatrix} \cdot \text{MPa}$$

The design buckling stress in the generatrix direction
(SS-EN 1993-1-6 equation 8.11)



$$\sigma_{x_Ed_mt} := \frac{N_{x_Ed}}{t} = \begin{pmatrix} -0.472 \\ -0.56 \\ -0.629 \\ -0.683 \\ -0.728 \\ -0.765 \end{pmatrix} \cdot \text{MPa}$$

$$\text{utilized}_{1st_mt} := \frac{\sigma_{x_Ed_mt}}{\sigma_{x_Rd}} = \begin{pmatrix} -0.306 \\ -0.366 \\ -0.413 \\ -0.451 \\ -0.483 \\ -0.509 \end{pmatrix} \cdot \%$$

The extend of which the 1st conditions
has been utilized

$$\sigma_{x_Ed1_la} := \frac{N_{x_Ed_la}}{t} - \frac{M_{x_Ed}}{\frac{t^2}{4}} = \begin{pmatrix} -1.709 \times 10^3 \\ -2.386 \times 10^3 \\ -2.38 \times 10^3 \\ -1.977 \times 10^3 \\ -1.571 \times 10^3 \\ -906.284 \end{pmatrix} \cdot \text{MPa} \quad \text{Equation 6.3 of SS-EN 1993-1-6}$$

$$\sigma_{x_Ed2_la} := \frac{N_{x_Ed_la}}{t} + \frac{M_{x_Ed}}{\frac{t^2}{4}} = \begin{pmatrix} 1.709 \times 10^3 \\ 2.385 \times 10^3 \\ 2.379 \times 10^3 \\ 1.976 \times 10^3 \\ 1.57 \times 10^3 \\ 904.949 \end{pmatrix} \cdot \text{MPa} \quad \text{Equation 6.3 of SS-EN 1993-1-6}$$

$$\text{utilized}_{1st_1_la} := \frac{\sigma_{x_Ed1_la}}{\sigma_{x_Rd}} = \begin{pmatrix} -1.106 \times 10^3 \\ -1.557 \times 10^3 \\ -1.564 \times 10^3 \\ -1.305 \times 10^3 \\ -1.041 \times 10^3 \\ -602.078 \end{pmatrix} \cdot \% \quad \text{The extend of which the 1st conditions has been utilized}$$

$$\text{utilized}_{1st_2_la} := \frac{\sigma_{x_Ed2_la}}{\sigma_{x_Rd}} = \begin{pmatrix} 1.105 \times 10^3 \\ 1.556 \times 10^3 \\ 1.563 \times 10^3 \\ 1.305 \times 10^3 \\ 1.04 \times 10^3 \\ 601.192 \end{pmatrix} \cdot \% \quad \text{The extend of which the 1st conditions has been utilized}$$

Note: If the ratio_buckling exceeds 100% the condition for the buckling is not fulfilled and the thickness of the tank wall has to be increased, or the tank has to be stiffened.

Second condition:

$$\sigma_{\theta_Ed_eff} \leq \sigma_{\theta_Rd_eff}$$

The buckling strength verification in the direction of the circumference for an equivalent single cylinder with uniform wall thickness and effective length l_{eff} , see Figure D.5 (SS-EN 1993-1-6 equation D.66)

$$C_{\theta_eff} := 1$$

A factor that should be 1 for stepwise variable wall thicknesses (SS-EN 1993-1-6 D.2.3.1(7))

The elastic critical circumferential buckling stress (SS-EN 1993-1-6 equations D.20-D.23 with corrections for stepwise variable wall thickness according to D.2.3.1(7)):

$$\sigma_{\theta_Rcr_eff} := 0.92 \cdot E \cdot \frac{C_{\theta_eff}}{\omega_{eff}} \cdot \frac{t_a}{\frac{D}{2}} = 56.353 \cdot \text{MPa}$$

$$\lambda_{\theta_eff} := \sqrt{\frac{f_{yk}}{\sigma_{\theta_Rcr_eff}}} = 2.042$$

The relative slenderness parameter in circumference direction (SS-EN 1993-1-6 equation 8.17)



$$\alpha_{\theta} = 0.5$$

The circumferential elastic imperfection reduction factor, determined for the chosen tolerance class (SS-EN 1993-1-6 Table D.5)

$$\lambda_{\theta 0} := 0.40$$

The circumferential squash limit slenderness (SS-EN 1993-1-6 equation D.26)

$$\lambda_{\theta p} := \sqrt{\frac{\alpha_{\theta}}{1 - \beta}} = 1.118$$

The plastic limit relative slenderness (SS-EN 1993-1-6 equation 8.16)



$$\chi_{\theta_eff} = 0.12$$

The buckling reduction factor in circumference direction (calculated from equations 8.13-8.15 of SS-EN 1993-1-6)

$$\sigma_{\theta_Rk_eff} := \chi_{\theta_eff} \cdot f_{yk} = 28.176 \cdot \text{MPa}$$

The characteristic buckling stress in the circumference direction (SS-EN 1993-1-6 equation 8.12)

$$\sigma_{\theta_Rd_eff} := \frac{\sigma_{\theta_Rk_eff}}{\gamma_{M1}} = 28.176 \cdot \text{MPa}$$

The design buckling stress in the circumference direction (SS-EN 1993-1-6 equation 8.11)



$$k_w = 0.65$$

Determined from equation D.29 of SS-EN 1993-1-6

$$c_{p0_max} := 1$$

The maximum external pressure coefficient without free-end flow (Figure 7.27 of SS-EN 1991-1-4).

$$c_{pe_max} := c_{p0_max} \cdot \psi \cdot \lambda_{\alpha}$$

The maximum pressure coefficient for the external pressure (equation 7.16 of SS-EN 1991-1-4 for c_{p0_max})

$$w_{e_max} := q_p(z_e) \cdot c_{pe_max}$$

The maximum wind pressure acting on the external surfaces (SS-EN 1991-1-4 equation 5.1)

$$q_{w_max} := w_{e_max} = 352.134 \cdot \text{Pa}$$

The maximum wind pressure

$$q_{eq} := k_w \cdot q_{w_max} = 228.887 \cdot \text{Pa}$$

The equivalent uniform external wind pressure (equation D.28 of SS-EN 1993-1-6)

$$q_s := \min(0, p_i) = 0 \cdot \text{MPa}$$

The internal suction (see SS-EN 1993-1-6 D.1.3.2(5))

$$\sigma_{\theta_Ed_eff} := (q_{eq} + q_s) \frac{D}{t_a} = 0.046 \cdot \text{MPa}$$

The circumferential design stress for the effective cylinder calculated with the equivalent wind (SS-EN 1993-1-6 equation D.30)

$$\text{utilized}_{2nd_eq_wind} := \frac{\sigma_{\theta_Ed_eff}}{\sigma_{\theta_Rd_eff}} = 0.162 \cdot \%$$

The extend of which the 2nd conditions has been utilized for the equivalent wind



$$\sigma_{\theta_Ed_eff_mt} := \frac{N_{\theta_Ed}}{t_a} = \begin{pmatrix} 2.973 \\ 5.773 \\ 8.573 \\ 11.373 \\ 14.173 \\ 16.973 \end{pmatrix} \cdot \text{MPa}$$

$$\text{utilized}_{2nd_mt} := \frac{\sigma_{\theta_Ed_eff_mt}}{\sigma_{\theta_Rd_eff}} = \begin{pmatrix} 10.551 \\ 20.489 \\ 30.426 \\ 40.363 \\ 50.301 \\ 60.238 \end{pmatrix} \cdot \%$$

The extend of which the 2nd conditions has been utilized

$$\sigma_{\theta_Ed_eff1_la} := \frac{N_{\theta_Ed_la}}{t_a} - \frac{M_{\theta_Ed}}{\frac{t_a^2}{4}} = \begin{pmatrix} -443.652 \\ -808.382 \\ -1.019 \times 10^3 \\ -1.003 \times 10^3 \\ -684.141 \\ 14.173 \end{pmatrix} \cdot \text{MPa}$$

Equation 6.3 of SS-EN 1993-1-6

$$\sigma_{\theta_Ed_eff2_la} := \frac{N_{\theta_Ed_la}}{t_a} + \frac{M_{\theta_Ed}}{\frac{t_a^2}{4}} = \begin{pmatrix} 449.598 \\ 819.928 \\ 1.036 \times 10^3 \\ 1.023 \times 10^3 \\ 706.887 \\ 14.173 \end{pmatrix} \cdot \text{MPa}$$

Equation 6.3 of SS-EN 1993-1-6

$$\text{utilized}_{2\text{nd}_1\text{la}} := \frac{\sigma_{\theta_Ed_eff1_la}}{\sigma_{\theta_Rd_eff}} = \begin{pmatrix} -1.575 \times 10^3 \\ -2.869 \times 10^3 \\ -3.618 \times 10^3 \\ -3.561 \times 10^3 \\ -2.428 \times 10^3 \\ 50.301 \end{pmatrix} \% \quad \text{The extend of which the 2nd conditions has been utilized}$$

$$\text{utilized}_{2\text{nd}_2\text{la}} := \frac{\sigma_{\theta_Ed_eff2_la}}{\sigma_{\theta_Rd_eff}} = \begin{pmatrix} 1.596 \times 10^3 \\ 2.91 \times 10^3 \\ 3.679 \times 10^3 \\ 3.631 \times 10^3 \\ 2.509 \times 10^3 \\ 50.301 \end{pmatrix} \% \quad \text{The extend of which the 2nd conditions has been utilized}$$

Note: If the ratio_buckling exceeds 100% the condition for the buckling is not fulfilled and the thickness of the tank wall has to be increased, or the tank has to be stiffened.

Third condition:

$$\tau_{x\theta_Ed_eff} \leq \tau_{x\theta_Rd_eff}$$

The buckling strength verification for shearing in the direction of the circumference for an equivalent single cylinder with uniform wall thickness and effective length l_{eff} , see Figure D.5 (SS-EN 1993-1-6 equation 8.18)

$$C_{\tau_eff} := 1$$

A factor that should be 1 for stepwise variable wall thicknesses (SS-EN 1993-1-6 D.2.3.1(7) with modification according to D.2.4.1(2))

The elastic critical shear buckling stress (equation D.32 of SS-EN 1993-1-6 with corrections for stepwise variable wall thickness according to D.2.4.1(2)):

$$\tau_{x\theta_Rcr_eff} := \frac{0.75 \cdot E \cdot C_{\tau_eff}}{\sqrt{\omega_{eff}}} \frac{t_a}{\frac{D}{2}} = 190.204 \cdot \text{MPa}$$

$$\lambda_{\tau_eff} := \sqrt{\frac{\frac{f_{yk}}{\sqrt{3}}}{\tau_{x\theta_Rcr_eff}}} = 0.845$$

The relative slenderness parameter for the shear stress in circumference direction (SS-EN 1993-1-6 equation 8.17)



$$\alpha_{\tau} = 0.5$$

The shear elastic imperfection reduction factor, determined for the chosen tolerance class (SS-EN 1993-1-6 Table D.6)

$$\lambda_{\tau 0} := 0.40$$

The shear squash limit slenderness (SS-EN 1993-1-6 equation D.39)

$$\lambda_{\tau p} := \sqrt{\frac{\alpha_{\tau}}{1-\beta}} = 1.118$$

The plastic limit relative slenderness (SS-EN 1993-1-6 equation 8.16)



$$\chi_{\tau \text{eff}} = 0.628$$

The buckling reduction factor for the shear stress in circumference direction (calculated from equations 8.13-8.15 of SS-EN 1993-1-6)

$$\tau_{x\theta \text{Rk_eff}} := \frac{\chi_{\tau \text{eff}} \cdot f_{yk}}{\sqrt{3}} = 85.273 \cdot \text{MPa}$$

The characteristic buckling shear stress in the circumference direction (SS-EN 1993-1-6 equation 8.12)

$$\tau_{x\theta \text{Rd_eff}} := \frac{\tau_{x\theta \text{Rk_eff}}}{\gamma_{M1}} = 85.273 \cdot \text{MPa}$$

The design buckling shear stress in the direction of the circumference (SS-EN 1993-1-6 equation 8.11)



$$\tau_{x\theta \text{Ed_mt}} := \frac{N_{x\theta \text{Ed}}}{t} = \begin{pmatrix} 0 \\ 0 \\ 0 \\ 0 \\ 0 \\ 0 \end{pmatrix} \cdot \text{MPa}$$

$$\text{utilized}_{3\text{rd_mt}} := \frac{\tau_{x\theta \text{Ed_mt}}}{\tau_{x\theta \text{Rd_eff}}} = \begin{pmatrix} 0 \\ 0 \\ 0 \\ 0 \\ 0 \\ 0 \end{pmatrix} \cdot \%$$

The extend of which the 3rd conditions has been utilized

$$\tau_{x\theta \text{Ed_eff1_la}} := \frac{N_{x\theta \text{Ed}}}{t_a} - \frac{M_{x\theta \text{Ed}}}{\frac{t_a^2}{4}} = \begin{pmatrix} 0 \\ 0 \\ 0 \\ 0 \\ 0 \\ 0 \end{pmatrix} \cdot \text{MPa}$$

Equation 6.4 of SS-EN 1993-1-6

$$\tau_{x\theta_Ed_eff2_la} := \frac{N_{x\theta_Ed}}{t_a} + \frac{M_{x\theta_Ed}}{\frac{t_a^2}{4}} = \begin{pmatrix} 0 \\ 0 \\ 0 \\ 0 \\ 0 \\ 0 \end{pmatrix} \cdot \text{MPa} \quad \text{Equation 6.4 of SS-EN 1993-1-6}$$

$$\text{utilized}_{3rd_1_la} := \frac{\tau_{x\theta_Ed_eff1_la}}{\tau_{x\theta_Rd_eff}} = \begin{pmatrix} 0 \\ 0 \\ 0 \\ 0 \\ 0 \\ 0 \end{pmatrix} \cdot \% \quad \text{The extend of which the 3rd conditions has been utilized}$$

$$\text{utilized}_{3rd_2_la} := \frac{\tau_{x\theta_Ed_eff2_la}}{\tau_{x\theta_Rd_eff}} = \begin{pmatrix} 0 \\ 0 \\ 0 \\ 0 \\ 0 \\ 0 \end{pmatrix} \cdot \% \quad \text{The extend of which the 3rd conditions has been utilized}$$

Note: If any of the ratio_buckling exceeds 100% the condition for the buckling is not fulfilled and the thickness of the tank wall has to be increased, or the tank has to be stiffened.

The following two conditions should be checked as an addition to the conditions above (SS-EN 1993-1-6 D.2.3.2(1):

Fourth condition:

$$\sigma_{\theta_Ed_j} \leq \sigma_{\theta_Rcr_j} \quad \text{Equation D.66 of SS-EN 1993-1-6}$$

▮

$$\sigma_{\theta_Rcr} = \begin{pmatrix} 60.378 \\ 52.831 \\ 46.961 \\ 42.265 \\ 38.422 \\ 35.221 \end{pmatrix} \cdot \text{MPa} \quad \text{The critical circumferential buckling stress of each cylinder section j (equations D.62 and D.65 of SS-EN 1993-1-6)}$$

$$\sigma_{\theta_Ed} := \left(q_{eq} + q_s \right) \frac{D}{t} = \begin{pmatrix} 0.049 \\ 0.043 \\ 0.038 \\ 0.034 \\ 0.031 \\ 0.029 \end{pmatrix} \cdot \text{MPa} \quad \text{The circumferential design stress for each section of a cylinder calculated with the equivalent wind pressure (SS-EN 1993-1-6 equation D.30)}$$

$$\text{ratio_buckling_}\theta := \frac{\sigma_{\theta_Ed}}{\sigma_{\theta_Rcr}} = \begin{pmatrix} 0.081 \\ 0.081 \\ 0.081 \\ 0.081 \\ 0.081 \end{pmatrix} \cdot \%$$

$$\sigma_{\theta_Ed} := \frac{N_{\theta_max_Ed}}{t} = \begin{pmatrix} 18.185 \\ 15.912 \\ 14.144 \\ 12.73 \\ 11.572 \\ 10.608 \end{pmatrix} \text{MPa} \quad \text{Equation D.68 of SS-EN 1993-1-6}$$

$$\text{utilized}_{4th} := \frac{\sigma_{\theta_Ed}}{\sigma_{\theta_Rcr}} = \begin{pmatrix} 30.119 \\ 30.119 \\ 30.119 \\ 30.119 \\ 30.119 \\ 30.119 \end{pmatrix} \cdot \% \quad \text{The extend of which the 4th conditions has been utilized}$$

Note: If the ratio_buckling exceeds 100% the condition for the buckling is not fulfilled and the thickness of the tank wall has to be increased, or the tank has to be stiffened.

Fifth condition:

$$\tau_{x\theta_Edj} \leq \tau_{x\theta_Rcrj} \quad \text{Equation D.66 of SS-EN 1993-1-6 with modification according to D.2.4.1(2).}$$

$$\tau_{x\theta_Rcrj} := \frac{t_a}{t_j} \tau_{x\theta_Rcr_eff} \quad \text{The elastic critical shear buckling stress of each section j (equation D.62 with corrections for according to D.2.4.1(2) SS-EN 1993-1-6)}$$

$$\tau_{x\theta_Rcr} = \begin{pmatrix} 203.79 \\ 178.316 \\ 158.503 \\ 142.653 \\ 129.685 \\ 118.878 \end{pmatrix} \text{MPa}$$

$$\tau_{x\theta_Ed} := \frac{N_{x\theta_max_Ed}}{t} = \begin{pmatrix} 0 \\ 0 \\ 0 \\ 0 \\ 0 \\ 0 \end{pmatrix}$$

Equation D.68 with modification according to D.2.4.1(2) of SS-EN 1993-1-6

$$\text{utilized}_{5th} := \frac{\tau_{x\theta_Ed}}{\tau_{x\theta_Rcr}} = \begin{pmatrix} 0 \\ 0 \\ 0 \\ 0 \\ 0 \\ 0 \end{pmatrix} \%$$

The extend of which the 5th conditions has been utilized

Note: If the ratio_buckling exceeds 100% the condition for the buckling is not fulfilled and the thickness of the tank wall has to be increased, or the tank has to be stiffened.